T.C.
IŞIK UNIVERSTIY
SCHOOL OF GRADUATE STUDIES

MASTER THESIS
DEPARTMENT OF CIVIL ENGINEERING PROGRAM
CIVIL ENGINEERING PROGRAM

Zineb BOULAHIAT

COMPARATIVE ANALYSIS OF SOIL-STRUCTURE INTERACTION (SSI) ACCORDING TO TURKISH AND MOROCCAN SEISMIC STANDARDS

SUPERVISOR
Prof. Dr. Ehsan ETMINAN

İSTANBUL, June 2025

T.C.
IŞIK UNIVERSTIY
SCHOOL OF GRADUATE STUDIES

MASTER THESIS
DEPARTMENT OF CIVIL ENGINEERING PROGRAM
CIVIL ENGINEERING PROGRAM

Zineb BOULAHIAT

(22CIVL5003)

COMPARATIVE ANALYSIS OF SOIL-STRUCTURE INTERACTION (SSI) ACCORDING TO TURKISH AND MOROCCAN SEISMIC STANDARDS

SUPERVISOR

Prof. Dr. Ehsan ETMINAN

İSTANBUL, June 2025

T.C.
IŞIK UNIVERSITY
SCHOOL OF GRADUATE STUDIES

MASTER'S THESIS
DEPARTMENT OF CIVIL ENGINEERING
CIVIL ENGINEERING PROGRAM

Zineb BOULAHIAT

(22CIVL5003)

COMPARATIVE ANALYSIS OF SOIL-STRUCTURE INTERACTION (SSI) ACCORDING TO TURKISH AND MOROCCAN SEISMIC STANDARDS

Date: 30-06-2025

Thesis Supervisor: Asst. Prof. Dr. Ehsan ETMINAN / Işık University

Jury Members:

Asst. Prof. Dr. Önder UMUT/ Işık University

Asst. Prof. Dr. Kaveh DEHGHANIAN / Aydın University

İSTANBUL, June 2025

ÖZET

TÜRKİYE VE FAS SİSMİK STANDARTLARINA GÖRE TOPRAK-YAPI ETKİLEŞİMİNİN (SSI) KARŞILAŞTIRMALI ANALİZİ

Bu tez, Türkiye (TBDY 2018) ve Fas (RPS 2000) sismik tasarım standartlarına göre inşa edilen yapılarda zemin-yapı etkileşiminin (ZYE) davranışlarını karşılaştırmalı olarak incelemektedir. Çalışmanın temel amacı, iki ülke arasındaki jeoteknik ve sismik düzenlemelerdeki farklılıkların, yapıların ZYE tepkileri üzerindeki etkilerini analiz etmektir. Bu kapsamda, hem Türkiye'nin hem de Fas'ın zemin özellikleri ile sismik koşulları dikkate alınarak, standartların mühendislik tasarımına etkisi değerlendirilmiştir.

Çalışmanın teorik altyapısı, ZYE'yi etkileyen bölgesel zemin parametreleri ile sismik faktörlerin belirlenmesini amaçlayan kapsamlı bir literatür taramasına dayanmaktadır. Sayısal analizler, PLAXIS sonlu elemanlar yazılımı kullanılarak gerçekleştirilmiştir. Modeller oluşturulurken, Türkiye'ye özgü karmaşık ve katmanlı zemin profilleri ile Fas'a özgü daha homojen zemin yapıları dikkate alınmıştır. Zemin sınıflandırmaları, sismik tepki katsayıları ve temel-zemin etkileşimleri gibi anahtar parametreler analiz edilmiştir.

Elde edilen bulgular, zemin özellikleri, sismik yükler ve düzenleyici gereklilikler bakımından farklılık gösteren standartların, yapıların oturma ve yük aktarım davranışlarını önemli ölçüde etkilediğini göstermektedir. Türkiye'deki standartların daha detaylı ve zemin derinliğini dikkate alan bir yaklaşım içerdiği, Fas standartlarının ise daha sade ve yüzeysel değerlere dayandığı görülmektedir. Bu farklılıklar, her iki ülkenin mühendislik çözümlerinde bölgeye özel tasarım yapılmasının gerekliliğini ortaya koymaktadır. Sonuç olarak, yapı güvenliğinin artırılması, ekonomik sağlanması

ve bakım maliyetlerinin azaltılması için yerel zemin koşullarına uygun, özelleştirilmiş temel tasarımlarının geliştirilmesi büyük önem taşımaktadır..
Anahtar Kelimeler: Zemin-Yapı Etkileşimi, Yüksek Katlı Binalar, Türkiye Bina Deprem Yönetmeliği, Fas Deprem Yönetmeliği, PLAXIS Analizi

ABSTRACT

COMPARATIVE ANALYSIS OF SOIL-STRUCTURE INTERACTION (SSI) ACCORDING TO TURKISH AND MOROCCAN SEISMIC STANDARDS

This thesis examines the soil-structure interaction (SSI) in structures built in accordance to seismic standards codes in both counties Turkey (TBDY 2018) and Morocco (RPS 2000). The study focuses on understanding how variations in geotechnical and seismic standards impact SSI behaviors across both countries. With the purpose of analyzing the development of SSI considerations in both nations and determining the similarities and differences between TBDY2018 and RPS2000. This study conducts a comprehensive review of the literature to investigate the regional soil parameters and seismic factors that influence SSI in each nation.

The findings are carried out by using finite element PLAXIS software to model SSI impacts, with a focus on how soil behavior differs between Turkey's complex, layered profiles and Morocco's generally uniform soils. The study's main focus is on analyzing soil classifications, seismic response modifications, and foundation interactions that differ according to local standards. The findings show that Turkish and Moroccan standards produce distinct settlement and load-transfer behaviors as a result of differences in soil qualities, seismic loads, and regulatory requirements. These findings highlight the necessity of customized and specialized foundation solutions that match regional circumstances in order to improve long-term structural integrity and reduce maintenance expenses for buildings.

Keywords: Soil-Structure Interaction, High-Rise Buildings, Turkish Building Seismic Code, Moroccan Seismic Code, PLAXIS Analysis

ACKNOWLEDGMENTS

I sincerely acknowledge and give all my warmest thanks to my advisor Prof Ehsan ETMINAN who guided and advised me through all the stages of writing this thesis, without forgeting his encouragement and his precious advices through the whole work. I am also grateful to the team of engineers at ESTA Construction for their contribution of the data that was indispensable for this investigation. Their technical guidance contributed to the findings. I want to thank also my family members that were from the beginning supportive mentally and financially, without forgetting my close friends that made me motivated in hard times.

Zineb BOULAHIAT

TABLE OF CONTENTS

LIST OF FIGURES

LIST OF TABLES

LIST OF ABBREVIATIONS

AASHTO: American Association of State Highway and Transportation Officials

AFAD: Disaster and Emergency Management Authority (Turkey)

ABAQUS: Commercial finite element analysis software

ASCE: American Society of Civil Engineers

BE: Boundary Element

BEM: Boundary Element Method

BKS: Bina Kullanım Sınıfı (Building Usage Class)

CAD: Computer-Aided Design

CM: Correction Magnitude

CRR: Cyclic Resistance Ratio

CPT: Cone Penetration Test

CSEM: European-Mediterranean Seismological Centre

DBD: Displacement-Based Design

DMT: Dilatometer Test

EC8: Eurocode 8

EAFZ: East Anatolian Fault Zone

ETABS: Extended 3D Analysis of Building Systems

FE: Finite Element

FEA: Finite Element Analysis

FEM: Finite Element Method

FLAC: Fast Lagrangian Analysis of Continua

HS: Hardening Soil

IBC: International Building Code

MMI: Modified Mercalli Intensity

NAFZ: North Anatolian Fault Zone

OCR: Overconsolidation Ratio

OpenSees: Open System for Earthquake Engineering Simulation

PBEE: Performance-Based Earthquake Engineering

PGA: Peak Ground Acceleration

PGV: Peak Ground Velocity

PLAXIS: Finite element software for geotechnical analysis

PMT: Pressuremeter Test

PSHA: Probabilistic Seismic Hazard Analysis

PIV: Particle Image Velocimetry

RC: Reinforced Concrete

RF: Friction Ratio

RPS: Moroccan Seismic Code (Règles de construction parasismique)

SD: Single-Sided Drainage

SDOF: Single Degree of Freedom

SPT: Standard Penetration Test

SSC: Model for Single-Sided Drainage (Exact acronym meaning unclear; often refers to Single-Sided Consolidation or Soft Soil Creep in software)

SSSI: Site-Specific Seismic Investigation

TBEC: Turkish Building Earthquake Code

TBDY: Türkiye Bina Deprem Yönetmeliği (Turkish Building Earthquake Code)

USGS: United States Geological Survey

UTC: Coordinated Universal Time

VST: Vane Shear Test

ZYE: Zemin-Yapı Etkileşimi (Soil-Structure Interaction in Turkish)

CHAPTER 1

1. INTRODUCTION

1.1 BACKGROUND AND JUSTIFICATION

Earthquakes are a serious concern in the building industry, particularly in places like Turkey and Morocco where there is a lot of seismic activity. One of the key goals of contemporary civil engineering is to make sure that structures are strong enough to withstand earthquakes. Understanding the aim of soil-structure interaction (SSI), or the interface between buildings and the soil, is a key part of this safety. SSI may change how a structure responds to seismic stresses in a big manner. This can affect settlement, lateral displacement, and overall stability. Sometimes, fixed-base designs don't take into account the effects of SSI, which may lead to consequences that are dangerous. (Stewart et al, 2014).

Turkey's code : Türkiye Bina Deprem Yönetmeliği (TBDY 2018) and Morocco's code : Règlement de Construction Parasismique du Maroc (RPS 2000) are examples of national seismic codes that take into account the dangers and hazards of earthquakes and the characteristics of the soil in each country. The goal of this thesis is to compare how SSI acts under different standards and regulations. The objective is to learn more about seismic design methods and to compare the code requirements of both countries.

1.2 RESEARCH PROBLEM AND RESEARCH QUESTION

The primary goal of the study is how the geotechnical earthquake engineering standards deal with soil-structure interaction in Turkey and Morocco. The main aim concerning the research is to understand how both nations' seismic design frameworks deal with SSI, similarities and differences.

Some of the most important questions of research are:

- What are the variations and similarities between Turkey's and Morocco's seismic design requirements when it concerns SSI?
- How do these criteria affect how soil-structure systems behave during earthquakes, particularly when it comes to how well the foundation is working and how energy is lost (energy dissipation)?
- What effects have prior earthquakes in Turkey and Morocco had on the performance of SSI?

In addition, the study intends to find out what problems there are with setting SSI measures into each country's standard and how well they work in real life to make buildings more resistant to earthquakes. Turkey and Morocco are both in areas where earthquakes happen a lot, but Turkey has more and stronger earthquakes. However, Morocco has also had significant earthquakes, which shows how important it is to have strong SSI design practices. The research looks at how SSI is now in TBDY 2018 (Turkey) and RPS 2000/2011 (Morocco) to find out how well each country's method works, what its problems are, and how it may be more effective. This comparison helps us to understand how ready a structure is for earthquakes, how safe it is, and how strong it will be in the long term, particularly when the geotechnical and structural conditions at different sites are not the same. It also provides a place for individuals from different countries to share knowledge and helps to improve earthquake design methods throughout the world.

1.3 OBJECTIVES AND CONTRIBUTIONS OF THE STUDY

The research’s objectives are as follows:

1. To look at and compare Turkey and Morocco's seismic standards, focusing on SSI-related terminology, provisions, and modeling methods.
2. To find out how well SSI requirements in these standards help prevent structure damage during earthquakes.

3. To find the best practices from both standards codes and suggest ways to make SSI modeling and design better.
4. To use PLAXIS 2Dsoftware to do a numerical study that simulates a 15-story structure on a raft foundation that is susceptible to seismic loads.

This will be done by using Turkish and Moroccan geotechnical data subject to 3 different combination equations that are:

G + Q

1.4G + 1.6G

G + Q + E

The research will provide a full picture of the similarities, differences, and results of SSI implementation under Turkish and Moroccan seismic codes. It will help to analyze how various rules affect SSI practices and how well structures work. The results will help to make suggestions for safer and more effective code implementations in both countries and to set a framework for future improvements.

1.4 METHODOLOGY

The first part of the methodology covers the function of soil-structure interaction in design of earthquakes and how is presented in TBDY 2018 and RPS 2011. The first chapter will explain the research challenge, goals, and contributions. In the second chapter, there will be a study of the literature that focuses on the basic ideas of SSI, how seismic waves move, and how the two nations regulate these aspects. The third section of the research will look at previous earthquakes in Turkey (as Kocaeli earthquake (1999) and Kahramanmaraş earthquake (2023)) and Morocco (like Al Hoceima earthquake (2004) and Al Haouz earthquake (2023)) to learn how SSI affected the damage and reaction patterns. Chapter 4 will go into further depth about a comparison of seismic standards, focusing on SSI elements including soil classification, foundation categories, seismic coefficients, structural significance factors, and importance factors. In Chapter 5, we will look at a case study that uses

PLAXIS 2D to model a 15-story structure with a raft foundation, we'll use geotechnical data from Turkey of an existing constructed project and seismic input parameters, then after simulation, the outputs like settlement, total strain, and stress distribution in both of horizontal (y) and vertical directions (x) we can be able to see how various codes change SSI behavior, for the Moroccan case, from a Moroccan project, soil parameters will be used under the same Turkish conditions of loads and foundation type, in order to compare the effect of change of each country’s soil parameters. The last chapter will go over the main points, talk about the pros and cons of both standards, and provide suggestions for how to make SSI integration better in future versions of national seismic design codes.

CHAPTER 2

2. LITERATURE REVIEW

2.1 DESCRIPTION OF SOIL-STRUCTURE INTERACTION (SSI)

2.1.1 Definition and Physical Mechanisms

Soil-Structure Interaction, or SSI, is the two-way link between a building and the soil it sits on, especially when there are active loads like earthquakes. Unlike the usual fixed-base design theory, which says that the foundation can't move, Soil-Structure Interaction takes into account how the soil can change form, which affects and is affected by the structure's reaction. This two-way interaction changes important factors like natural frequency, damping ratios, and displacement magnitude, all of which have significant effects on how well buildings and infrastructure withstand earthquakes.(Kramer ,1996). To put it simply, SSI is made up of three main parts: the building (the part above soil), the base system, and the supporting soil medium. A lot of things affect how this system works, such as the stiffness of the dirt, its damping properties, the type and depth of the base, and the structure's own dynamic properties. (Wolf, 1985). The system may be defined mechanically in terms of how compliance of the soil influences the dynamic reaction of the structure. Energy dissipation (as a result of radiation damping) and changes in natural vibration modes are the outcomes of a flexible foundation placed in a flexible soil. Soil and structural element seismic demand and stress distribution are affected by these changes. (Wolf, 1985; Gazetas, 1991; Kramer, 1996) A common mathematical representation of the SSI effect is the dynamic equilibrium of a system with the coupled soil-structure system's stiffness matrix [K], mass matrix [M], and damping matrix [C] integrated into the governing equation of motion: (Chopra, 2012)

$$M\_total \times \ddot{u}(t) + C\_total \times \hat{u}(t) + K\_total \times u(t) = F(t) \qquad (2.1)$$

Where:

M_total = overall mass matrix including added mass of soil C_total = damping matrix which incorporates material and radiation damping K_total = matrix that accounts for soil compliance and stiffness u(t) = displacement vectorF(t) = dynamic load vector (for instance, input of earthquake) The figure 2.1 illustrates the interaction mechanism showing the transfer of energy between the structure and the soil, which occurs through foundation compliance and ground motion amplification.

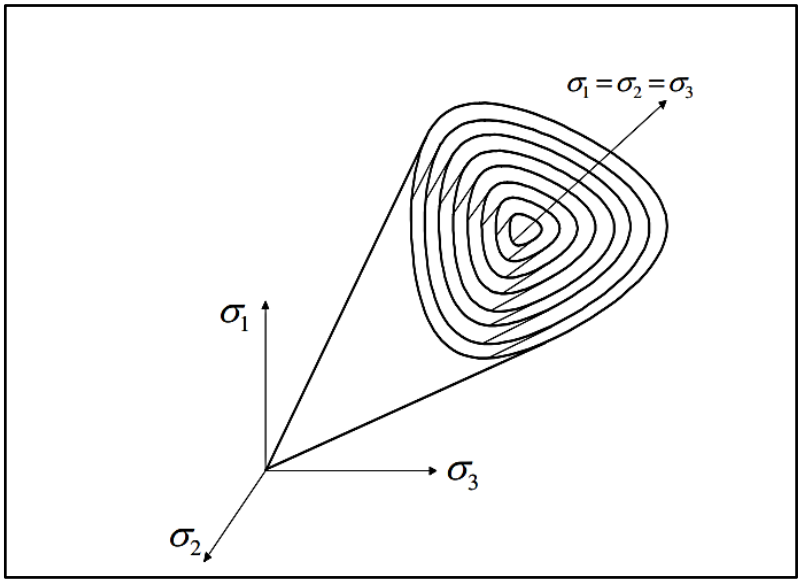

Figure 2.1 Multi Lade Duncan yield surfaces configuration in main stress space (Yang and Elgamal, 2004).

The principal impacts noted from SSI are-Extension of period length: resulting from less overall stiffness.

Base shear modification: generally a decrease, which may be advantageous or risky depending on the structural capability.

Enhanced lateral displacement: especially in compressible soft soils.

Rocking and foundation uplift: more common in shallow or inflexible foundations subjected to intense seismic activity.

SSI behavior is significantly site-specific. Structures constructed on rock or rigid soils exhibit little soil-structure interaction effects, whereas those situated on soft clays or loose sands may undergo significant amplification of seismic waves. The height and mass distribution of the structure influence the degree of interaction, with tall and slender structures displaying more significant SSI effects (Gazetas, 1991).

Consequently, identifying and measuring these processes is essential for precise earthquake analysis and design. Disregarding SSI may result in cautious or hazardous consequences, impacting the safety and cost-effectiveness of geotechnical and structural systems.

2.1.2 Historical Development of SSI Concepts

The development of Soil–Structure Interaction (SSI) as a distinct field of research has paralleled advancements in geotechnical and structural engineering, driven by significant worldwide seismic events. The notion developed attention in the mid-20th century, when failures during seismic events exposed significant limits of fixed-base design assumptions. (Clough & Penzien , 1975).

One of the earliest recorded examples of SSI recognition was during the 1940 California El Centro earthquake. Engineers noted that structures on soft soil sustained greater damage than those on rock, despite comparable architectural design. This resulted in first versions including adaptable foundations utilizing simpler springs and dashpots. (Veletsos & Newmark , 1960).

The earthquakes of 1964 Niigata (Japan) and 1971 San Fernando (California) were crucial in illustrating that soil can amplify soil motion and significantly affect foundation performance. The significant tilting and overturning of structures in Niigata, primarily caused by liquefaction, underscored the necessity of including soil flexibility and site reactivity into engineering models. (Tokimatsu & Seed, 1987).

In the 1970s and 1980s, researchers such Veletsos, Gazetas, and Wolf developed the idea of Soil-Structure Interaction (SSI) using dynamic system modeling. Analytical and computational methodologies, encompassing finite element (FE) and boundary element (BE) approaches, were devised in order of assessing the mutual interaction between the soil and the structure. (Wolf ,1985).

These approaches considered impedance functions, radiation damping, and complex wave propagation in soil media. The 1985 Mexico City earthquake underscored the significance of soil-structure interaction (SSI). Structures located on soft lakebed soils experienced significant amplification and resonance, resulting in failures despite conformity of seismic design standards. This incident caused extensive study into dynamic site response, soil damping, and nonlinear soil behavior in soil-structure interaction analysis. (Bard & Durand , 1986).

Since the 1990s, the development and rise of computational tools like PLAXIS, FLAC, and ABAQUS has transformed SSI research. Engineers can now accurately simulate nonlinear material behavior, interface slide, and foundation uplift. Codes like Eurocode 8, ASCE 7, and TBEC have started to incorporate these improvements by advising or mandating the incorporation of SSI in particular scenarios. (Gazetas, 1991).

In recent years, SSI has been examined not just for individual structures but also for essential infrastructure such as bridges, tunnels, and dams. Research has progressed into probabilistic Soil-Structure Interaction (SSI), integrating uncertainties in soil characteristics, seismic input, and structural performance.

Currently, SSI is acknowledged as a crucial component of seismic design. Nonetheless, its practical implementation differs among countries, and several national building standards codes such as RPS 2000 in Morocco do not comprehensively include contemporary SSI principles. (Wolf, 1985) (Kramer, 1996)

2.1.3 Aim of SSI in Seismic Design

The significance of soil–structure interaction (SSI) in seismic building design has grown according to its substantial and major influence on the structural framework response of buildings and infrastructure during seismic events. In conventional plan methodology, engineers have often minimized the issue by supposing that the foundation of the structure is inflexible and has no interaction with the underlying soil. This fixed-base assumption has consistently demonstrated inadequacy, particularly for buildings constructed on soft soils or those characterized by substantial bulk or narrow geometries. (Stewart & Fenves, 1998)**.**

The importance of SSI is especially apparent in seismic zones, where dynamic soil behavior and wave propagation significantly affect foundation reaction. Neglecting Soil-Structure Interaction in these situations may lead to erroneous assessments of essential structural attributes, such as natural period, damping, base shear, and lateral displacement. This may result in either overprotective or hazardous designs, contingent upon the soil conditions and structural characteristics. (Kramer , 1996).

Soil-construction Interaction (SSI) can modify the seismic demands placed on a construction. For instance, increasing the basic period of vibration via soil flexibility can change the structure's reaction to a segment of the response spectrum characterized by lower spectral accelerations. This often leads to a reduced base shear force, which can be advantageous in structural design. This advantage experiences the expense of amplified displacements and inter-story drifts, necessitating assessment to prevent non-structural damage and loss of function. (Mylonakis et al, 2006).

Figure 2.2 illustrates a comparative analysis of fixed and flexible-based bases behavior of the identical building, highlighting the alteration in natural period and the associated decrease in seismic acceleration requirement.

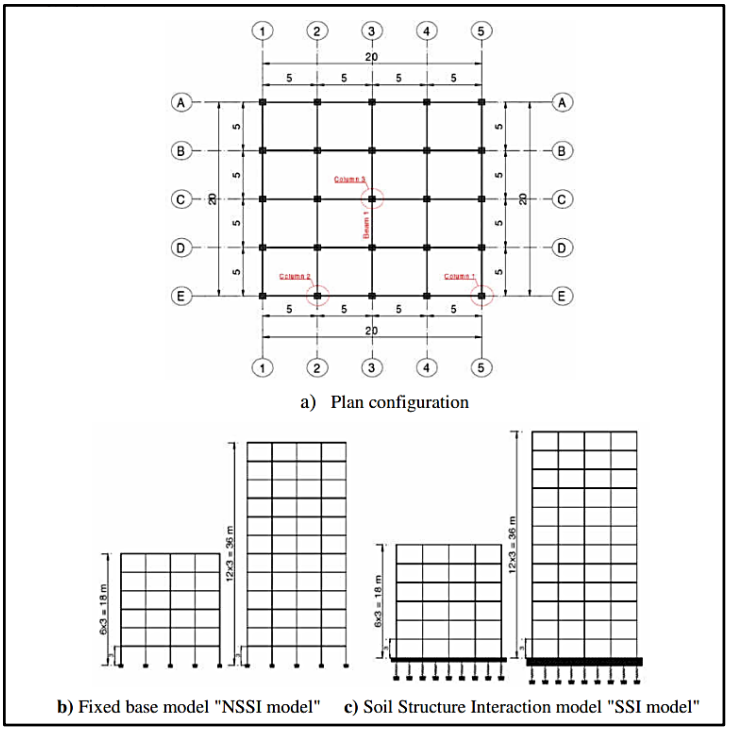

Figure 2.2 Schematic Of 6-Story and 12-Story Buildings' Models (Madabhushi & Haigh, 2014)

Moreover, SSI may cause rocking, elevation, and differential settlement, especially in shallow foundations during intense soil motion. This is particularly vital in crucial infrastructures such as hospitals, power plants, or bridges, where operational integrity must be maintained following an earthquake.

Contemporary design philosophies like Performance-Based Earthquake Engineering (PBEE) and Displacement-Based Design (DBD) propose for the explicit incorporation of Soil-Structure Interaction (SSI) in the analytical process. SSI impacts the comprehensive deformation requirements, causes of failure, and methods of energy dissipation in structural systems. International codes, like Eurocode 8, ASCE 7, and TBEC 2018, increasingly include sections that either promote or require SSI analysis under specific scenarios. Eurocode 8 - Part 5 (EN 1998-5).

Conversely, seismic codes that do not adequately incorporate SSI considerations, such as Morocco's RPS 2000/2011 are susceptible to design inaccuracies, particularly for structures situated on soft soil. These codes often depend on basic soil categorization and empirical coefficients, constraining their capacity to accurately represent real and actual dynamic interactions.

2.1.4 Classification of SSI Effects: Kinematic vs. Inertial Interaction

Soil-Structure Interaction (SSI) involves two principal effects resulting from the dynamic interplay between the soil and the superstructure: kinematic interaction and inertial interaction. Comprehending the difference between these two mechanisms is crucial for precision of seismic analysis and the formulation of resilient structure models. Kinematic interaction transpires when seismic waves propagate via the soil and are modified by the existence of a foundation. As seismic waves rise, they are modified by the soil layers and subsequently influenced by the variation in stiffness between the soil and the foundation. This leads to modified soil motion at the structure's base, usually marked by diminished high-frequency components and amplified motion amplitude at the surface**.** (Mylonakis & Gazetas , 2000)

Kinematic interaction in shallow foundations, particularly on rigid soils, can lead to considerable variations in base motion compared to free-field ground motion. The impact is also affected by the foundation's embedment depth and the geometric configuration of the base.(Stewart & Fenves , 1998).

Inertial interaction is related to the soil's response to the dynamic forces conveyed by the vibrating structure. When a structure reacts to seismic activity, its inertia generates forces that act onto the foundation, resulting in the deformation of the underlying soil. The reciprocal interaction of forces modifies the overall system dynamics and can affect the natural frequency, damping ratio, and base shear of the structure. (Veletsos & Meek , 1974).

The substructure technique, referred to as a 'multi-step approach,' addresses an SSI problem by integrating solutions from the previously

mentioned kinematic and inertial interaction phenomena, shown in the figure 2.3:

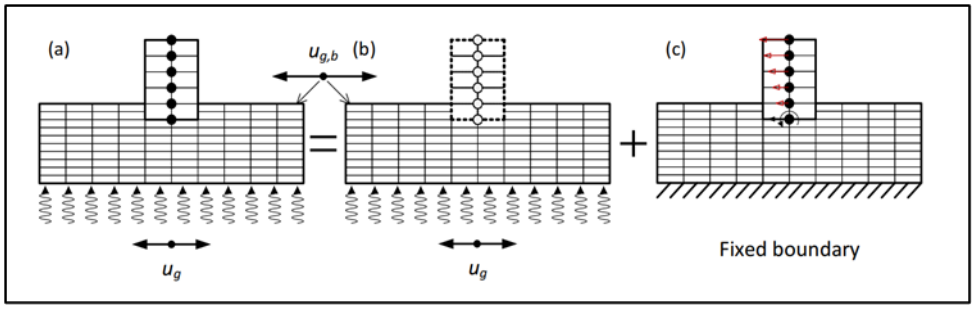

Figure 2.3 The evaluation of (a) an SSI issue may be devided into (b) a kinematic interaction analysis and (c) an inertial interaction analysis.(Zhang et al. Zhang & Tang , 2014)

In modeling practice, these two impacts are treated distinctly: Kinematic interaction is frequently integrated through changing input ground motion using transfer functions or de-convolution methods. Inertial interaction is implemented by connecting structural mass and foundation stiffness in dynamic response simulations, commonly employing finite element or substructure techniques. Kinematic contact modifies the boundary conditions of the entering seismic wave, whereas inertial interaction adds further damping and stiffness to the system.
The interactions are affected by several aspects, including:

- Soil stiffness and stratification
- Foundation geometry and depth of embedment
- Height, mass, and flexibility of the structure
- Type and frequency characteristics of the seismic motion

Neglecting to include these elements in seismic design may lead to an underestimation of displacements or an overestimation of structural stresses. Contemporary seismic design standards such as Eurocode 8 and TBEC 2018 advocate for the incorporation of both impacts for essential structures and soft-

soil locations, however RPS 2000 in Morocco doesn't properly classify or address the two components.

2.2 THEORETICAL FOUNDATIONS OF SSI MODELING

2.2.1 Spring-Dashpot and Subgrade Models

The spring-dashpot system is one of the earliest and most prevalent methods of modeling Soil–Structure Interaction (SSI), as it reduces complicated soil dynamics into a comprehensible mechanical estimation. The spring element signifies soil stiffness, whereas the dashpot denotes energy dissipation via damping. These models are fundamental in SSI theory and continue to be applied today, especially in initial design or simplified studies.(Wolf, 1985; Kramer, 1996; Veletsos & Meek, 1974)

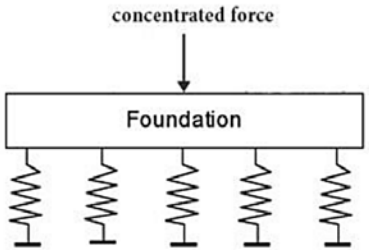

Figure 2.4 Winkler Model (Subgrade Reaction Model) (Selvadurai, A. P. S., 1979)

The Winkler model as shown in figure 2.4 is the fundamental subgrade model in which the soil is shown as a collection of independent, elastic linearly springs. The foundation is considered such a beam supported by these springs. The relationship between pressure and displacement in this model is defined as:

$$p(x) = ks \times y(x) \quad (2.2)$$

Where:

p(x): contact pressure at point x

ks: modulus of subgrade reaction (N/m³)

y(x): vertical displacement at point x

The Winkler model, although easy to understand and computationally efficient, assumes a lack of interaction between nearby soil components, consequently it is misrepresenting actual soil behavior under significant deformations or dynamic loads. (Winkler , 1867)

2.2.1.1 Elastic Continuum Models

Elastic continuum models illustrated in figure 2.5 generally conceptualize the subgrade as a layer situated above a rigid foundation, characterized by three parameters: the elastic modulus, Poisson's ratio, and layer thickness (Horvath, 2002) All continuum models impose specific assumptions to facilitate the mathematical computations required. The comprehensiveness of a certain model is dependent upon the nature of its simplifying presumptions. Reissner's model disregards in-plane stresses (Reissner 1958). Vlasov and Leont'ev proposed a model that neglects horizontal deformations and assumes a predetermined function for vertical deformation (Vlasov and Leont'ev 1966). Kerr and Rhines, besides ignoring the in-plane stresses, also excluded the horizontal deformations to develop a model comparable to that of Vlasov and Leont'ev (Kerr and Rhines 1967). Horvath excluded all stress components, except for the vertical one, to formulate a Winkler-type model (Horvath , 1983).

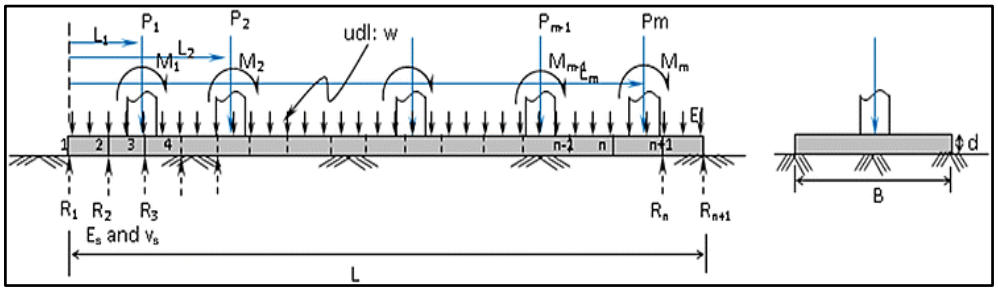

Figure 2.5 Definition sketch of elastic continuum model (Gulhane & Bajad , 2018)

In order to address the shortcomings and constrains of the Winkler model, more sophisticated models grounded in elastic half-space theory were created. These models regard the soil as a continuous, elastic material and consider shear interactions among adjacent soil components. Popular formulations involve the following:

Boussinesq's solution (concerning point loads on elastic half-space).

Mindlin's solution (concerning buried loads).

These continuum models yield superior anticipates for settlements and stresses, particularly for wide or irregular foundations. (Poulos & Davis ,1974)

2.2.1.2 Lumped Parameter Models (Spring-Dashpot System)

Lumped parameter models are employed for illustrating foundation impedance in dynamic SSI analysis.The following models have been included:

Translational spring: K_t (horizontal and vertical).

Rotational spring: K_r (rocking resistance).

Dashpot: C (damping in each mode)

These characteristics are often computed using empirical methods or obtained from field or laboratory investigations. Gazetas (1991) presented closed-form formulas for surface and embedded foundation's stiffness and demping, taking into account soil type, foundation geometry, and embedment depth. (Gazetas ,1991)

2.2.1.3 Motion Equation For Soil-Structure Interaction

A simplified dynamic model that includes SSI can be defined as

$$(M \times \ddot{u}) + (C \times \dot{u}) + (K \times u) = -M \times \ddot{u}_g \quad (2.3)$$

Where: M, C and K= mass, damping, and stiffness matrices of the soil-structure system.

ü= relative acceleration of structure.

üg = ground acceleration.

In this layout, the foundation is regarded as a changeable factor, with dynamic stresses from the ground being reduced by the spring-dashpot

components, which contain both soil compliance and damping in the table 2.1 the advantages and limitations of common SSI models were presented. .

Table 2.1 Advantages and Limitations of Common Soil-Structure Interaction Models (Gerolymos & Gazetas, 2006)

Model Type	Advantages	Limitations
Winkler Model	Simple, easy to implement	Ignores shear interaction in soil
Elastic Continuum	More realistic for wide foundations	Requires complex calculations
Spring-Dashpot	Useful in dynamic analysis	Needs calibration with site data

Although their simplifications, spring-dashpot models continue to be significant for seismic analysis, especially in software applications like as SAP2000, ETABS, and PLAXIS (within simplified substructure methodologies). They provide an equilibrium between computing efficiency and physical realism when well calibrated.

2.2.2 Wave Propagation in Soil Media

Wave propagation in soil is mandatory for comprehending soil-structure interaction (SSI), especially under seismic stress. During an earthquake, seismic waves go through the earth and engage with structure foundations. The properties of these waves, such as velocity, amplitude, and frequency content, are profoundly affected by the soil type and its stratification. Three primary categories of seismic waves important to SSI analysis that are:

Primary (P) waves: Compressional waves that are the swiftest and propagate through both solids and liquids.

Secondary (S) waves: Shear waves that propagate perpendicularly to their direction of motion; they cause higher damage on structures.

Surface waves (Rayleigh and Love waves): Propagate along the Earth's surface and often induce the most substantial ground motion closer to the surface (Kramer , 1996)

The velocity of these waves is dependent upon soil rigidity and density. The shear wave velocity (Vs) is crucial and frequently employed in seismic site categorization (e.g., Vs30 in Eurocode 8 and TBEC). The correlation between wave velocity and dynamic soil stiffness is as follows:

$$G = \rho \times Vs^2 \quad (2.4)$$

Where: G = shear modulus

(Pa) ρ = soil density (kg/m³)

Vs = shear wave velocity (m/s)

2.2.2.1 Wave Reflection and Refraction

Seismic waves reflect and refract while encountering various soil layers. These activities induce changes in wave amplitude and frequency content, frequently resulting in resonance effects when the soil's primary frequency aligns with the structure's natural frequency. (Idriss & Boulanger , 2008).

The concepts of reflection and refraction are dictated by Snell's Law.

$$(\sin\theta^1 / V^1) = (\sin\theta^2 / V^2) \quad (2.5)$$

Where: θ_1, θ_2 = angles of refraction and incidence

V_1, V_2 = wave velocities in each medium.

These transitions affect the amount of seismic energy transmitted to the foundation and must be carefully evaluated in SSI modeling.

2.2.2.2 Site Amplification

Site amplification indicates the enhancement of seismic motion intensity resulting from soft soil layers. This is especially important in areas with substantial accumulations of soft clay or alluvium. Soft soils often increase low-frequency seismic vibrations, resulting in the resonance with tall and flexible structures. (Bard , 1999). To illustrate, seismic wave amplification through layered soil profiles were shown in figure 2.6.

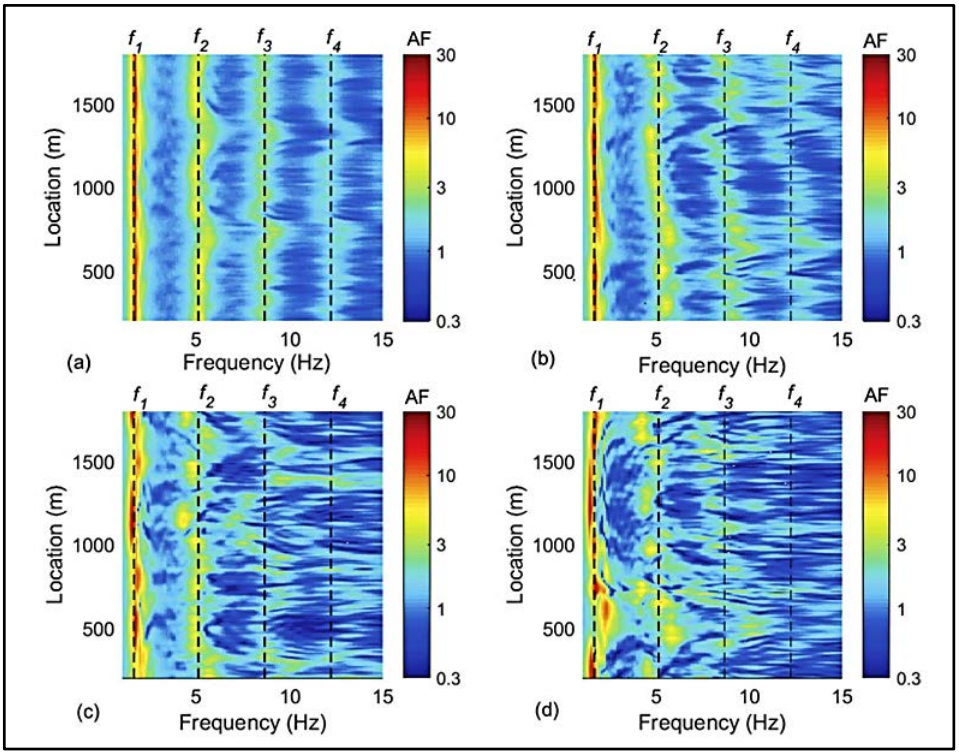

Figure 2.6 Seismic wave amplification through layered soil profiles (Source: Huang et al. Huang et al , 2018)

2.2.2.3 Implications for SSI Modeling

Accurate modeling of wave propagation is essential in both direct and substructure methodologies for SSI.

-In the *direct approach*, wave propagation is modelled using absorbing limitations and realistic soil stratification.

In the *substructure technique*, the ground motion input at the base is modified via transfer functions based on wave propagation theory.

Advanced numerical models, such as **PLAXIS** and **OpenSees**, integrate these concepts through allowing users to specify soil classification, damping characteristics, and dynamic material features.

2.2.3 Radiation and Material Damping Mechanisms

Damping is essential for the dynamic response of soil-structure systems since it dissipates vibrational energy. Whiting the framework of soil-structure interaction (SSI), two primary types of damping are considered: material damping (also known as hysteretic damping) and radiation damping (often referred as geometric damping). (Wolf, 1985; Kramer, 1996; Gazetas, 1991)

2.2.3.1 Material Damping (Hysteretic Damping)

When soil experiences inelastic deformations, it loses energy internally, a process known as material damping. In soils subjected to dynamic or cyclic loading, this kind of damping is linked to the stress-strain hysteresis. To put it into practical terms, it is symbolized by a damping ratio (€) that measures the quantity of energy lost for each vibration cycle. (Idriss & Sun , 1992)

The following are examples of common soil damping ratios

Dense sand : **1–2%**

Soft clay : **5–10%**

Stiff clay : **2–5%**

Due to its frequency dependence, material damping is often represented by either sophisticated nonlinear hysteresis models or similar linear approaches. Users of PLAXIS and similar finite element programs have the option of using constitutive models, such the hardening soil type with small-strain strength, or user-defined damping ratios to incorporate material damping. (Brinkgreve et al, 2019).

2.2.3.2 Radiation Damping (Geometric Damping)

Radiation damping occurs due to the propagation of seismic waves from the foundation into the infinite soil media. When a structure vibrates, part of the energy passes into the adjacent soil, where it dissipates outward and is successfully dissipated from the system. This form of damping is dependent upon:

Soil rigidity and compaction

Foundation geometry and depth

Wave transmission velocity

Radiation damping is often represented in analytical or semi-analytical models by using impedance functions or frequency-dependent dashpots. The fundamental formulations for impedance and damping were established by Lysmer and Richart (1966) and subsequently enhanced by Gazetas (1991). The horizontal damping coefficient (Ch) for a circular surface foundation can be estimated as: $Ch = \rho \times Vs \times (8/3) \times R$ (2.6)

Where:

ρ = soil density (kg/m³)

R = foundation radius (m)

Vs = shear wave velocity (m/s)

This expression assumes a half-space model and linear elastic soil behavior. For embedded or irregular foundations, numerical models are preferred.

2.2.3.3 Combined Damping in SSI Models

In SSI analysis, total damping is often considered as a combination of material and radiation damping. However, care must be taken to avoid double-counting. For example:

In time-domain finite element models: Rayleigh damping coefficients are adjusted to match the expected frequency content.

In frequency-domain substructure models: Both hysteretic damping and impedance-based radiation damping are explicitly defined. Amplitude and phase of the dynamic compliance in 3 types of plates were illustrated as charts in figure 2.7.

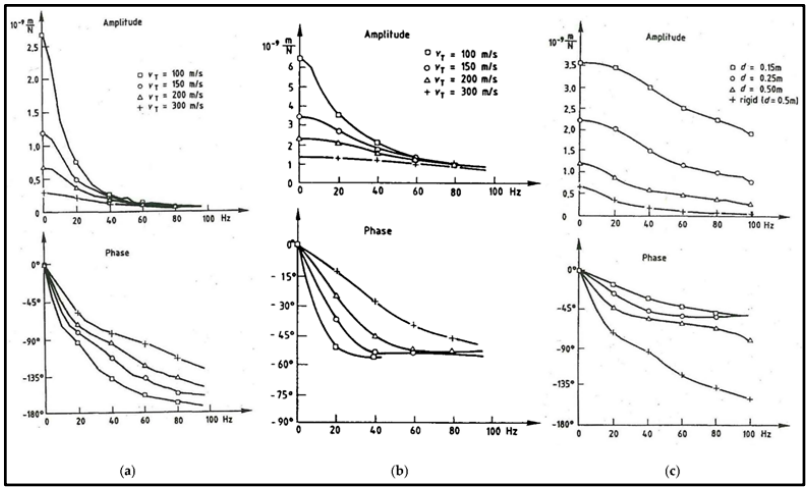

Figure 2.7 Amplitude and phase of the dynamic compliance (a) rigid plate, (b) concrete plate, and (c) plates of different heights (Auersch, 2025)

In order to provide precise predictions of seismic reaction, damping must be accurately modelled. It is possible to overestimate dynamic demand and underestimate displacements and accelerations by overestimating damping, and vice versa.

2.2.4 Limitations of Fixed-Base Assumptions

The fixed-base assumption is a common one in traditional structural design; it states that the building's base should be totally solid and unmovable with respect to the earth underneath. This oversimplification makes structural analysis simpler, but it doesn't do justice to the reality of (SSI), that is particularly Investigating the effects of soil characteristics and flexibility on seismic energy transmission reveals the weaknesses of the fixed-base assumption. The fixed-base model errors lateral displacements and inter-story drifts since it does not account for the soil's deformability.

Causes conservative designs by exaggerating natural frequencies

Overestimates damping behavior while neglecting the effects of radiation and instability

In shallow or soft-soil situations, foundation shaking, sliding, and uplift are ignored. (Kramer , 1996)

2.2.4.1 Impact on Seismic Response

The fixed-base assumption yields higher calculated accelerations according to reduced structural periods. In actuality, the soil's flexibility prolongs the vibration duration, modifying the response to a segment of the design spectrum that may exhibit lowered spectral acceleration values. This could reduce the design base shear but leads to increased displacement demand, which a fixed-base model may not account for (Mylonakis & Gazetas, 2000). The chart in figure 2.8 is an illustration of response spectrum curve of the acceleration (g) within period of the earthquake.

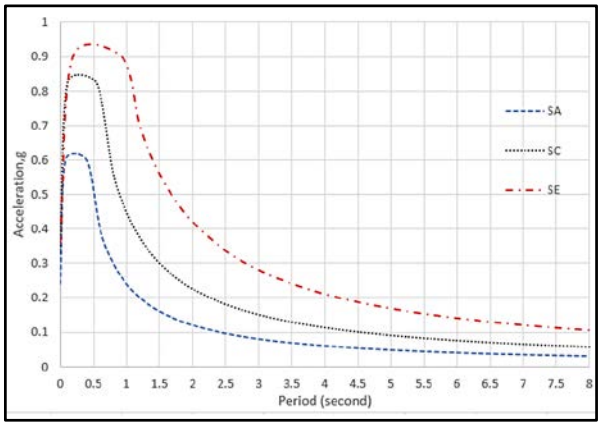

Figure 2.8 Response spectrum curve (Nouri-Borujerdi & Rahgozar , 2018)

2.2.4.2 Inadequacy for Soft Soil and Tall Structures

The uncertainty resulting from fixed-base assumptions becomes significant for:

Tall structures: The additional bulk and slenderness make them more susceptible to soil flexibility.

Structures on soft soils: Regions where seismic waves are enhanced and longer-period phenomena occur.

Critical infrastructure: Hospitals, power plants, and bridges, where precise performance prediction is needed (ASCE 7-22, 2022)

Neglecting SSI in these instances may lead to hazardous designs, unforeseen damage, or serviceability problems post-seismic event.

2.2.4.3 Code Evolution and Recommendations:

Current seismic codes are progressively deviating from the fixed-base assumption, especially in the context of performance-based design. Standards such as Eurocode 8, ASCE 7, and TBDY 2018 provide guidelines for incorporating Soil-Structure Interaction

(SSI) in certain contexts, including:

- Plastic or saturable soils
- Structures of significant significance or unusual configuration
- Locations exhibiting significant ground motion amplification Despite these developments, several regional codes such as RPS 2000 (Morocco) still exhibit inadequate SSI integration, often depending on empirical coefficients that may not accurately represent genuine dynamic behavior.

The fixed-base assumption, while it simplifies seismic analysis, leads to considerable errors for several site-structure combinations. Advanced SSI modeling provides a more precise and realistic evaluation of structural performance under seismic loads and is crucial for contemporary, solid construction methodologies.

2.3 INTERNATIONAL APPROACHES TO SSI IN SEISMIC CODES

2.3.1 Eurocode 8 Provisions

Comprehensive recommendations for the seismic design of structures throughout Europe are provided by Eurocode 8 (EN 1998), with Part 5 (EN 1998-5) focusing on foundations, retaining walls, and the geotechnical

components of earthquake-resistant construction. The code offers both straightforward and sophisticated ways to include soil-structure interaction (SSI) into design, and it expressly recognizes the significance of SSI in altering structural response.(CEN, 2004).

2.3.1.1 Site Classification and soil Types

Shear wave velocity (Vs30), standard penetration resistance (SPT), and undrained shear strength are the variables used by Eurocode 8 to identify soil types (A to E). Soil type coefficients are applied to modify the spectrum of design reaction, which is influenced by these classifications. For soil categories D and E, which reflect soft soils with significant amplification effects, SSI consideration is especially emphasized. (Pitilakis et al., 2004).

2.3.1.2 Conditions Requiring SSI Consideration

Eurocode 8 specifies that SSI analysis is required in accordance:

- The basic structure's surpasses 0.6 s.
- The construction is situated on soft or liquefiable soils.
- The building is classified as important class III or IV (e.g., educational institutions, medical facilities, emergency response centers).
- The structure has profound or atypical foundation systems (e.g., piles, caissons).

In many instances, the fixed-base assumption is inadmissible, necessitating the use of either a substructure or direct technique to address SSI effects. (Clough & Penzien, 1993).

2.3.1.3 Substructure Method

This method separates the soil and structural domains. It encompasses conducting a site reaction study to identify ground motion at the foundation level.

Simulating foundation springs and dashpots by impedance functions (e.g., Gazetas formulations).

Implementing resultant loads onto the structural model.

2.3.1.4 Direct Method

This advanced method involves modeling the whole soil-structure system concurrently, usually by finite element analysis (FEA). This technique may involve:

- Layered soil profiles showing nonlinear behavior.
- Interface components connecting soil and structure.
- Motion input is applied at the bedrock level

Eurocode 8 enables this procedure where enhanced precision is required and determined resources are sufficient. This is particularly important for irregular geometries and performance-oriented designs (Fardis, 2009).

2.3.1.5 Spectral Shape Adjustment

The response spectra defined by Eurocode 8 can be modified by using the soil factor **(S)** and the damping correction factor **(η)**. These modifications instinctively include SSI impacts through changing the seismic load on the structure:

S = soil type-dependent amplification factor $\eta = 10 / (5 + \xi)$ (2.7)

Here, ξ denotes the damping ratio, typically set at 5% for fixed-base buildings, and elevated when soil-structure interaction (SSI) is considerable.

2.3.1.6 SSI-Related Design Recommendations

- Foundations should be designed with regard to seismic bearing capacity, uplift, and sliding.
- SSI analysis should confirm that foundation displacements correspond to serviceability restrictions.

- The potential for liquefaction and subsequent settlement after an earthquake must be evaluated when relevant.

Eurocode 8 highlights the need of transparency in (SSI) assumptions and argues for the documenting of :

- Employed damping models
- Soil study methodologies.
- Boundary conditions in computational models (CEN, 2004; Pitilakis et al, 2004)

Eurocode 8 provides a comprehensive and systematic framework for SSI, integrating analytical precision with pragmatic guidelines. It recognizes the need of SSI in soft soils and for essential structures, recommending for both empirical simplifications and sophisticated numerical analyses based on project requirements and seismic risk assessments.

2.3.2 ASCE 7 and FEMA Guidelines

The American standards, specifically ASCE 7-22 (Minimum Design Loads and Associated Criteria for Buildings and Other Structures) and guidelines from FEMA (Federal Emergency Management Agency), are crucial in defining the approach to soil-structure interaction (SSI) in earthquake design throughout the United States. These reports offer prescriptive and performance-based methodologies that require and stimulate SSI integration based on structural and geotechnical conditions. (ASCE , 2022).

2.3.2.1 ASCE 7-22 Provisions for SSI

ASCE 7-22 outlines specific requirements for the consideration of SSI. The structural period is 0.5 seconds at least.

The building is constructed on soft soil (Site Class E or F).

- The structure is categorized under risk category III or IV, including important facilities.

- The structure has base isolation systems or deep foundations as per ASCE (2022).

The standard permits two analytical methodologies:

- Fixed-base analysis is authorized for standard constructions situated on stiff soils. ASCE 7 enables the use obstructure techniques in which soil and foundation stiffness are represented by springs and dashpots. It additionally supports investigation in the time domain or frequency domain with site-specific ground motion data.

2.3.2.2 Modeling Foundations in ASCE 7

ASCE 7 includes instructions for simulating foundation flexibility via the use of:

- Translational and rotational springs.
- Differentiating between structural damping.
- Soil radiation damping.
- Damping.

Embedment effects that may enhance foundation stiffness and damping. Impedance functions are suggested for modeling foundation behavior. These functions, determined by soil characteristics and foundation design, establish dynamic stiffness and damping in vertical, horizontal, and rocking modes.

2.3.2.3 FEMA Guidelines and SSI

FEMA Guidelines and SSI FEMA publications, including FEMA P-1050 (NEHRP Recommended Seismic Provisions) and FEMA P-440A, provide supplementary technical guidelines for incorporating SSI in both new constructions and retrofitted projects. FEMA highlights the use of nonlinear site response analysis, probabilistic earthquake risk analysis (PSHA) in addition to performance-based design.

2.3.2.4 According to FEMA P-440A

- SSI may have advantageous outcomes, including the decrease of seismic forces (base shear).
- Nonetheless, it may exacerbate displacements and ductility requirements, particularly in flexible structures.
- The impacts of SSI are more significant in tall, flexible, or isolated structures situated on deep or loose soil profiles (FEMA, 2009).
- FEMA articles recommend the use of software tools like as OpenSees, SAP2000, and deep soil for precise SSI modeling, highlighting the need of time-history and modal analysis.

2.3.2.5 Damping Modifications in ASCE

ASCE 7 changes the spectral response using the damping adjustment factor (β), which considers the enhanced system damping resulting from soil-structure interaction (SSI). This reduces the design response spectrum for systems showing high damping ratios ($\xi > 5\%$). The factor is based on empirical correlations and site characteristics.

2.3.2.6 SSI in U.S. building Codes (IBC)

The International Building Code (IBC), by referencing ASCE 7, automatically integrates SSI rules for essential and atypical structures. Standard design does not necessitate SSI, but allows engineers to include it in performance-based designs or where local circumstances permit.

2.3.3 Comparison of Global Standards: Similarities and Differences

A review of the seismic codes from across the world, including Eurocode 8 (Europe), ASCE 7/FEMA (United States), TBEC 2018 (Turkey), and RPS 2000/2011 (Morocco), shows that there are both similarities and differences in how Soil–Structure Interaction (SSI) is used in seismic design. These variances

show different ideas about seismic risks, how the soil might change, and how do engineers in practices concerning this domain.

The majority of contemporary seismic codes have four essential SSI-related characteristics in common, notwithstanding regional variations:

- Recognition of the impact of SSI on structural performance and dynamic responsiveness.
- To evaluate amplification effects, site categorization techniques (such as Vs30, SPT, or Su-based) are used.
- The necessity or suggestion that SSI be added to: o Soft or liquefiable soils.
- Significant or unbalanced structures.
- Long-term behavior cases (Pitilakis et al, 2015)

From basic spectrum modifications (such as soil factors and damping adjustments) to sophisticated modeling strategies employing time-history or frequency-domain research, each standard provides a variety of methods and techniques. The table 2.2 shows the differences of those codes.

Table 2.2 Distinctive Differences of Eurocode8, ASCE7, TBDY2018 and RPS2011

Feature	Eurocode8	ASCE 7 / FEMA	TBDY 2018 (Turkey)	RPS 2000/2011 (Morocco)
Site classification	Vs30, Su, NSPT	Vs30-based (Site Class A–F)	Vs30 + soil type (ZC–ZE)	Broad SPT categories
SSI requirement	Mandatory for soft soil and T > 0.6s	Required for soft soil, T > 0.5s	Based on Earthquake Design Class	No explicitly is required

Table 2.2 Distinctive Differences of Eurocode8, ASCE7, TBDY2018 and RPS2011

Feature	Eurocode8	ASCE 7 / FEMA	TBDY 2018 (Turkey)	RPS 2000/2011 (Morocco)
Analysis methods	Substructure & Direct	Substructure & Direct	Both methods supported	Not defined
Foundation modeling	Impedance functions, springs/dashpots	Impedance functions + embedment	Raft, pile, or shallow with flexibility	Basic empirical rules
Liquefaction/ settlement	Included	Emphasized via FEMA	Considered in site class	Rarely addressed
Dynamic damping adjustment	η factor	β factor	ξ-based design spectra	Absent

2.3.3.1 Observations on Eurocode 8 vs. ASCE 7

- The two codes enable thorough SSI simulations and support performance-based engineering.
- Eurocode 8 tends to be more conservative in foundation design and is more often used
- in multinational projects.
- Whereas Eurocode use fixed forms, ASCE 7 offers flexibility and adjustment variables to match seismic demand to actual damping levels.

2.3.3.2 Gaps in TBDY 2018 and RPS 2011

- The comparatively advanced TBDY 2018 incorporates site-specific spectral response analysis and SSI considerations based on Earthquake Design Class.

- In contrast, RPS 2000/2011 does not explicitly address SSI beyond empirical seismic coefficients and fundamental soil classifications. SSI modeling is neither standardized nor supported.
- Using a categorization based on Vs30

2.3.3.3 Implications for Comparative Research

Some regional codes lack standardized SSI applications, which makes it difficult to compare foundation performance and seismic resistance. This emphasizes how crucial code-to-code parameter mapping and standardized simulation tools (like PLAXIS and OpenSees) are for facilitating cross-border engineering examination. (Mylonakis & Nikolaou. 2010).

2.4 NUMERICAL MODELING TECHNIQUES IN SSI RESEARCH

2.4.1 Finite Element vs. Boundary Element Methods

Two of the most often utilized numerical techniques for simulating soil-structure interaction (SSI) are the finite element method (FEM) and the boundary element method (BEM).

Both strategies have advantages and disadvantages, and how well they work will rely on the problem's complexity, the degree of information that is required, and the available computing resources.

2.4.1.1 Finite Element Method (FEM)

FEM is a domain-specific numerical method that subdivides the whole problem area into a mesh of finite elements. It is exceptionally adept in managing heterogeneous soil conditions.

- Nonlinear behavior of soil and structures.
- In SSI modeling, FEM facilitates the simulation of:
- Structural components including footings, piles, and retaining walls.
- Stratified soil profiles with differing stiffness.

- Interfaces between soil and foundation via contact elements or interface elements.

Finite Element Method (FEM) is often used in software such as PLAXIS, ABAQUS, and ANSYS. It resolves the governing equations of motion below:

$$[M]\ddot{u} + [C]\dot{u} + [K]u = F(t) \quad (2.8)$$

Where: [M], [C], [K]: Mass, damping, and stiffness matrices

ü, û, u: Acceleration, velocity, and displacement vectors

F(t): External force vector (e.g., seismic loading)

Advantages:

- Exceptional precision for intricate geometries
- Capability to simulate nonlinear, time-varying behavior
- Comprehensive study of the stress-strain response

Constraints:

- Significant computational expense
- Necessitates comprehensive input data

The specification of boundary conditions is essential to prevent spurious reflections in dynamic analysis.

2.4.1.2 Boundary Element Method (BEM)

BEM is a boundary-focused method that reduces the issue's dimensionality (for example, modeling a 3D problem on a 2D surface). It works very well for issues involving:

- Infinite or semi-infinite domains (perfect for soil).
- Consistent soil characteristics
- Assumptions of linear behavior

BEM is especially well-suited for dynamic SSI issues like wave propagation and vibration analysis of embedded foundations because it can effectively describe radiation damping and far-field effects. (Dominguez, 1993). The comparison between (FEM) and (BEM) in accordance to their main features is shown below in table 2.3.

Table 2.3 General comparison between (FEM) and (BEM) in accordance to their main features.

Feature	Finite Element Method (FEM)	Boundary Element Method (BEM)
Modeling Domain	Entire Volume	Only Boundaries
Handling of Heterogeneity	Excellent	Limited
Radiation Damping	Requires Special Boundaries	Built-In
Nonlinear Behavior	Well-Suited	Less Suitable
Computational Demand	High	Moderate

4.2.1.3 Hybrid Approaches

Coupled FEM-BEM models are sometimes used in practice to combine the advantages of both approaches. For example, in order to effectively capture radiation effects, the far field is modelled using BEM, whereas the near field (foundation and immediate soil) is represented using FEM. In seismic SSI research, where accuracy and computational effectiveness are crucial, this method is advantageous and well useful. (Zienkiewicz & Taylor , 2005)

2.5 COMMONLY USED SOFTWARE (PLAXIS, OPENSEES, ETC.)

In the last twenty years, several software tools have been developed to help in the modeling and analysis of Soil–Structure Interaction (SSI). The selection of these programs, which vary from general-purpose finite element

platforms to experts geotechnical software, is dependent upon the problem's complexity, the needed precision, and the availability of input data.

2.5.1 PLAXIS

(PLAXIS 2D-Version 8 Tutorial Manual, 2004) PLAXIS Version 8 is a finite element software designed for two-dimensional study of deformation and stability in geotechnical engineering. Geotechnical applications need precise constitutive models to simulate the non-linear, time-dependent, and anisotropic behavior of soils and/or rock. Furthermore, according to the multi-phase nature of soil, specialized processes are necessary to address hydrostatic and non-hydrostatic pore pressures inside of the soil. While modeling the soil is significant, several tunnel projects need the model of structures and their interaction with the soil. PLAXIS has functionalities to address multiple components of complicated geotechnical structures. A brief description of key aspects of the software is provided below.

2.5.1.1 Graphical Input of Geometry Models

The integration of soil layers, structures, designing phases, loads, and boundary conditions is facilitated by efficient CAD drawing techniques, enabling precise modeling of the geometric cross-section. A 2D finite element mesh may be readily created from this geometric model.

The main interface modeling screen in software is illustrated in figure 2.9.

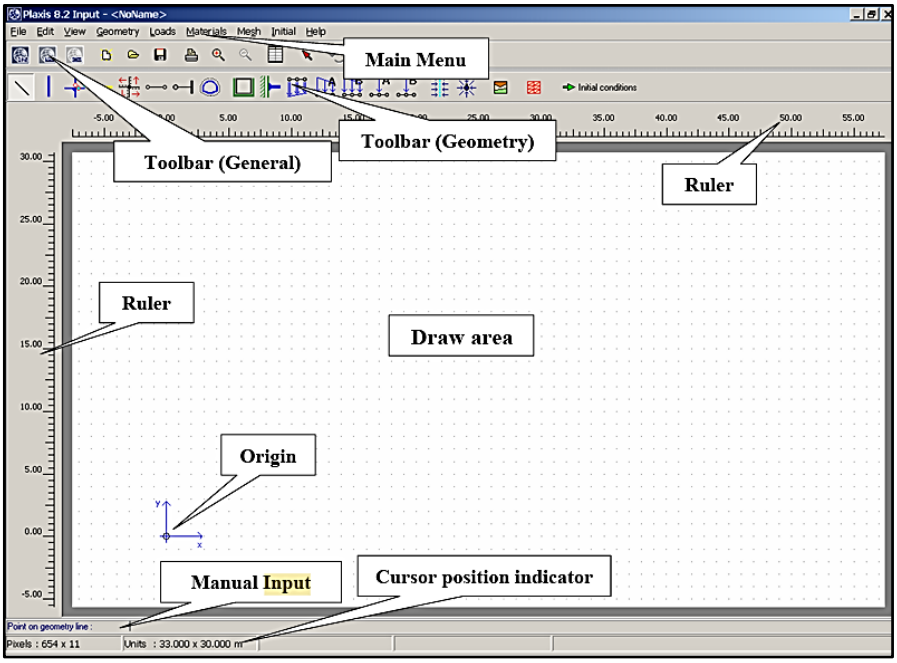

Figure 2.9 Primary Interface of the Input Program (PLAXIS, 2004)

2.5.1.2 Tool Bar

This toolbar shown in figure 2.10has options for operations related to the design and creation of the geometric model. The options are placed so that, generally, progressing from left to right on the toolbar results in a completed geometric model.

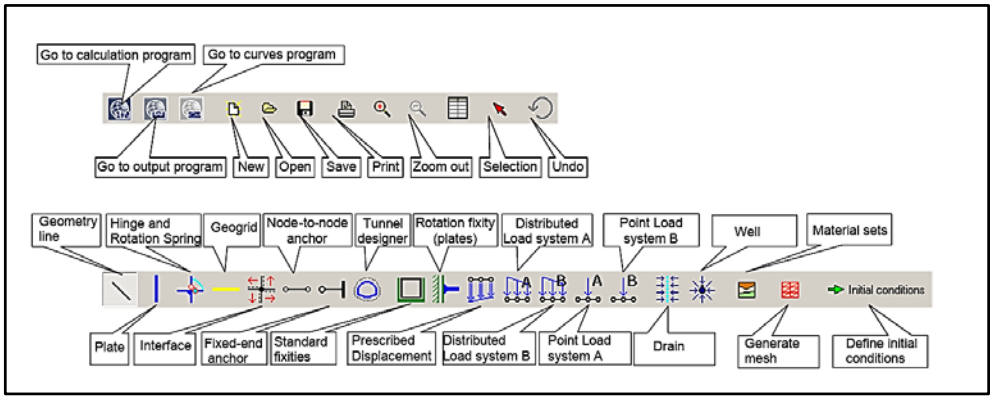

Figure 2.10 PLAXIS Toolbars (PLAXIS, 2004)

2.5.1.3 Automated Mesh Generation

PLAXIS allows the computerized creation of unstructured 2D finite element meshes, like in figure 2.11 and figure 2.12, with options for both global and local mesh refinement. The 2D mesh generator is a specialized variant of the Triangle generator, created by Sepra. Higher-order elements: Quadratic 6-node and fourth-order 15-node triangular components are offered for modeling soil deformations and stresses.

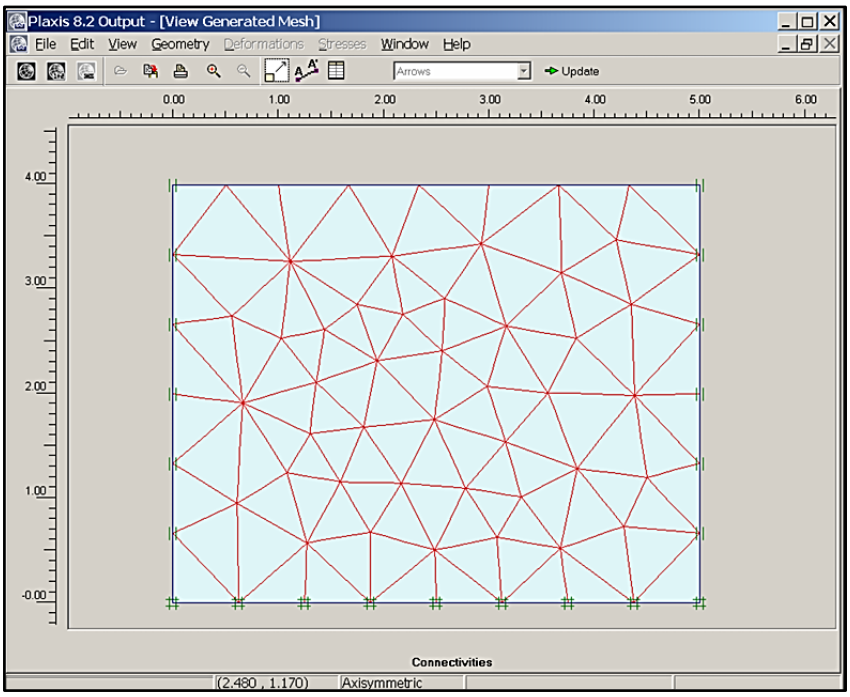

Figure 2.11 Axisymmetric finite element mesh representing the geometry around the footing (PLAXIS, 2008)

2.5.1.4 Reviewing Output Findings

Upon concluding the computations in PLAXIS, the analysis findings can be shown in the output program. This setting enables users to see essential outputs, including displacements, stresses, and structural reactions, either over the whole geometry or within specified cross-sections. Deformations may be

shown by arrows, color gradients, or contour lines, providing clear insight into the behavior of the soil and structure. In addition, numerical findings are presented in tabular format, facilitating both visual analysis and quantitative evaluation. This output system is crucial for assessing settlement, stress distribution, and other SSI-related responses.

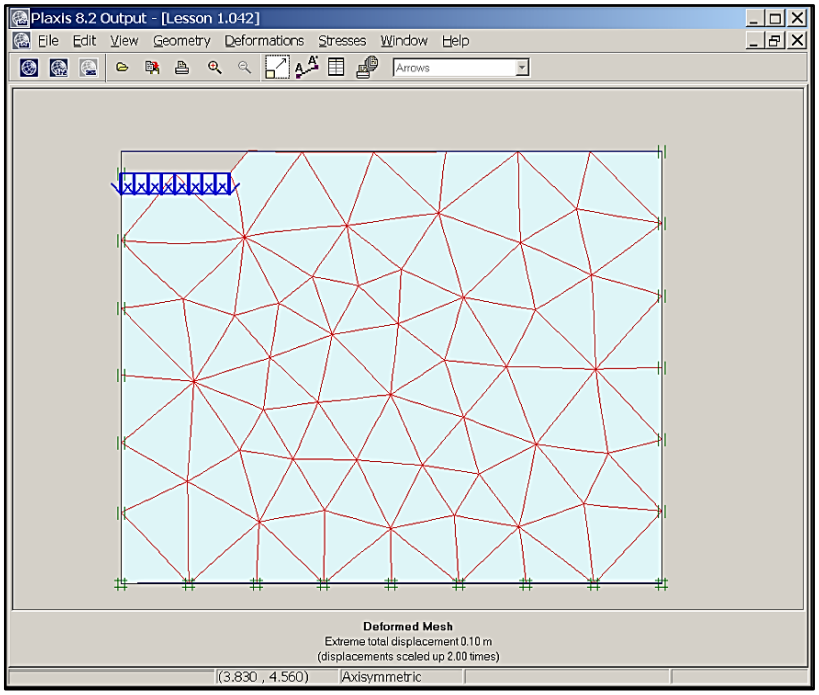

Figure 2.12 Deformed mesh (PLAXIS, 2008)

PLAXIS 2D V8 is a popular finite element program developed for two-dimensional research on deformation and stability in geotechnical engineering. It can represent intricate soil-structure interaction (SSI) processes under static and dynamic circumstances. This version covers plane strain and axisymmetric models, including material models such as Mohr-Coulomb, Hardening Soil, and Soft Soil. Its dependability in reproducing authentic geotechnical behavior has been corroborated by comparisons with empirical data (Bouaanani & Lu, 2009) and its application is supported by the official instructional manual (Brinkgreve et al, 2004).

2.5.2 Advanced Editions:PLAXIS 2D CONNECT Edition and PLAXIS 3D

Recent revisions, including PLAXIS 2D CONNECT Edition and PLAXIS 3D, offer upgraded functionalities with advanced meshing techniques, three-dimensional modeling, and refined user interfaces. PLAXIS 3D allows comprehensive three-dimensional modeling of soil-structure interaction, crucial for asymmetric or spatially complicated systems, as represented in figure 2.13. The selection of PLAXIS 2D in this research is justified by the two-dimensional nature of the case study and the dependable validation of V8 in analogous SSI applications, despite the availability of advanced simulation tools.

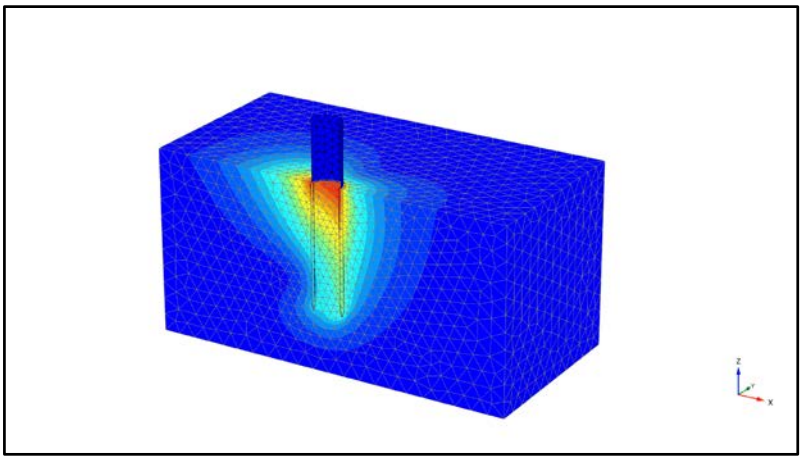

Figure 2.13 PLAXIS 3D Structural Mesh (Bentley, 2023)

2.5.3 Alternative Software Solutions for SSI Analysis

Additional software tools often used in SSI analysis are FLAC (as shown in figure 2.14) (Fast Lagrangian Analysis of Continua), OpenSees (Open System for Earthquake Engineering Simulation), ABAQUS, and MIDAS GTS NX. These tools provide diverse functionalities for constitutive models, boundary condition configurations, and dynamic analysis. For more description concerning those softwares, the table 2.4 shows the capabilities of common software tools numerical 2D model.

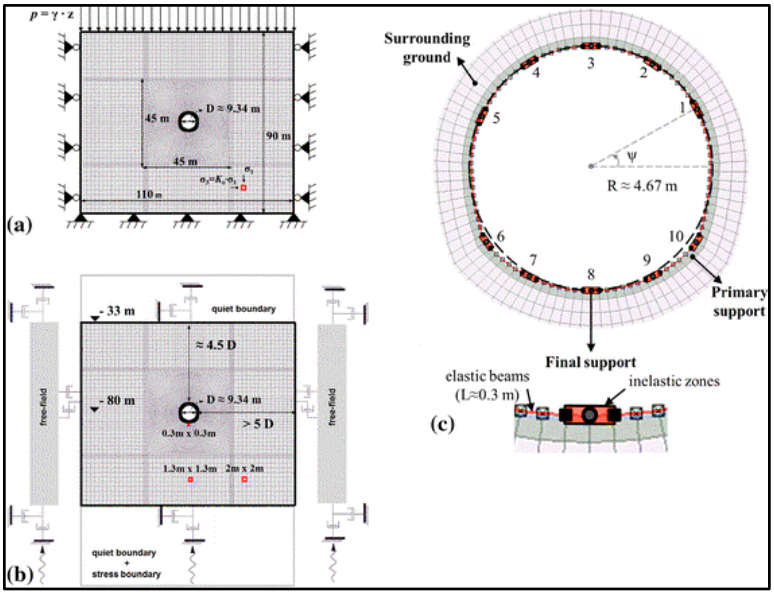

Figure 2.14 Numerical FLAC 2D model (Andreotti, G., & Lai, C. G., 2017)

Table 2.4 Comparison Table: SSI Capabilities of Common Software Tools Numerical 2D Model

Software	SSI Modeling Type	Constitutive Models	Dynamic Analysis Capability
PLAXIS 2D	2D FEM, Direct & Substructure	Mohr-Coulomb, HS, Soft Soil	Yes (Dynamic Module)
PLAXIS 3D	3D FEM	Mohr-Coulomb, HS Small, Jointed Rock	Yes
FLAC	2D/3D Explicit Dynamic	Customizable, built-in models	Yes
OpenSees	3D FEM (User-Defined Elements)	Highly Customizable	Yes
ABAQUS	3D FEM	Advanced plasticity, UMAT support	Yes

2.5.4 The Selection Of Software For SSI Analysis

The selection of software for SSI analysis must be determined by many critical aspects. Nonlinear time domain SSI analysis necessitates the consideration of material nonlinearity, foundation behavior, soil-structure interactions, and seismic isolation systems (Coleman et al., 2013). The selection of element size and time step is essential for accurately capturing nonlinear behavior at appropriate frequencies (Coleman et al., 2013). In benchmarking analytic tools, it is crucial to determine unique user requirements, comprehend solver algorithms, and assess methodologies ranging from finite element to finite volume approaches (Ghosh, 1998). Essential software attributes to evaluate include database integrity, internal operational processes, documentation accessibility, output clarity, and developer reliability (Frank & Pelican, 1986). Factors that may differ in significance based on the user's circumstances include the capacity to modify the database, standard operating procedures, output functionalities, and service rules (Frank & Pelican, 1986). Thorough evaluation of these parameters could ensure perfect software selection for SSI analysis.

2.6 GEOTECHNICAL PARAMETERS FOR SSI ANALYSIS IN PLAXIS

2.6.1 Elastic Parameters: E, ν

Young's modulus and Poisson's ratio are essential soil characteristics in geotechnical evaluations with PLAXIS 2D. Young's modulus (E) indicates the rigidity of the soil and directly impacts strain levels, with higher values corresponding with reduced strain (Raper & Erbach, 1990). This modulus is a fundamental input for the finite element analysis of soil dynamics (Waheed & Asmael, 2023). Poisson's ratio (ν) impacts the distribution of stress and strain, as well as volumetric modifications, with higher values increasing stress and reducing strain. In SSI and slope stability analyses, ν may considerably affect safety factors and plastic zones (Chen, 2006), however E is more related to

settlement and deformation predictions (Mehdi Hosseinzadeh Sutubadi & Khatibi, 2013). Das (2010) argues that elastic parameters are crucial to soil models used in Soil–Structure Interaction (SSI) research. Young's modulus and Poisson's ratio characterize the elastic properties of soil and determine its deformation and load transmission abilities. The modulus of elasticity is expressed by the equation:

$$\boldsymbol{E = \sigma / \varepsilon} \quad (2.9)$$

Where:

σ = applied stress

ε = resulting strain

Young's modulus is significantly impacted by soil type, density, moisture content, and stress history. Normal ranges include: Loose sand (5–20 MPa), Medium dense sand (20–60 MPa), Dense sand (60–150 MPa), Soft clay (1–10 MPa), and Stiff clay (25–100 MPa) (Das, 2010; Bowles, 1996). In PLAXIS, the modulus of elasticity (E) is modified according to the chosen constitutive model: E50 (secant stiffness), Eoed (oedometer stiffness), and Eur (unloading/reloading stiffness) (Brinkgreve et al., 2020).

Poisson's ratio (ν) is referred to the negative ratio of lateral strain to axial strain. It impacts lateral deformation and volumetric alteration under stress. Typical ranges include: Sands (0.25–0.35) and Clays (0.3–0.45) (Das, 2010; Bowles, 1996). In SSI modeling, ν is essential for determining volumetric response and is used to calculate the shear modulus (G) using the formula:0)

$$G = E / [2(1 + \nu)] \quad (2.10)$$

This equation specifically associates Poisson's ratio with soil shear behavior, which is important under seismic loads (Das, 2010).The precise measurement of E and ν in SSI analysis is dependent upon reliable field and laboratory measurements. Common field testing include the Pressure-meter Test (PMT), Dilatometer Test (DMT), and seismic experiments (cross-hole and down-hole). Laboratory examinations contain triaxial, oedometer, and unconfined compression tests (Das, 2010; Bowles, 1996). In PLAXIS, the interpretation of E and ν is dependent upon the chosen constitutive soil model.

Dynamic analysis necessitates modifications to small-strain stiffness to precisely reflect strain-dependent behavior. E-modulus profiles are established for each soil layer to reflect stratigraphy and heterogeneity (Brinkgreve et al, 2020).

(Zhang and Bentley, 2005) examined the physical and mineralogical parameters affecting Poisson's ratio. They noted that ν is variable and contingent upon the interactions between elastic modulus and void structure. Their research demonstrates that the E/G ratio is responsive to ν and is often used to assess elastic properties in rock and soil. For similar soils, it has been found that minor variations in ν may lead to significant changes in shear modulus, hence influencing dynamic and seismic responses in SSI models, as an illustration of their investigation, figures 2.15 and 2.16 poisson's ratio in comparison with young's modulus of dried and wet rock at 10 MPa .

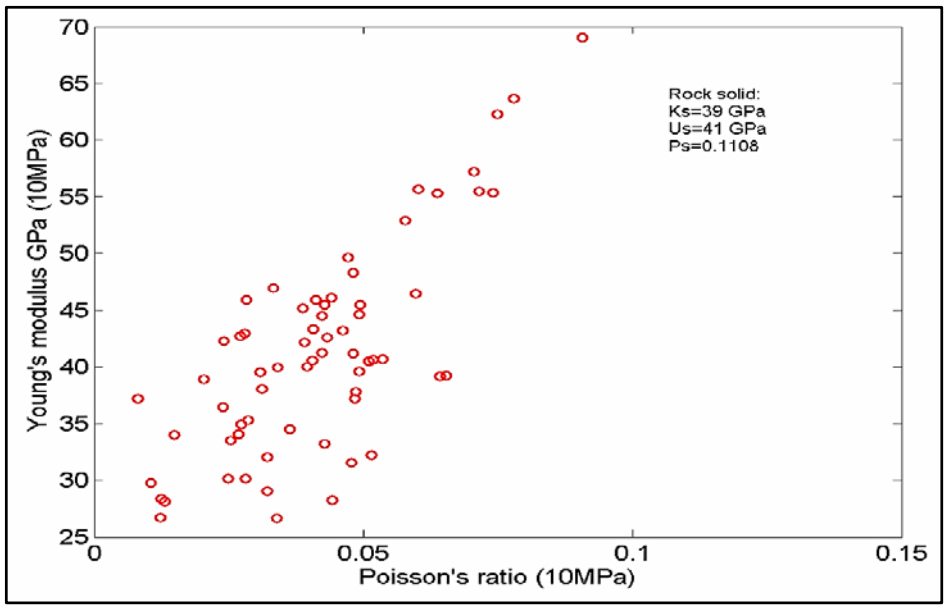

Figure 2.15 Poisson's Ratio In Comparison With Young's Modulus of Dried Rock At 10 Mpa. (Zhang & Bentley, 2005)

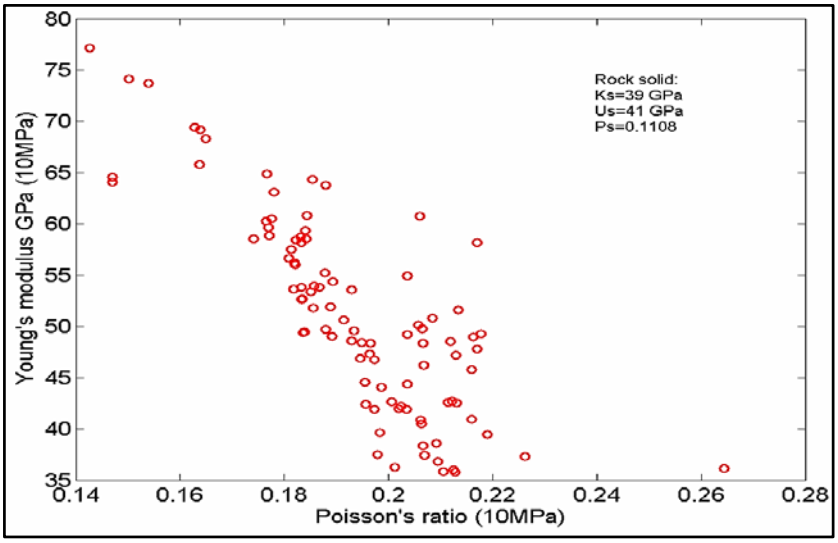

Figure 2.16 Poisson's Ratio In Comparison With Young's Modulus of Wet Rock At 10 Mpa. (Zhang & Bentley, 2005)

The association between Poisson's ratio and Young's modulus at an effective pressure of 10 MPa provides critical insights into the mechanical behavior of rock under different pore conditions. A general beneficial relationship occurs in dry rocks, where higher Poisson's ratio often corresponds to an increased Young's modulus. This is due to the fact that a smaller amount of cracks, which rise Poisson's ratio, simultaneously increase stiffness (Young's modulus). The relationship is broken by the presence of round pores that affect stiffness regardless of cracking density. In water-saturated rocks, the relationship reverses wet fractures increase Poisson's ratio while decreasing Young's modulus owing to the softening impact of pore fluid. At higher pressures, when fractures close and round pores dominate the mechanical response, the relationship between Poisson's ratio and Young's modulus decreases, especially in dry conditions. Furthermore, heterogeneity in rock mineral composition (rock solid) adds complexity, particularly at low pressures, reducing the predictive power of Poisson's ratio for determining elastic modulus. Finally, although some connection occurs under controlled circumstances (dry rocks, constant rock solid), the link between Poisson's ratio

and Young's modulus is very context-dependent. This emphasizes the necessity of taking into account saturation state, pore type, and effective stress when interpreting or using elastic parameters in geo-mechanical modeling.

2.6.2 Strength Parameters: c, φ, Su

PLAXIS 2D v8 depends significantly on cohesion (c), friction angle (φ), and undrained shear strength (Su) to accurately describe soil behavior in geotechnical assessments. These characteristics are applied in constitutive models such as Mohr-Coulomb to simulate soil reaction under different situations (Zakaria & Basha, 2024). PLAXIS 2D can assess pavement constructions on unsaturated subgrade soils, taking into account water table level, suction, and saturation degree (Jaffer, 2019). The program allows for the analysis of soil profiles, deformation, stability, and stress in geotechnical engineering projects (Singh and Jain, 2020). It can also back-analyze shear strength for cement-stabilized soils using several constitutive models, including Mohr-Coulomb and Hardening Soil, to compare stress-strain behavior to laboratory test findings (Toyeb, 2020). These examples highlight PLAXIS 2D's flexibility in simulating complicated soil dynamics, as well as its usefulness in geotechnical engineering practice.

2.6.2.1 Cohesion(c)

Cohesion (c) is considered as a part of shear strength that remains unaffected by the applied normal stress. It is primarily due to inter-particle bonding, clay flexibility, and cementation in fine-grained soils. According to (Das, 2010) and (Budhu, 2010), cohesion normally varies from 10-25 kPa for soft clays, 25-75 kPa for hard clays, and could reach more than 100 kPa for cemented soils, however cohesion for sands is frequently considered to be zero. The Mohr-Coulomb failure criteria uses this parameter as the intercept on the shear stress axis, shown in the equation below

$$\tau = c + \sigma \times tan(\varphi). \quad (2.11)$$

In PLAXIS, c is directly entered into soil models such as Mohr-Coulomb and Hardening Soil, and it influences the study of slope stability, bearing capacity, and lateral earth pressure. (Brinkgreve et al., 2020).

2.6.2.2 Internal Friction Angle (φ)

The angle of internal friction (φ) reflects the soil's resistance to shearing that results from inter-granular friction and particle interlocking. It represents the slope of the Mohr-Coulomb failure envelope and is especially important for granular soils. Loose sand typically has φ values of 28°-32°, thick sand has φ values of 34°-42°, and gravel has φ values of 40°-45°. Over-consolidated clays may have φ values of 25° to 35° (Das, 2010; Budhu, 2010). Particle form, void ratio, and effective stress level all have an impact on φ. In PLAXIS, φ is crucial in simulating earth pressures, deep foundation resistance, and stability of slopes, particularly under loads of earthquake (Brinkgreve et al, 2020).

2.6.2.3 Undrained Shear Strength (Su)

Undrained shear strength (Su) is It describes cohesive soils exposed to fast loading in situations when drainage is not achievable, such as seismical events. It reflects the highest shear stress that soil can endure in undrained situations. Su values typically vary from <25 kPa for extremely soft clays to 100-200 kPa for stiff clays (Das, 2010; Budhu, 2010). Su is often obtained from unconfined compression tests, vane shear tests, or triaxial testing done under undrained circumstances. Su is employed in PLAXIS in undrained soil types (Types A and B) for short-term seismic or loading research studies in saturated cohesive soils.

2.6.2.4 Determination of Parameters

The strength parameters c, φ, and Su are determined by laboratory and in situ experiments. Direct shear, triaxial, and unconfined compression tests are among the laboratory procedures used. In situ tests, such as the Standard

Penetration Test (SPT), Cone Penetration Test (CPT), and Vane Shear Test (VST), offer field-based predictions. Wang and Akeju (2016) suggest employing correlation approaches with limited site data to predict links between c and φ using Bayesian integration and Monte Carlo simulations, particularly when complete testing datasets are missing. Empirical correlations based on CPT are common, including

$Su = Nk \times qc - \sigma vo$ (2.12) and φ calculation based on friction ratio (Rf) (Das, 2010).

2.6.2.5 Implementation using PLAXIS

The strength parameters used in PLAXIS are determined by the constitutive model and analysis type chosen. The Mohr-Coulomb and Hardening Soil models specify c and φ directly. Su is used to represent undrained behavior with the right soil type variables. Soil saturation, loading duration, and drainage channel availability all play a role in distinguishing drained and undrained environments. These strength parameters define the failure envelope and are critical for appropriately representing seismic behavior and foundation interaction (Brinkgreve et al, 2020; Das, 2010).

2.6.3 Consolidation and Stress History: E50, Eoed, Eur, OCR, K_o

Soil-structure interaction (SSI) is a complicated process that involves a variety of consolidation factors and soil parameters. Moghaddasi et al. (2012) found that the stiffness ratio between structure and soil, as well as the structural aspect ratio, had a substantial influence on SSI effects. Soil shear wave velocity and degradation ratio are important elements in determining structural response variation (Moghaddasi et al, 2012). Preliminary soil state, material characteristics, and confinement circumstances all play important roles in local and global interface behavior, with relative density and particle characteristics having the most influence (DeJong & Westgate, 2009). Loading history and boundary circumstances impact soil constitutive model parameters, especially strain parameters such as K, G, and Eoed modules (Kowalska, 2012). Standard

non-interaction analysis, which considers unyielding column support and neglects structural stiffness in foundation design, may result in overly expensive or dangerous structures (Garg, 2012). A more logical approach to SSI may increase computational reliability and precision in geotechnical engineering (Garg, 2012).

E50, Eur, and Eoed: Parameters in the Hardening Soil Model
The Hardening Soil Model (HS) in PLAXIS demands three stiffness modulus to represent soil reaction under various loading situations (Brinkgreve et al., 2020).

-E50: Secant stiffness measured in a conventional drained triaxial test; it indicates soil stiffness under primary stress.

Eur: Unloading/reloading modulus; often higher than E50 and applied for elastic recovery.

Eoed: Oedometer modulus; indicates stiffness during one-dimensional compression in an oedometer test. The relationships between these modulus represent soil behavior throughout several loading and unloading cycles. Eur is often calculated as 3 × E50 for sands and hard clays (Budhu, 2010). These characteristics are stress-dependent and vary according to confining pressure and relative density. They affect elastic deformation during seismic trembling, cyclic behavior of shallow foundations, and ground settlement under static and dynamic loading (Brinkgreve et al., 2020).

2.6.3.1 Over-consolidation Ratio (OCR)

The Overconsolidation Ratio (OCR) stress history measurement, expressed as OCR = σ'p_max / σ'p_current, with σ'p_max representing the largest historical effective vertical stress and σ'p_current denoting the current effective vertical stress (Terzaghi et al., 1996). An OCR greater than 1 indicates over-consolidated soils, characterized by increased stiffness and higher resistance to deformation. OCR substantially influences modulus values, shear strength, and settling potential. In SSI, higher OCR results in less

deformation, increased foundation stiffness, and a lower risk of seismic-induced settlement (Budhu, 2010).

2.6.3.2 Coefficient of Earth Pressure at Rest (K_0)

K_0 signifies the ratio of horizontal to vertical effective stress under at-rest conditions: $K_0 = \sigma'h / \sigma'v$ Standard values are:

Typically cemented clay: $K_0 \approx 1 - \sin(\varphi)$

Overconsolidated soil: $K_0 > 1$

Loose sand: 0.3–0.5 (Terzaghi et al., 1996; Budhu, 2010). Parameter Identification Consolidation and stress history parameters are often obtained via laboratory experiments (such as oedometer and triaxial tests), empirical correlations, and field observations. Common predictions are $E50 \approx 2.5 \times$ NSPT (MPa) for sandy soils. OCR is calculated from consolidation curves or geological histories (Budhu, 2010; Terzaghi et al, 1996).

2.6.3.3 Implementation using PLAXIS

In the PLAXIS Hardening Soil (HS) model, E50, Eoed, and Eur are parameters specified for each soil layer. The OCR and K_0 affect the setting of the geostatic stress field. The presence of strain-dependent stiffness in HS provides a precise representation of soil behavior under varying load magnitudes, making these characteristics essential for modeling settlement, stress redistribution, and foundation interaction in both static and dynamic aspects (Brinkgreve et al, 2020).

2.6.4 Dynamic Parameters: Vs, ξ, PGA

Dynamic soil characteristics are essential in soil-structure interaction (SSI), influ encing the structural response during seismic events. Important requirements include soil compliances, which may be represented by mass-spring-dashpot systems (Sarrazin et al., 1972). The advantageous effects of SSI are notably significant for substantial structures on soft soils, possibly

decreasing base shear while improving structural flexibility (Karthika & Gayathri, 2018). While SSI often has a little or advantageous impact, it can improve structural responsiveness by as much as 20% under some situations (Sarrazin et al., 1972). Uncertainties in SSI analysis arise from combined modeling and parameter uncertainties, which can be examined by response surface approach (Wong, 1984). Soil-Structure Interaction (SSI) impacts the dynamic response of structures, altering their natural frequencies and vibration modes. Parametric assessments on different reinforced concrete and masonry structures have been performed to assess SSI impacts across different structural typologies (Ceroni et al., 2012). Accurate identification of foundation soils is necessary for properly considering soil-structure interaction in structural calculations.

Dynamic parameters are important for precisely describing the seismic response of soil-structure systems. In SSI modeling, especially for earthquake events, characteristics include shear wave velocity (Vs), damping ratio (ξ), and peak ground acceleration (PGA) define the transmission, amplification, and dissipation of energy inside the soil and structure (Kramer, 1996; Idriss & Boulanger, 2008).

2.6.4.1 Shear Wave Velocity (Vs)

Shear wave velocity refers to the rate at which shear waves move through the soil. It indicates the soil's small-strain stiffness and is used as an essential measure in seismic site categorization (e.g., Vs30). It is also directly associated with the soil's shear modulus (G):

$$G = \rho \times Vs^2 \quad (2.13)$$

Where:

G = shear modulus

ρ = soil density

Vs indicates shear wave velocity.

Average Vs values (m/s):

Soft clay: 100 to 200

Stiff clay: 200–400

Coarse sand: 150–300

Dense sand and gravel: 400–800

In PLAXIS, Vs may be indirectly supplied by specifying G or computed determined by modulus and density. Vs is essential for:

- Site categorization (e.g., EC8, TBEC, ASCE)
- Dynamic loading and wave propagation
- Calculation of Rayleigh damping coefficients (Brinkgreve et al., 2020).

2.6.4.2 Damping Ratio (ξ)

The damping ratio indicates the percentage of seismic energy dissipated during each cycle of motion. Damping in SSI originates from two primary sources: material damping, which involves hysteretic energy loss in the soil, and radiation damping, which involves energy loss via wave transmission to the far field.

Average values:

- Sands: 2 to 5 percent
- Clay content: 5–10%
- Rocks: 0.5%–2%

The damping ratio affects the design spectral response via correction factors:

- Eurocode 8: $\eta = \frac{10}{(5+\xi)}$
- ASCE 7: β factor used in spectral analysis

In PLAXIS, ξ is often applied by Rayleigh damping, using mass and stiffness proportional factors (α and β) to attain the appropriate ξ at specified frequencies (Brinkgreve et al., 2020).

2.6.4.3 Peak Ground Acceleration (PGA)

PGA indicates the peak ground acceleration measured at the surface during an earthquake. It signifies the magnitude of seismic loading and is an

essential factor in seismic design. Peak Ground Accelerations (PGA) vary by area and are shown in seismic hazard maps. For example:

TBEC 2018 offers PGA according to designated seismic levels (DD-1 to DD-4).

RPS 2000/2011 offers zonation maps indicating PGA values between 0.05g and 0.25g

In PLAXIS, PGA serves to: Scale acceleration time histories during dynamic loading. Specify input motion at bedrock or free-field boundaries. -Perform pseudo-static studies (e.g., using kh = 0.1 × PGA) (Brinkgreve et al., 2020).

2.6.4.4 Practical Considerations in SSI Modeling

Dynamic parameters must adhere to local seismic regulations. The frequency content of the input motion must correspond to site-specific circumstances. Calibration using in-situ Vs and damping parameters improves simulation reliability (Kramer, 1996; Brinkgreve et al., 2020).

2.6.5 Interface and Boundary Conditions

Interface and boundary circumstances are essential in soil-structure interaction (SSI) investigations. Improved numerical simulations employing nonlinear hysteretic materials and plasticity models can precisely replicate soil-structure interactions, encompassing permanent deformations and damping foundation impedances (Forcellini & Gobbi, 2015). The concrete-soil interface significantly affects forces on structures, requiring enhanced models that incorporate concurrent variations in normal and shear stresses, along with stress reversals (Gómez et al, 2000). The parameters of soil constitutive models, especially strain parameters, are variable and contingent upon loading history and boundary conditions (Kowalska, 2012). Parametric studies in PLAXIS may assess the impact of parameters such as geogrid length, strength, and soil friction angle on wall displacements in mechanically stabilized earth (MSE) walls (Tomar et al., 2024). These investigations yield significant

knowledge into SSI behavior and furnish reference information for comprehending design techniques and specifications.

2.6.5.1 Interface Conditions

(Brinkgreve et al, 2020) The accurate description of interface and boundary conditions plays an important role in the numerical modeling of Soil-Structure Interaction (SSI), particularly in finite element software such as PLAXIS. These elements govern the physical interaction between the soil and structure, the transmission of seismic waves, and the model's capacity to accurately predict energy dissipation and structural responses.

Interfaces are artificial elements situated between structural elements and soil to replicate:

The separation or gapping

Shear transfer as well as bond degradation

Interface elements in PLAXIS describe:

R_{inter}: 0.6–1.0 factor for reducing of interface strength

Kn, Ks: Interface shear and normal stiffness

Coulomb friction either with or without cohesion: contact behavior

Interface elements have several uses including:

Foundation for raft and pile buildings

Retention systems and tunnels

Piled high and with diaphragm walls

Good use of interfaces helps to replicate:

Load movement in reaction to seismic changes

Slippage of ground near deep foundations

Concerning the illustration of soil and interface material configuration window is demonstrated in figure 2.17, and soil and interface material configuration window is shown in figure 2.18.

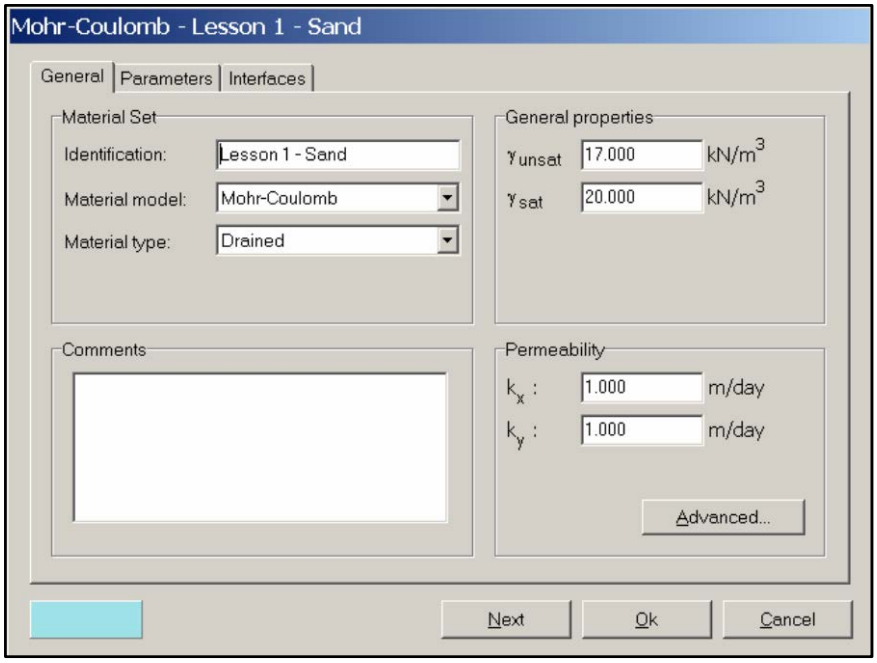

Figure 2.17 Soil and Interface Material Configuration Window (Interfaces tab sheets) (PLAXIS, 2008**)**

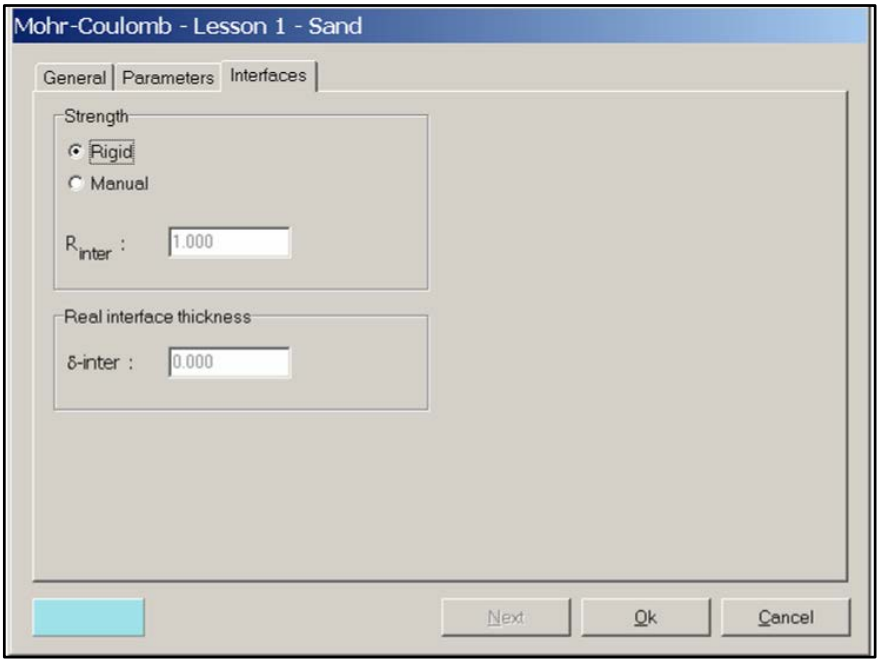

Figure 2.18 Soil and Interface Material Configuration Window *(Interfaces tab sheets)* (PLAXIS, 2008)

2.6.5.2 Boundary Conditions

(Lysmer & Kuhlemeyer, 1969)Boundaries indicate the physical limitations of the numerical domain and the application of external loads or displacements. In SSI models, particularly for dynamic analysis, authentic boundary conditions are essential for preventing unrealistic wave reflections and non-physical responses.

Categories of boundary conditions:

Fixed boundaries: Completely constrained in all directions (typical in static analysis)

Absorbing boundaries: Facilitate the escape of outgoing waves from the domain without reflection; frequently realized by dashpots (e.g., Lysmer–Kuhlemeyer boundaries)

Unconstrained boundaries: Model lateral propagation in infinite domains, particularly in two-dimensional dynamic analysis.

Prescribed displacements or loads: Employed for the application of time histories (e.g., seismic motion at the foundation)

Dynamic Absorbing Boundaries In dynamic SSI:

(Brinkgreve et al, 2020) Absorption of boundaries is implemented to replicate an infinite soil medium. This is generally accomplished with viscous dashpots, computed by:

$$C = \rho \times A \times V \quad (2.14)$$

Where:

C represents the damping coefficient.

ρ = density of soil

A = border region

V = wave velocity (Primary or Secondary wave)

These boundaries mitigate the probability of inaccurate seismic responses resulting from wave absorption inside the mesh. The geometry model in the input window showing the boundaries is demonstrated in the figure 2.19.

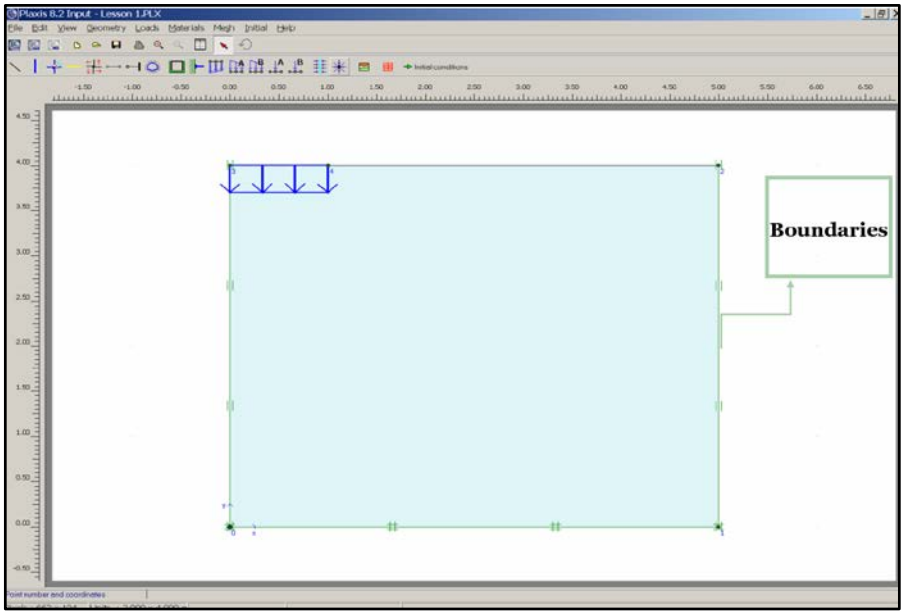

Figure 2.19 Geometry Model in The Input Window Showing The Boundaries (PLAXIS, 2008)

2.7 INTERPRETATION OF KEY PLAXIS OUTPUTS FOR SSI

2.7.1 Displacement Fields and Structural Deformation

Soil-structure interaction (SSI) is essential for comprehending structural behavior under diverse situations. PLAXIS software is frequently used for analyzing soil-structure interaction, offering insights into displacement fields and structural deformation (Samuel et al., 2023; Nasasira & Srivastava, 2020).The impact of live loads on soil-steel constructions can be examined with PLAXIS, demonstrating displacement patterns during vehicular transit (Machelski & Mumot, 2016). Soil saturation levels influence structural seismic performance, since raised saturation results in higher lateral roof displacement due to diminished soil stiffness (Göktepe et al., 2019). These findings show the significance of incorporating SSI in the structural design and analysis, especially for offshore wind turbines, foundations, and structures that experience seismic loads (Samuel et al., 2023; Göktepe et al., 2019).

The article "Effect of Mesh Size on Soil-Structure Interaction in Finite Element Analysis" by Nasasira Derrick and Amit Kumar Srivastava (IJERT, 2020) highlights the substantial impact of mesh size on the precision of simulated outcomes, especially regarding displacement behavior and foundation deformation. PLAXIS software generates output as contour plots and vector fields, showing vertical (Uz) and horizontal (Ux) displacement factors.

(Derrick and Srivastava, 2020) study indicates that finer mesh configurations, such as "very fine" and "fine" settings in PLAXIS, provide more precise and uniform displacement fields. As mesh sizes transitioned from "very coarse" to "very fine," the assessment of displacement magnitudes become progressively more dependable, especially in pinpointing areas of highest settlement right under the filled foundation. The use of 15-node components, in contrast to 6-node elements, enhanced the precision of deformation patterns, enabling greater resolution of the stress-strain behavior at the foundation contact. The structural deformation in this context is assessed by examining the response of the raft base to soil settlement. The paper contrasts vertical displacements across different mesh sizes and demonstrates that smaller mesh models more accurately represent the reality of non-uniform settlements (i.e., differential settlement). This is essential because such deformations, if not well understood, might result in misinterpretations of structural safety assessments.

PLAXIS facilitates the viewing of the deformed mesh, an essential output for evaluating the physical behavior of the structure and the surrounding soil.

Essential PLAXIS outputs important to this analysis comprise:

- Total Displacement: Reflects the aggregate soil movement and structural displacement.
- Vertical Displacement (Uz): Supplies settlement values, crucial for serviceability assessments.
- Horizontal Displacement (Ux): Essential for lateral load or seismic analyses.

Deformed Mesh Visualization: Illustrates regions of stress concentration and failure zones graphically, as it is observed in figure 2.20.

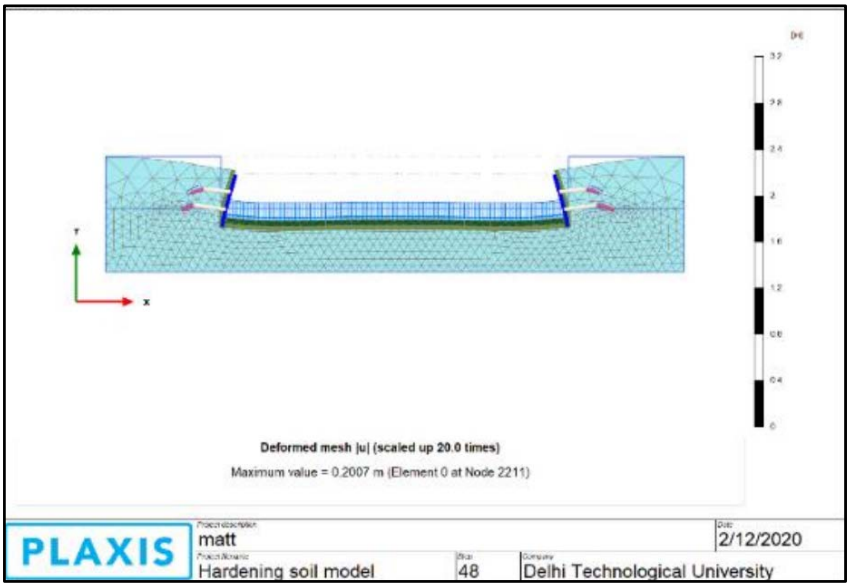

Figure 2.20 Deformed Mesh Showing Settlement (Nasasira&Srivastava, 2020)

The research emphasizes that precise displacement and deformation analysis in SSI investigations need mesh refinement and suitable soil modeling (e.g., Hardening Soil Model) in PLAXIS (Brinkgreve et al, 2018) (Nasasira & Srivastava, 2020). This methodology guarantees accurate interpretation of displacements and assists engineers to make informed design choices.

2.7.2 Pore Pressure Generation and Dissipation

The patterns of pore pressure development and dissipation in soils are essential for comprehending soil behavior under cyclic loading and seismic activity. Studies indicate that energy dissipation in soil directly influences pore pressure generation, demonstrating distinct patterns in load-controlled and displacement-controlled studies (Polito et al, 2024). Pore pressure generation patterns remain essentially indistinguishable when plotted against the energy dissipation ratio, independent of the loading type (Polito & Martin, 2024).

Saturation significantly affects pore water pressure dissipation patterns in one-dimensional consolidation tests of fine-grained soils (Szczepan & Olek, 2023).

The formation of extra pore water pressure in silty sands during earthquakes is mostly affected by relative density and fines material, with little influence from cyclic stress ratio, initial vertical effective stress, and soil fabric (Tomasello & Porcino, 2024). These results enhance models for estimating pore pressure behavior in diverse soil types under varying loading scenarios.

In SSI modeling, extra pore pressure often occurs during undrained loading situations, particularly during fast or cyclic loading instances. The dissipation rate of this surplus pressure is reliant upon parameters like soil permeability, drainage conditions, loading frequency, and soil structure. The study by Cetin and Seed (2024) illustrates that energy dissipation and pore pressure accumulation vary markedly between displacement-controlled and load-controlled testing. Displacement-controlled tests provide more efficient energy dissipation paths via enhanced regulation of deformation energy.

Pore pressure improvement in PLAXIS and finite element models is simulated by connected consolidation or dynamic analysis. Excess pore pressure is shown using isopleth maps illustrating geographical distributions at various time intervals. This enables engineers to pinpoint areas of possible liquefaction or structural instability. The formation of high pore pressure zones under a foundation may result in softening and a reduction in bearing capacity (Brinkgreve et al, 2018).

The appropriate selection of constitutive models—such as the Hardening Soil model with draining capabilities or fully linked flow-deformation models—is crucial for accurately describing pore pressure response. Research demonstrates that layered soils or those with reduced permeability experienced decreased dissipation rates and sustained higher pore pressure levels (Cetin & Seed, 2024).

(Seed & Idriss, 1971) The formation and dissipation of pore pressures are key processes in Soil–Structure Interaction (SSI) as these processes affect both the strength and stiffness of the soil during and after shaking.

2.7.2.1 Generation of Pore Pressure

During fast cyclic loading, the soil framework experiences shear deformations which contribute to the compaction of the soil mass. In undrained surroundings, common during seismic occurrences, water cannot rapidly depart, resulting in elevated pore water pressure. This decreases the effective stress and, therefore, the shear strength (Seed & Idriss, 1971):

$$\sigma' = \sigma - u \quad (2.15)$$

Where:

σ' = effective stress

σ = total stress

u = pore water pressure

If the produced pore pressure near the original effective stress, the soil may attain a liquefied condition, hence losing its load-bearing ability. PLAXIS may replicate this using models like the UDSM PM4Sand/PM4Silt or by dynamic analysis using coupled flow-deformation computations (Brinkgreve et al, 2020). In the figure 2.21, the mechanism of pore pressure production under cyclic loading is presented.

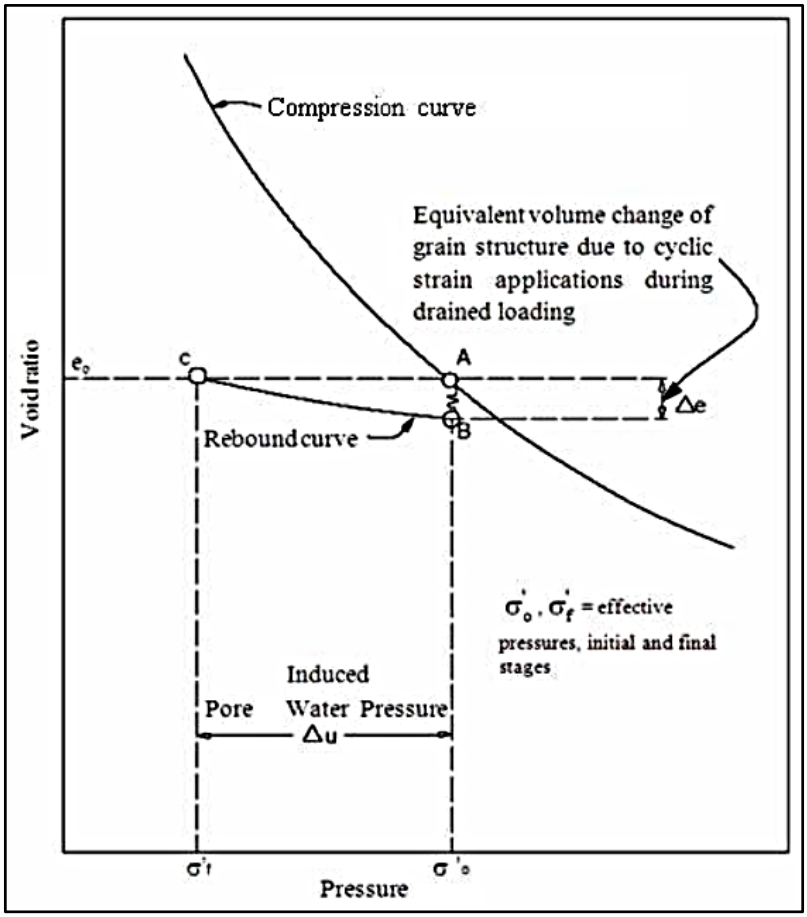

Figure 2.21 Schematic Representation Of The Mechanism Of Pore Pressure Production Under Cyclic Loading. (Seed, 1979)

2.7.2.2 Pore Pressure Dissipation

Boulanger and Idriss, 2014 Upon end of seismic shaking, surplus pore pressures start dissipation by drainage, a phenomenon referred to as consolidation. The dissipation rate is contingent upon: Soil permeability (k), thickness of layers and drainage pathway and soil compressibility.

PLAXIS facilitates time-dependent consolidation analysis using linked flow-deformation formulations. The dissipation is shown by (Brinkgreve et al, 2020)

Pore pressure graphs vs time iso-contours of increased pore pressure and settlement-time curves. As an illustration of the content, both of pore pressure

measurements at four depths below an embankment and Distribution of excess pore pressures after six years of an embankment (measured in meters), as forecasted by the modified SSC model for single-sided drainage are demonstrated respectively in figure 2.22 and figure 2.23.

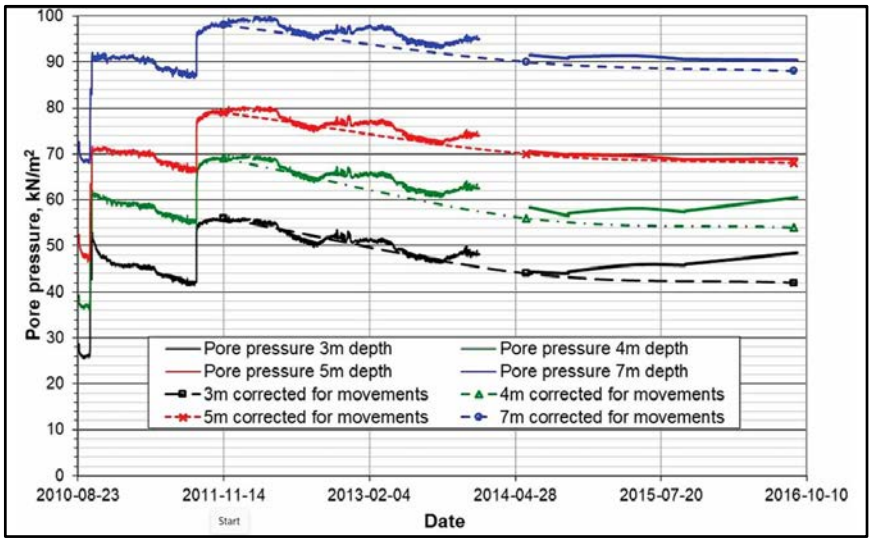

Figure 2.22 Pore Pressure Measurements at Four Depths Below An Embankment (Seed, 1979)

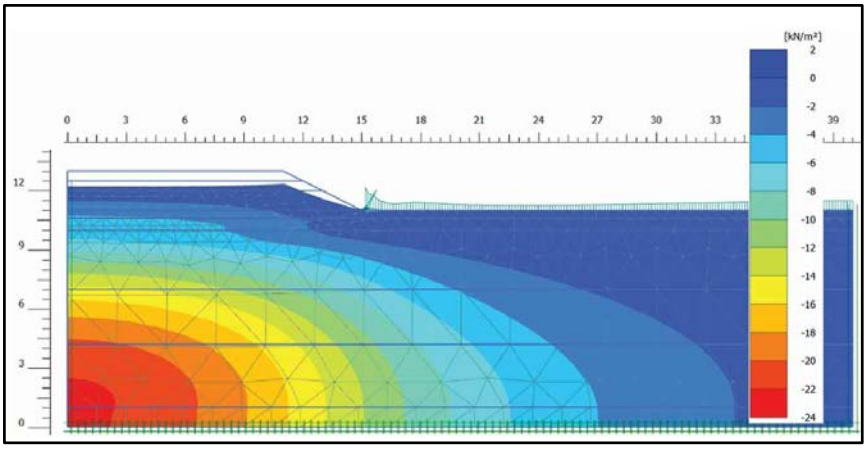

Figure 2.23 Distribution Of Excess Pore Pressures After Six Years Of An Embankment (Measured In Meters), As Forecasted By The Modified SSC Model For Single-Sided Drainage. (Seed, 1979)

2.7.3 Shear and Normal Stress Distribution

Soil-structure interaction (SSI) is essential in seismic response and structural design. Numerical studies using tools such as PLAXIS 3D and OpenSees may simulate intricate soil-structure interaction circumstances, including nonlinear soil behavior and interface situations (Medzvieckas et al., 2019; Forcellini & Gobbi, 2015). Critical determinants affecting SSI impacts consist of soil shear wave velocity, the stiffness ratio between structure and soil, and the structural aspect ratio (Moghaddasi et al., 2012). The distribution of normal and shear stresses at soil-structure interfaces substantially influences structural loads and behavior (Gómez et al., 2000; Medzvieckas et al., 2019).

Interface models must precisely represent concurrent variations in normal and shear stresses, stress reversals, and unload-reload cycles to reflect authentic field circumstances (Gómez et al., 2000). Integrating SSI into design methodologies might enhance the precision of seismic performance evaluations and provide possible cost savings (Forcellini & Gobbi, 2015).

2.7.3.1 Analysis of Shear and Normal Stresses in PLAXIS

(Brinkgreve et al, 2018) In PLAXIS, analyzing shear and normal stress distributions is essential for interpreting the behavior of soil-structure systems under diverse loading circumstances. The program enables users to extract stress components along specified cross-sections, offering insights into the transmission of stresses through the soil mass.

PLAXIS specifically calculates:

- Normal Stress (σ_n): Stress acting perpendicular to a designated plane or cross-section.
- Shear Stress (τ): Stress exerted parallel to a designated plane or cross-section.

The stress components are crucial for assessing possible failure surfaces and comprehending the interaction between soil and structural elements. The capacity to visualize these stresses across cross-sections facilitates the

identification of stress concentration zones, which are essential for design and safety evaluations.

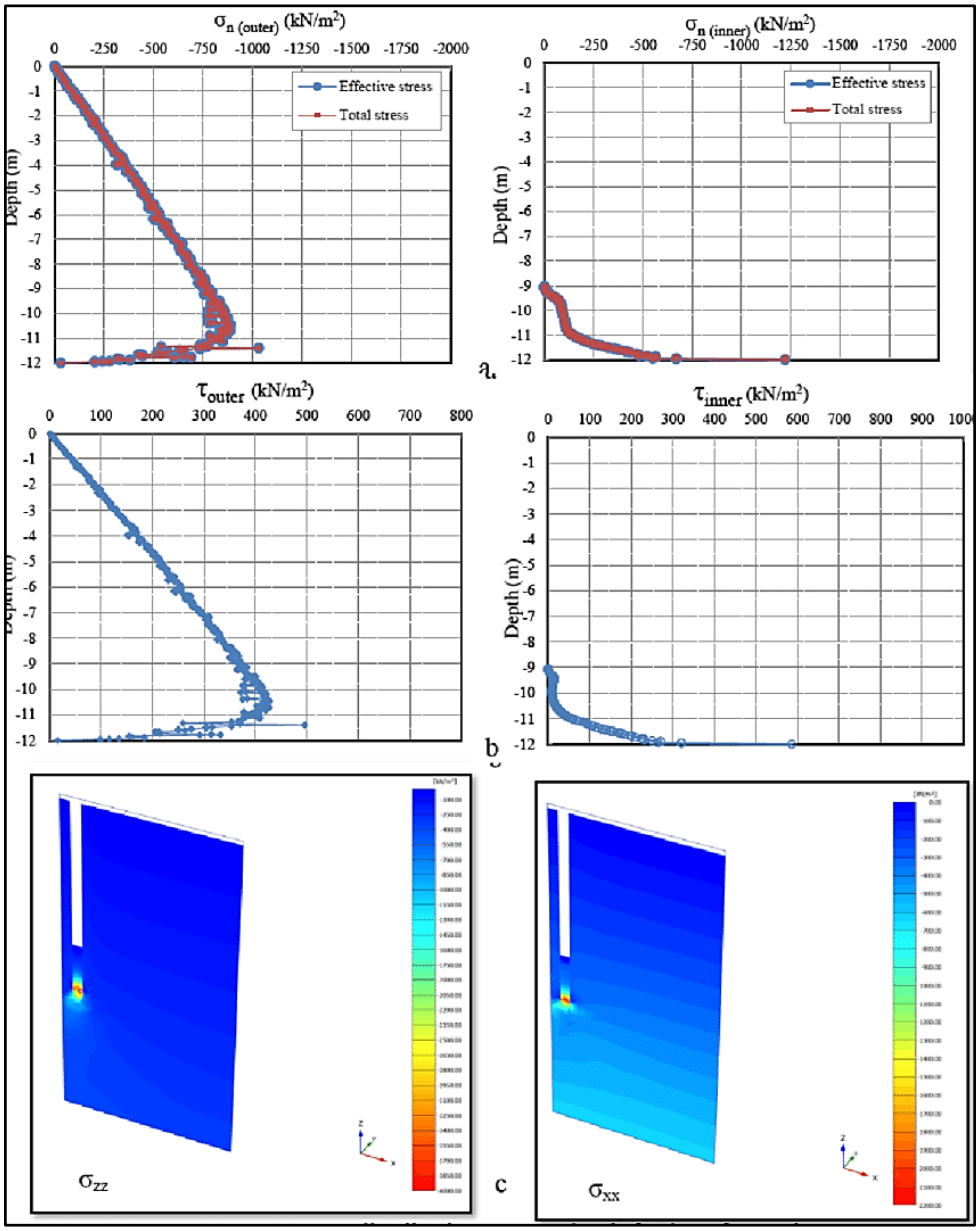

Figure 2.24 Example of stress distribution relative to depth for interface components between soil and pile in a (2x2) group with a separation of (3D) between piles. (a) Normal stress at the outer and inner interfaces, (b) Shear stress at the outer and inner interfaces, (c) Cross-sectional planes for σ zz and σ xx distribution. (Fattah et al, 2019)

2.7.3.2 Shear Stress Distribution

(Potts and Zdravkovic, 1999)The distribution of shear and normal stresses within the soil mass and at the soil-structure interface is a vital result of soil-structure Interaction (SSI) studies. These stress patterns facilitate knowledge of failure processes, foundational behavior, and internal stability of both soil, and structural components under static and dynamic loading situations.

Shear stresses arise from lateral loads, including seismic forces or wind, and are accountable for soil deformation, sliding, or collapse. In SSI modeling using PLAXIS, shear stress (1) outputs are available at element integration points, interface surfaces, and along key planes (e.g., under foundations or next to retaining walls) (Brinkgreve et al. 2020).

Significant findings comprise:

- High shear stress regions under the corners of raft or strip footings
- Activated resistance at pile-soil interfaces
- Formation of shear bands, signifying possible failure zones

In seismic SSI research, observing shear stress variations during shaking helps in assessing the initial stage of plasticity or liquefaction (Potts & Zdravkovic, 1999).

2.7.3.3 Normal Stress Distribution

(Brinkgreve et al, 2020) Normal stresses (σ) are mostly vertical, resulting from self-weight and structural loads; but, horizontal stresses arise from confinement and lateral soil pressure. In SSI models, these stresses are used to assess:

- Contact pressure under foundations.
- Evaluate ground pressure on retaining structures
- Analyse the displacement of vertical loads during settlement or uplift.

Standard stress distributions are essential inputs for assessing carrying capacity and ensuring compliance to limit states (Budhu, 2010).

2.7.3.4 Influence of Mesh Size on Stress Distribution Accuracy

(Nasasira & Srivastava, 2020) The precision of stress distribution outcomes in finite element analysis is greatly affected by the mesh size used in the model. A finer mesh may more precisely capture stress gradients, particularly in regions of high stress concentration, such as along foundation margins or around inclusions. In contrast, a coarse mesh may too simplify these gradients, resulting in diminished predictive accuracy.

A research by Nasasira and Srivastava (2020) indicated that optimizing the mesh size in PLAXIS models resulted in more accurate evaluations of bearing capacity and settling. The research highlighted the significance of mesh refinement in accurately representing stress distribution, especially in complicated soil-structure interaction scenarios, for a visual illustration of stress distribution on software, it is shown in figure 2.24.

2.7.3.5 Stress Distribution in Direct Shear Tests: Numerical Analysis

(Medzvieckas et al, 2019) Numerical models of direct shear testing provide significant insights into the distribution of vertical and shear stresses inside the soil material. A research using PLAXIS 3D, like in figure 2.25, it examined the vertical stress distribution in direct shear box tools, demonstrating that the stress distribution is non-uniform over the shear plane. Boundary conditions, sample shape, and loading processes affect the stress patterns seen during testing.

Comprehending these stress distributions is essential for analyzing test outcomes and for adjusting numerical models to appropriately simulate laboratory circumstances.

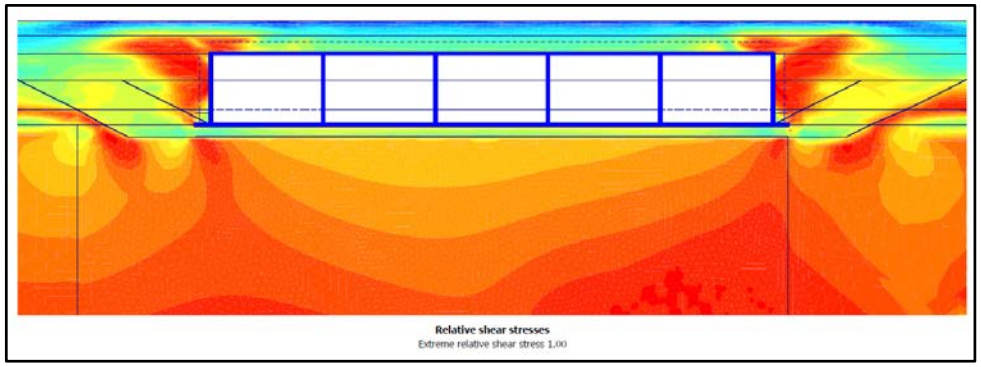

Figure 2.25 Relative Shear Stress Contours From PLAXIS Modelling (Fattah Et Al, 2019)

2.7.3.6 Application in SSI: Stress Distribution Under Foundations

(Brinkgreve et al. 2018) In the context of soil-structure interaction, evaluating the distribution of shear and normal stresses under foundations is crucial for determining bearing capacity and possible settlement. PLAXIS facilitates the visualization of stress trajectories and magnitudes across many loading situations, assisting in the design of secure and efficient foundation systems; it is demonstrated in the figure 2.26.

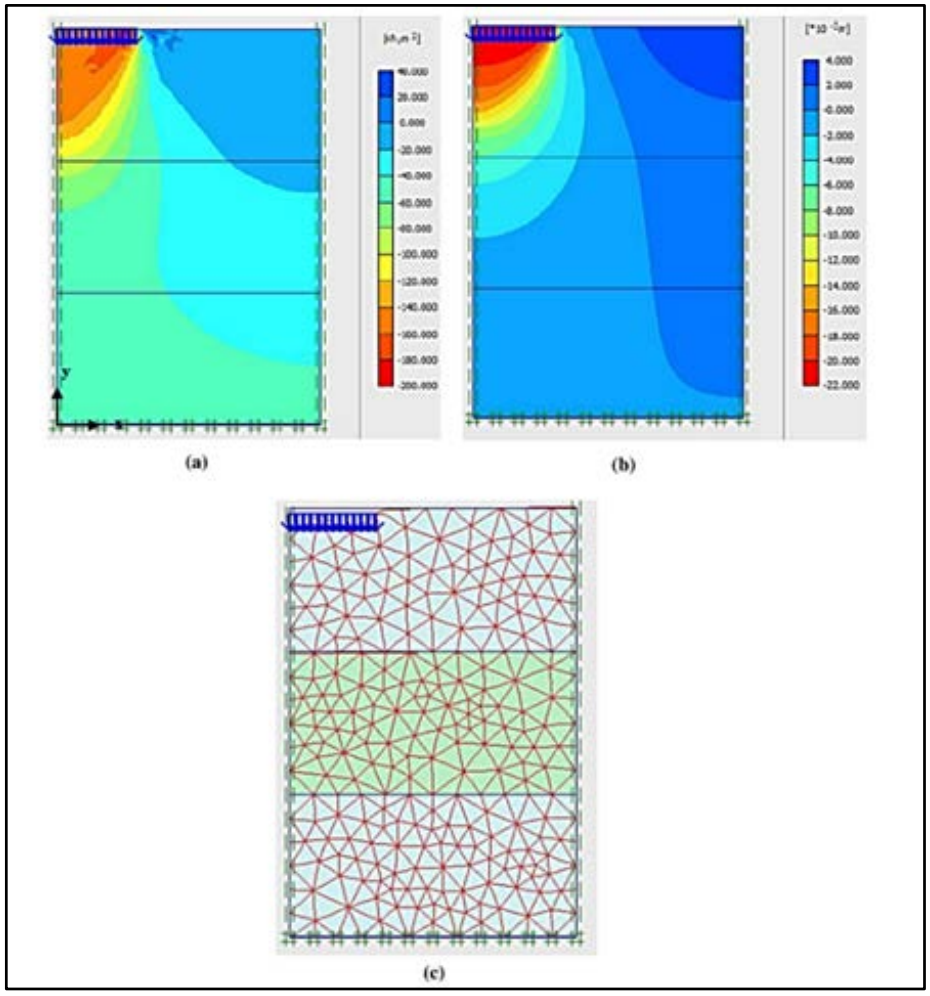

Figure 2.26 **P**LAXIS 2D Results Indicate An Applied Vertical Displacement Uy Of -2.162 Cm For The Natural Clay. (a) Contour Plot of Total Vertical Stress, (b) Contour Plot Of Vertical Displacement, and (c) Deformed Mesh Without Scaling (Cabalar Et Al, 2021)

2.7.4 Acceleration Records and Spectral Response

Soil-structure interaction (SSI) profoundly affects the seismic response of structures and bridges. Research indicates that ignoring SSI may result in hazardous designs, particularly in softer soils and elevated seismic regions (Awchat & Monde, 2021; Abdel Raheem et al., 2014). The consequences of SSI encompass enhanced lateral displacements, spectral acceleration, and

spectral velocity (Awchat & Monde, 2021). Finite element modeling (FEM) is often used to assess soil-structure interaction (SSI), with both temporal and frequency domain methodologies demonstrating efficacy (Abate et al, 2017). In the context of bridges, soil-structure interaction (SSI) may enhance base shear responses and increase isolator displacement requirements, especially in softer soil conditions (Cheshmehkaboodi et al, 2023). The ratio of peak ground acceleration to peak ground velocity (PGA/PGV) in earthquake records substantially influences dynamic responses, with reduced ratios resulting in increased displacements and accelerations/forces (Cheshmehkaboodi et al, 2023). Records obtained near fault often provide greater dynamic responses than those collected from far-field locations (Cheshmehkaboodi et al., 2023). These results emphasize the significance of using SSI in seismic design and analysis.

Kramer (1996) valuation Acceleration recordings and spectral response outputs are essential elements in the understanding of seismic Soil-Structure Interaction (SSI). These results clarify the transmission of seismic waves through soil and their impact on structural reaction, assisting engineers in evaluating vibration intensity, resonance hazards, and energy requirements on foundations.

2.7.4.1 Acceleration Time Histories

In dynamic SSI modeling, PLAXIS enables the input of ground motion as acceleration time histories, often obtained from actual earthquakes or synthetically produced to align with site spectra. (Brinkgreve et al, 2020) The program calculates the reaction at various nodes or monitoring locations, producing acceleration output in the form of:

- Acceleration versus time graphs.
- Peak ground acceleration (PGA) measurements at various depths.
- Comparisons between free-field motion and foundation-level motion.

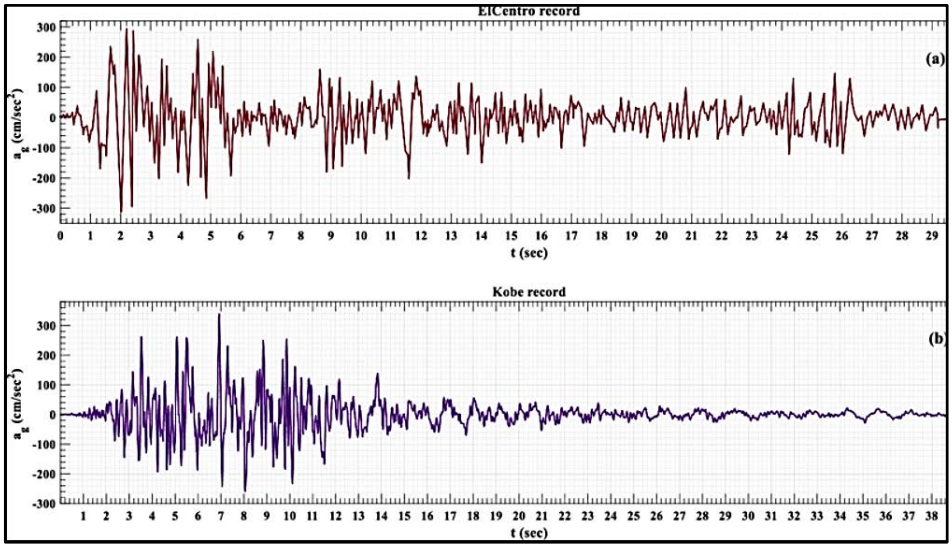

Figure 2.27 The Ground Motion Functions: A El-Centro Earthquake, B Kobe Earthquake (Mehdi Babaei, 2025)

An example of registrations of 2 earthquakes' ground motions: El-Centro and Kobe are shown in figure 2.27.

Kramer (1996) These outputs assist in assessing:

- Amplification or amplification effects resulting from layers of soil.
- Temporal delays and phase alterations in wave propagation.
- Variations in motion attributable to interfacial dynamics and soil absorption.

2.7.4.2 Analysis of Spectral Response

(Chopra, 2012) Spectral response is the maximum acceleration, velocity, or displacement of a single-degree-of-freedom (SDOF) system with various natural frequencies that responds to a certain ground motion. The response spectrum often illustrating :

-Spectral acceleration (Sa) against period (T):

Valuable for determining resonance between soil/structure systems and input motion

(Chopra, 2012) In SSI research, spectral response is used to:

- Evaluate the modification in the basic period of the soil-structure system resulting from base flexibility.
- Analyze structural demand based on fixed-base vs flexible-base assumptions.
- Measure damping modifications and energy dissipation.

For an illustration, a response spectra compared with TBDY-2018 at two different stations is illustrated below in figure 2.28.

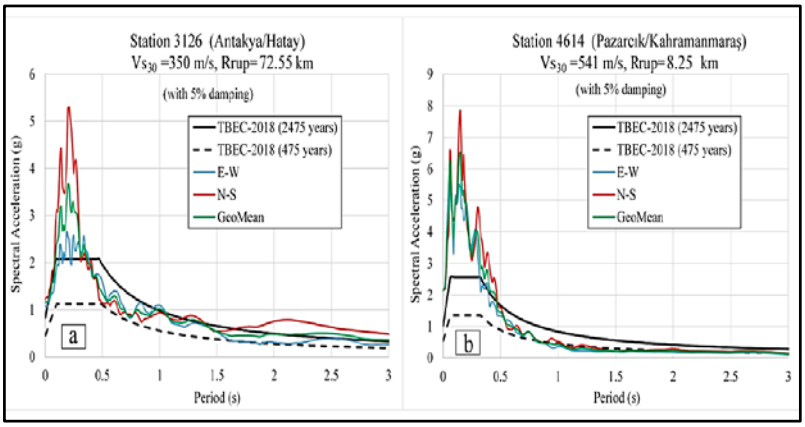

Figure 2.28 Response Spectra Compared With TBDY-2018 At Stations (A) 3126 And (B) 4614, Concerning The Pazarcık Earthquake (Mw = 7.7).(Alpyürür, M., & Ulutaş, H, 2024)

2.7.4.3 Significance of SSI

(Kramer, 1996) The interaction between the soil and structure changes the natural period and damping properties. This leads to:

- An extended natural period due to soil flexibility.
- A reduction in peak spectral acceleration, particularly in rigid soils.
- An increase in displacement requirement for flexible or soft soil.

2.7.4.4 Application of PLAXIS

(Brinkgreve et al, 2020) In PLAXIS, users can:

- Monitor nodal accelerations to create customised response spectra.

- Compare foundation-level accelerations with bedrock or input motion.
- Validate damping assumptions by analyzing energy dissipation.

2.7.5 Foundation Forces and Rocking Behavior

The rocking behavior of foundations is impacted by many elements, including embedment depth, foundation dimensions, form, and structural configuration. Increasing embedment depth increases recentering capabilities, diminishes damping, and elevates moment capacity (Moradi et al, 2024).

Increased foundation dimensions often reduce soil-structure interaction (SSI) impacts on lateral displacements and foundation rocking (Bapir et al, 2024). The configuration of the footing influences rocking performance, with greater length-to-width ratios resulting in improved recentering ability (Khezri et al, 2024). Wall-frame systems are more affected by SSI effects than moment-resisting frame systems, demonstrating increased period elongation and base shear pressures (Bapir et al, 2024). Rocking foundations may attenuate energy and reduce structural requirements, possibly improving overall stability and seismic performance (Al-Janabi et al, 2024). However, these advantages can lead to residual deformations and settlements (Moradi et al, 2024).

2.7.5.1 Foundation Forces

(Brinkgreve et al, 2020) In PLAXIS and other finite element software's, foundation forces are calculated using stress integration along the base and interface components. The primary force outputs comprise:

- Vertical loads (Qz): Arise from the self-weight of the structure and axial forces.
- Horizontal forces (Qx, Qy): Resulting from earthquake inertia, wind, or ground pressure.
- Moments (Mx, My): Indicate inclinations for overturning and rocking.
- These forces assist in assessing:
- Foundation bearing capacity under combined loads.

- Load redistribution resulting from SSI effects.
- Critical load combinations that may cause tilting or failure.

2.7.5.2 Rocking Behavior

Recent experimental results (Moradi et al, 2024) demonstrate that increasing the embedment depth of shallow foundations improves rotational stiffness and moment capacity, concurrently reducing settlement and damping. This behavioral change is ascribed to a change in soil deformation processes, changing from wedge-type failure in surface foundations to a scoop-like mechanism in immersed scenarios. Rocking is a kind of rotational motion of a foundation that occurs when one side of the base elevates due to intense seismic activity. It illustrates the moment-rotation response of shallow foundations and is a critical nonlinear soil-structure interaction when it occurs.

Essential indications comprise:

- Moment versus rotation graphs: Nonlinear hysteresis loops demonstrating energy dissipation.
- Temporal progression of foundation rotation: Illustrates the timing and amplitude of rocking cycles.
- Uplift detection: Areas showing zero contact pressure during movement (Gajan & Kutter, 2008). Displacements of soil particles during the second-phase quarter cycle of loading for foundations with embedment depths of 0 mm; 25 mm and100 mm are shown in figure 2.29.

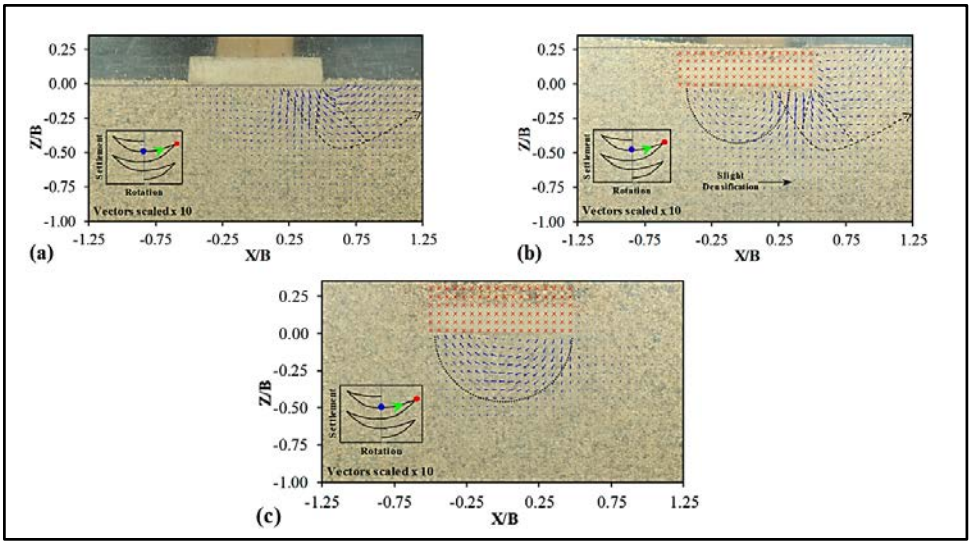

Figure 2.29 Displacement of soil particles during the second-phase quarter cycle of loading for foundations with embedment depths of (a) 0 mm; (b) 25 mm; and (c) 100 mm. (Khezri A. et al. 2024)

The PIV analysis findings for the third quarter cycle in the second loading phase of each experiment, which examine the soil–foundation deformation process throughout a loading quarter cycle (from zero to maximum rotation), are shown in Figure below. The second phase is selected for in-depth analysis, since the first phase shows negligible deformations and the third phase has a significant rotation amplitude that is improbable in real-world situations. The displacement vectors of soil particles above the foundation and the foundation's movement are excluded (shown by red crosses), since these substantial displacements obscure the more pertinent motions of the surrounding soil. Forcellini and Gobbi (2015) underscored the significance of accurately predicting the nonlinear rotational behavior of shallow foundations, particularly under seismic loading circumstances. Their numerical simulation demonstrated that rocking behavior is considerably influenced by the stiffness of the superstructure and the nonlinear properties of the underlying soil. Forcellini & Gobbi (2015) have demonstrated that excluding SSI effects in structural comparisons may lead to an underestimation

of displacements or an overestimation of internal challenges, so compromising structural safety margins and economic efficiency. They determined that in seismically active regions, specifically considering soil-structure interaction and rocking behavior might result in more efficient foundation designs that minimize superfluous construction expenses while preserving performance.

CHAPTER 3

3. EARTHQUAKE HISTORY AND THE ROLE OF SSI

3.1 INTRODUCTION TO EARTHQUAKE ACTIVITY IN MOROCCO AND TURKEY

3.1.1 Morocco

(El Hassani and Cherkaoui, 2012) One of the natural disasters that humans are still most afraid of is earthquakes. Buildings, infrastructure, public facilities, transportation networks, and more might all be lost in a matter of seconds due to their erratic nature and intensity. Several natural disasters, such as floods, landslides, tsunamis, fires, and soil liquefaction, may be carried on by an earthquake. Sometimes, they might cause more damage than the actual earthquake. There is still insufficient data to anticipate the precise date, magnitude, and location of an earthquake, but this might be decreased by considering suitable precautions that reduce the number of earthquake-related deaths and property damage. Therefore, when earthquakes cannot be predicted, it is necessary to improve prevention by identifying seismically sensitive places and evaluating the seismic risks in these areas.

Compared to nations like Japan, California, Greece, and Turkey, Morocco experiences less earthquake activity. Morocco does however, have a considerable background seismicity, that has generated many local magnitude historical and instrumental earthquakes greater than 6. 12,000 people were killed in the 1960 Agadir earthquake, which destroyed the city and nearby settlements. Significant earthquakes then occurred, most notably at Al Hoceima in Northern Morocco in 2004, which claimed 629 lives. Enough is known about the variables influencing the frequency and geographic distribution of these earthquakes. With a maximum convergence rate of around 5 mm per year, the ongoing collision between Africa and Europe is probably

the origin of the deformation that contributes to the seismicity of northern Morocco and the Atlas Mountains.

Morocco has low seismic activity compared to other Mediterranean countries (Algeria, Italy, Greece, Turkey, etc.), mostly related to the African and Eurasian tectonic plates' convergence. But every year, people suffer earthquakes that may sometimes cause serious local damage. We still remember the devastating Agadir earthquake, which killed 12,000 people, and the Al Hoceima earthquake with a loss of 629 people. Analysis of historical documents shows that far stronger earthquakes occurred in Morocco's history, have impacted cities include: Fez, Meknes, Melilla, and those on the Atlantic coast. With no instrumental data before to 1937, when the Cherifian Scientific institute now the Scientific institute-opened the first seismic station, seismicity in Morocco could be assessed independent of macro-seismicity.

The activity of earhquakes is primarily located in the Rif region, specifically in Al Hoceima, as well as in the the western Rif middle and high Atlas, where a notable NW-SE seismic alignment is noticeable, starting close to Fez and extending between Larache and Asilah via Ouezzane, as shown in the study of the seismicity map of Morocco and the neighboring regions from 1901 to 2010 (Fig. 3.1). Although most of the seismicity is shallow and centered in the first 30 k. there is considerable seismicity in the eastern half of the Gibraltar Strait (40-150 km). The Gibraltar Strait has little to no seismic activity (Hatzfeld 1978, Cherkaoui 1991). In the Middle Atlas, we also see around 30 intermediate earthquakes (40–170 km).

(Hatzfeld & Frogneux 1981, Cherkaoui 1991). According to the seismicity map of Morocco and the surrounding areas from 1901 to 2010.

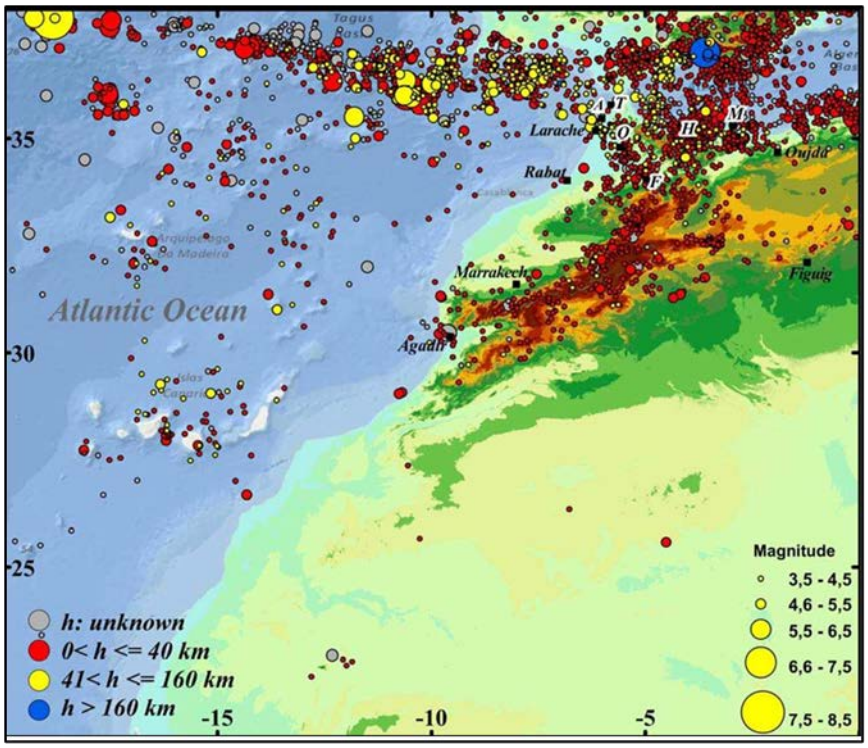

Figure 3.1 Morocco and the surrounding region's seismic activity from 1901 to 2010 with M ≥ 3.5. Abbreviations: A: Asilah, F: Fez, H: Al Hoceima, M: Melilla, O: Ouezzane, T: Tangier (Cherkaoui, 1991)

3.1.2 Turkey

(Orak et al, 2023) Even though storms, hurricanes, and cyclones may be predicted with the help of modern technology, an important number of natural disasters still happen without warning. Turkey is vulnerable to a number of natural catastrophes, including earthquakes, floods, landslides, avalanches, and wildfires, because of its topographical features. Earthquakes are responsible for more than 60% of disaster-related deaths in Turkey. It is known that Turkey is located in one of the world's most seismically active regions of the Mediterranean-Alpine-Himalayan area. The Ministry of Interior, Disaster and Emergency Management Presidency (AFAD) of the Republic of Turkey reports that 905 natural catastrophes happened in this country in 2020. 321 of them had an earthquake magnitude greater than 4.0 Mw. Five Catastrophic 7.7

Mw and 7.6 Mw earthquakes struck the southeast regions of Syria and Turkey on February 6, 2023.

(Yılmaz & Aydın, 2025) Turkey's substantial seismic risk in relation to its geographic position is evident from the European Seismic Hazard Map (Figure 3.2) (Giardini, Woessner, & Danciu, 2013). Turkey, Italy, and Greece have the greatest seismic risk in Europe, according to the statistics shown below. With 77 major earthquakes recorded between 1900 and 2018, Turkey ranks fourth in the world for the number of major earthquakes.

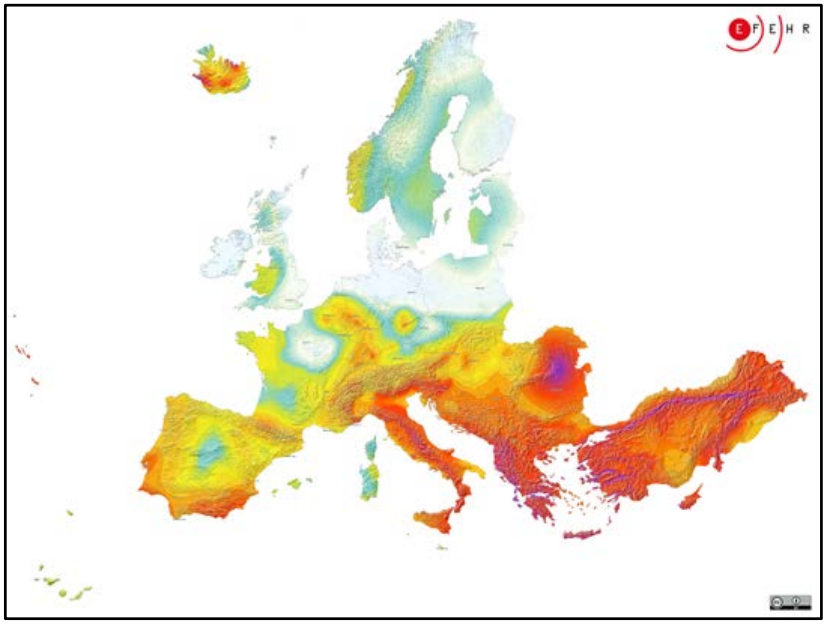

Figure 3.2 European Seismic Hazard Map (Afet ve Acil Durum Yönetim Başkanlığı, 2018).

In a 1996 study, Demirtaş and Yılmaz examined historical records from 2000 to 1900 BC, instrumental seismic data from 1900 to 1995, and some ancient texts dating back to 2000 BC. They identified seismic gap areas in Turkey that are more likely to have earthquakes by using this data. Yılmaz and Demirtaş, 1996, under the Marmara Sea, the northern section of the North Anatolian Fault, the Bingöl-Yedisu fault, the eastern part of the Ardahan, Hakkari, Isparta angle Aksu Thrust, and the Cyprus Arc south of Antakya are

among the numerous seismic regions that the study finds to be unruptured (Figure 3.3). The northern region of the Anatolian Fault, which directly affects Istanbul, is the most important zone among these seismic gap zones. According to Barka (2000), a 4-meter-high stress zone has developed in the Sea of Marmara, meaning that if a single fault ruptures, an earthquake with a magnitude of 6.5-7 could occur, while if several faults rupture simultaneously, an earthquake with a magnitude of 7.2-7.5 could occur (Barka et al., 2003). According to scientists, there is now a 47% likelihood that the earthquake will occur within 30 years from 1999. Significant seismic risk still exists despite differences in the intensity of seismic activity across different geological regions, especially in the graben systems of Western Anatolia, the East Anatolian Fault Zone (EAFZ), and the North Anatolian Fault Zone (NAFZ). According to recent studies, the northern part of the Anatolian Fault is under the Bingöl-Yedisu area and the Marmara Sea. One of the most important seismic gaps is a fault. Additionally, there is a significant danger of earthquakes in the Cyprus Arc, Ardahan, Hakkari, and the eastern portion of the Isparta Angle.

Figure 3.3 Earthquakes Occurred in Seismic Gap Areas Between 1996 and 2023

In conclusion, earthquake risks are a necessary component of Turkey's geological and tectonic system. However, it is crucial to develop and

implement efficient risk management strategies grounded on scientific research in order to avoid these dangers from developing into catastrophes. Turkey's resistance against future earthquakes should be strengthened by raising public awareness, enforcing stringent building inspections, and continuously improving disaster management regulations.

(Mekki, 2014) The soil-structure system has a major impact on how structures react to earthquakes. Predicting the interdependent behavior of the building and soil is crucial in soil-structure interaction (SSI) problems, and this calls for integrated soil and structure models. The external environment around its base, including the interaction between the structure, foundation, and soil, affects the structure's response in addition to its dynamic characteristics and its level of seismic excitation.

3.2 MOROCCO: DESCRIBING THE EARTHQUAKE EVENT AND GENERAL IMPACTS

3.2.1 2004 Al Hoceima Earthquake

(Van der Woerd et al. 2014) A major Mw6.4 earthquake (CSEM, USGS, Harvard) struck the Al Hoceima region of Morocco at 2:27 AM on February 24, 2004 (Jabour et al., 2004). The Al Hoceima region, known as Morocco's most seismically active location, had seen no major earthquake in at least 200 years until this one, as demonstrated in figure 3.4 and figure 3.5; On May 2, 1994, around 10 km west-northwest of the 2004 event, an earthquake with a magnitude of Mw6.0 occurred on a spring morning.

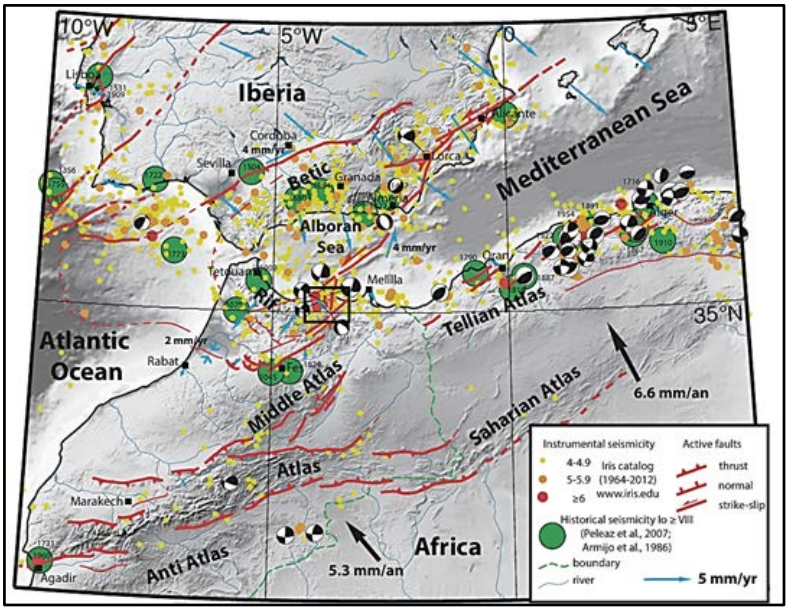

Figure 3.4 Seismotectonic map of western Mediterranean showing active structures of Africa-Iberia collision zone. (El Mrabet, 2005) (Pelaez et al. 2007)

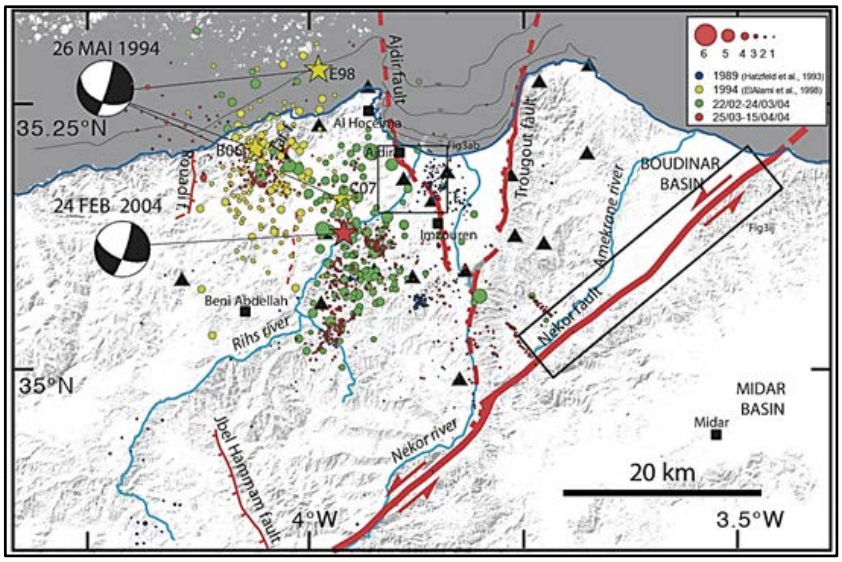

Figure 3.5 Seismotectonic map of epicentral region of Al Hoceima (El Mrabet, 2005), (Pelaez et al, 2007)

(Elmrabet et al, 2014) Approximately 628 to 631 people were died, 926 were harmed, and 12,539 to 15,000 people lost their homes as a result of the catastrophe. While reinforced concrete buildings in Al Hoceima city survived better during the earthquakes, the most serious damage occurred in rural villages when traditional stone and adobe structures with thick roofs fell. In areas like Ajdir and Beni Abdallah, geotechnical problems like as landslides and ground fissures were reported; at Imzourene, the highest ground acceleration reached 0.24g.

In 2014, Van der Woerd et al. Following the main earthquake on February 24, 2004, there were a number of aftershocks, some of which were stronger than a magnitude of 5, that occurred on March 20 and between February 25 and 28, as shown in table 3.1. The European-Mediterranean Seismological Center and the national seismological networks of Spain and Morocco independently recognized the first earthquake and its aftershocks. The most powerful aftershocks and the primary tremor were moved. After then, the P and SH waveforms that were recorded at teleseismic distances were inverted.

Table 3.1 List Of Aftershocks That Were Moved For Events That Took Place Before To The Temporary Network's Development (Van Der Woerd Et Al, 2004)

Year	M	D	H	Min	Sec	Latitude (° ')	Longitude (° ')	Magnitude
2004	02	24	02	27	46.68	35° 7.72'	-3° 57.31'	6.4
2004	02	24	02	36	38.93	35° 10.07'	-3° 57.63'	4.5
2004	02	24	02	38	59.55	35° 8.15'	-3° 53.54'	3.7
2004	02	24	02	41	10.40	35° 10.61'	-3° 59.79'	3.7

Table 3.1 List Of Aftershocks That Were Moved For Events That Took Place Before To The Temporary Network's Development (Van Der Woerd Et Al, 2004)

Year	M	D	H	Min	Sec	Latitude (° ')	Longitude (° ')	Magnitude
2004	02	24	02	48	2.64	35° 4.23'	-3° 56.69'	4.7
2004	02	24	02	59	2.68	35° 11.28'	-3° 0.76'	4.9
2004	02	24	03	17	44.97	35° 7.83'	-3° 58.62'	4.2
2004	02	24	03	25	10.57	35° 9.43'	-3° 57.56'	3.8
2004	02	24	03	27	14.14	35° 10.35'	-3° 57.04'	4.0
2004	02	24	03	32	24.83	35° 6.79'	-3° 59.25'	4.3
2004	02	24	03	53	57.74	35° 3.75'	-3° 55.41'	4.0
2004	02	24	04	4	45.61	35° 10.66'	-3° 57.62'	3.6
2004	02	24	04	6	37.61	35° 4.37'	-3° 57.59'	4.4

(El Janous et al, 2024) Significant lessons for seismic resilience in Morocco were brought to light by the Al Hoceima earthquakes, particularly the need to include the effects of soil-structure interaction (SSI) into urban planning and seismic design. One noteworthy finding was that, in comparison to reinforced concrete buildings in Al Hoceima city, traditional masonry and adobe structures in rural areas failed disproportionately, underscoring the risk of unengineered structures in seismically active places. This pattern of damage

showed how inadequate seismic details and neglect for local soil conditions significantly increased ground motion and ultimately led to structural collapse.

The significance of including site-specific soil response analysis and soil-structure interaction elements into Moroccan and regional seismic codes is highlighted by geotechnical issues like as landslides, lateral spreading, and earth fissures. Soft soils and uneven terrain increased the effects of shaking, highlighting the need for updated geotechnical studies and increased compliance of seismic zoning regulations. These incidents demonstrated the need of revising national seismic design regulations by enacting standards that include SSI analysis, improved foundation details, and structural reinforcements to increase resilience, especially for rural and informal structures. Furthermore, raising public and engineer knowledge is essential to creating safe building methods and reducing future fatalities and financial losses.

3.2.2 2023 Al Haouz Earthquake

(Yeck et al, 2023) Known as the Al Haouz earthquake due to the region that is known the most damaged by the vibrations, the magnitude 6.8 earthquake struck Morocco's High Atlas Mountains at 11:11 p.m. local time (22:11 UTC) on September 8, 2023, some 75 km southwest of Marrakesh. In the weeks after the Al Haouz earthquake, around 3,000 people lost their lives and 5,500 were injured (International Blue Crescent Relief and Development Foundation [IBC], 2023). "Have You Had That Experience?" The epicenter had a modified Mercalli intensity (MMI) of 9 (severe shaking), whereas Marrakesh had an MMI of 7 (very destructive shaking), according to Quitoriano and Wald (2020). Significant structural damage is consistent with the high observed intensities across the area.

The map of detailing seismicity surrounding the high Atlas mountains is represented in figure 3.6. The building infrastructure's susceptibility to the earthquake and the fact that it happened at night, when more people were at home, made its impacts worse. Destructive earthquakes within 500 kilometers

of this event have occurred in Morocco since 1900. In particular, the 1960 M5.912,000-15,000 people, or around 40% of the city's population, died in the Agadir earthquake series (Figure below), which completely destroyed the city (Tillotson, 1960). The shallow depth, proximity to a populated area, and susceptibility of the area's stone and brick structures to ground shaking were the primary causes of the Agadir series' fatal outcome (Paradise, 2005).

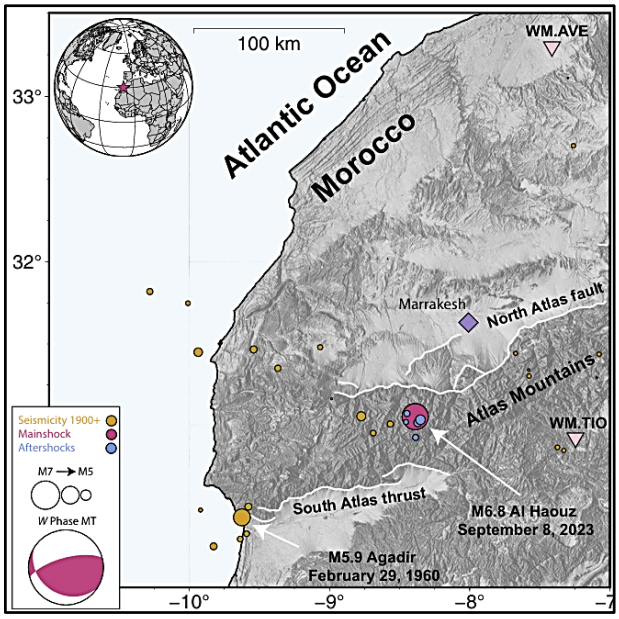

Figure 3.6 Map detailing seismicity surrounding the High Atlas Mountains (Chellai et al, 2024)

With a magnitude of 6.8, the 2023 Al Haouz earthquake in Morocco caused significant structural and geotechnical damage, especially in the High Atlas area. Over 40,000 dwellings collapsed and almost 3,000 towns were damaged as a result of the particularly fragile nature of traditional constructions made of adobe and unreinforced masonry. Whole villages were destroyed in rural regions like Amizmiz and Talat N'Yaaqoub. Significant damage was also sustained by urban areas, such as Marrakesh; historic buildings like as the Kutubiyya Mosque and the medieval walls of the Medina partially collapsed.

Geotechnically, the earthquake made rescue and repair activities more difficult by causing landslides, rockfalls, and ground deformations, especially in hilly areas. The damage caused was made worse by a mix of bad soil conditions and inferior construction methods, underscoring the need for better building regulations and consideration of soil-structure interaction in seismic design.

(Messaoudi & Chennaoui Aoudjehane, 2024) The destruction brought about by earlier seismic events such as the 1960 Agadir earthquake and the 2004 Al Hoceima earthquake highlights the negative effects of inadequate construction resilience. Inadequately constructed infrastructure and buildings, which sometimes fail to comply with current seismic regulations, are particularly vulnerable to collapse during earthquakes, which may cause significant property damage and fatalities. One of the most important ways to increase resilience is to retrofit older buildings to meet earthquake-resistant requirements.

Furthermore, zoning laws and land use planning are highlighted as preventative steps to ensure that new construction prioritizes seismic safety, reducing vulnerabilities and minimizing the risk of infrastructure collapse during seismic events. Together, these strategies seek to mitigate the consequences of design flaws and structural problems, enabling safer and more resilient communities in seismically active regions. (Malusà et al, 2024); (Deverchère et al, 2009).

Damage seen in hilly areas with complicated landscape and soft soils indicated shortcomings in accounting for local site impacts and dynamic soil-structure interaction, particularly with traditional masonry and non-engineered structures. The earthquake highlighted that existing design standards inadequately accounted for the influence of flexible soil layers in enhancing seismic wave amplification and modifying structure responses. Consequently, it is advised that future revisions to Moroccan seismic codes include sophisticated SSI modeling techniques, site-specific response assessments, and more rigorous geotechnical investigation standards to enhance resilience in

similar areas. The detailed geological cross sections of the eastern and central regions of Al Haouz is illustrated in figure 33.7.

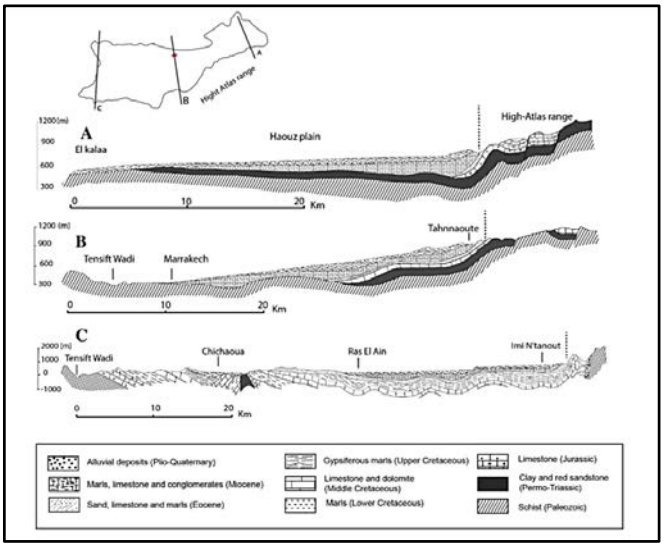

Figure 3.7 Geological cross sections of the eastern and central regions of Al Haouz, Al Haouz-Mejjate plain. (Boukhari et al, 2015)

3.3 DESCRIBING THE EARTHQUAKE EVENT AND GENERAL IMPACTS

3.3.1 1999 İzmit Earthquake

(Yazgan & Sucuoglu, 2001) After the Erzincan earthquake in 1939, the two largest natural disasters that occurred in Turkey in the 20th century were the Kocaeli earthquake on August 17, 1999, and the Düzce earthquake on November 12, 1999. The Kocaeli earthquake has a verified death toll of 17,322, whereas the Düzce earthquake has a confirmed death toll of 950. The cities of Gölcük, Değirmendere, Derince, Adapazarı, Gölyaka, Düzce, and Kaynaşlı were all on the verge of being destroyed due to these two earthquake occurrences. 330,000 structures were affected, of which 118,000 were considered to be lightly damaged, 112,000 to be severely damaged, and 100,000 to be significantly damaged or to have collapsed. During the Kocaeli

and Düzce earthquakes, 32 stations recorded grave, considerable vibrations of engineering relevance, seven of which are in close proximity of the fault. Only near-field ground vibrations after an earthquake above magnitude 7 have been recorded in Europe.

The table 3.2 shows the main characteristics of the near-field strong moves. Here, FD stands for the distance closest to the fault, while teff denotes the important part's duration, which is the period of time between 5% and 95% of the integrated square acceleration over time. As expected for a magnitude of 7.4, the Kocaeli earthquake demonstrated extended durations but low near-field Peak Ground Accelerations (PGA), except for the Düzce station. This might be the result of a series of several ruptures. However, PGVs are often greater.

Table 3.2 Features of Kocaeli and Düzce Earthquake Near Field Strong Motions (Efe, R., & Öztürk, M.Eds, 2017).

Earthquake	Station	Soil Type	FD (km)	Component	PGA (cm/s^2)	PGV (cm/s)	$t_e$ff (s)
Kocaeli	Gebze	S	15	NS	255	41	30
Kocaeli	Gebze	S	15	EW	141	35	16
Kocaeli	Yarımca	S	3	NS	226	72	31
Kocaeli	Yarımca	S	3	EW	316	74	31
Kocaeli	İzmit	R	8	NS	163	28	34
Kocaeli	İzmit	R	8	EW	226	38	34
Kocaeli	Sakarya	R	7	EW	396	57	44
Kocaeli	Düzce	S	11	NS	306	56	12
Kocaeli	Düzce	S	11	EW	357	59	12
Düzce	Düzce	S	7	NS	400	68	9
Düzce	Düzce	S	7	EW	507	88	9
Düzce	Bolu	S	6	NS	725	55	11
Düzce	Bolu	S	6	EW	790	65	11

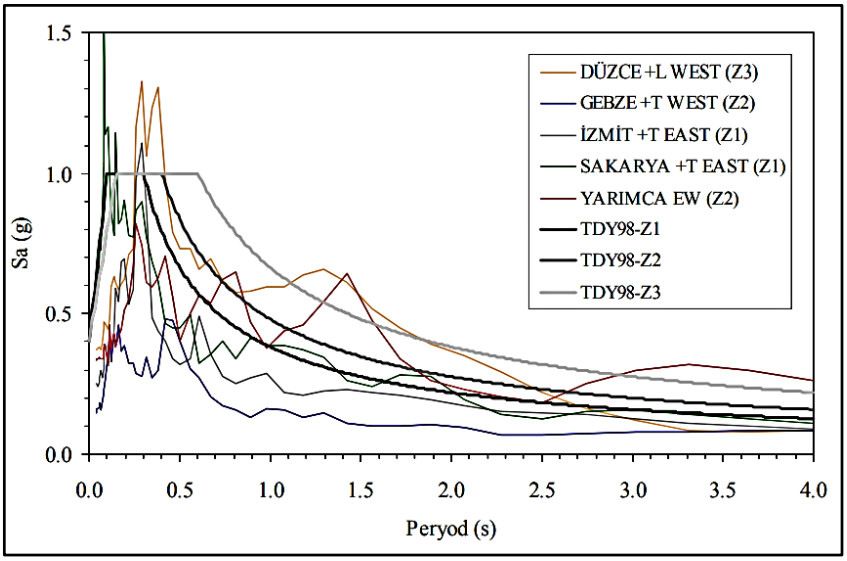

Figure 3.8 Comparison of the Acceleration Response Spectra (Sucuoğlu, 2000)

The Code design spectra and the east-west acceleration response spectra of the near field accelerograms captured during the Kocaeli earthquake are compared. Rock, stiff soil, and soft soil are denoted by Z1, Z2, and Z3, accordingly. Table 3.2 and figure 3.8 show that the rock movements recorded at the İzmit and Sakarya stations are much less intense than the ground vibrations reported at Düzce and Yarımca on soft soils.

As observed in figure 3.9 (damage distribution with the number of stories), there is a significant relationship between the number of stories and the degree of structural damage. Gravitational pressures are just as important in short buildings as seismic stresses, and even though they were not intended in their construction, the structural elements designed to sustain the building's self-weight also provide a large amount of resistance to lateral forces. Seismic forces, however, take over the structural response when the number of stories surpasses three or four. Five- to eight-story reinforced concrete buildings are the most important constructions for reducing seismic risks. Seismic demands are higher for shorter structures as they do not take use of their inherent extra lateral load capacity; rather, their vibration periods coincide with the main

frequencies of seismic ground movements. Nonetheless, they are often constructed by regional contractors using traditional methods, providing customers with the most affordable unit floor space. The Kocaeli earthquake caused very little damage to apartment buildings in the İzmit housing development zone, which ranged in height from eight to fourteen floors.

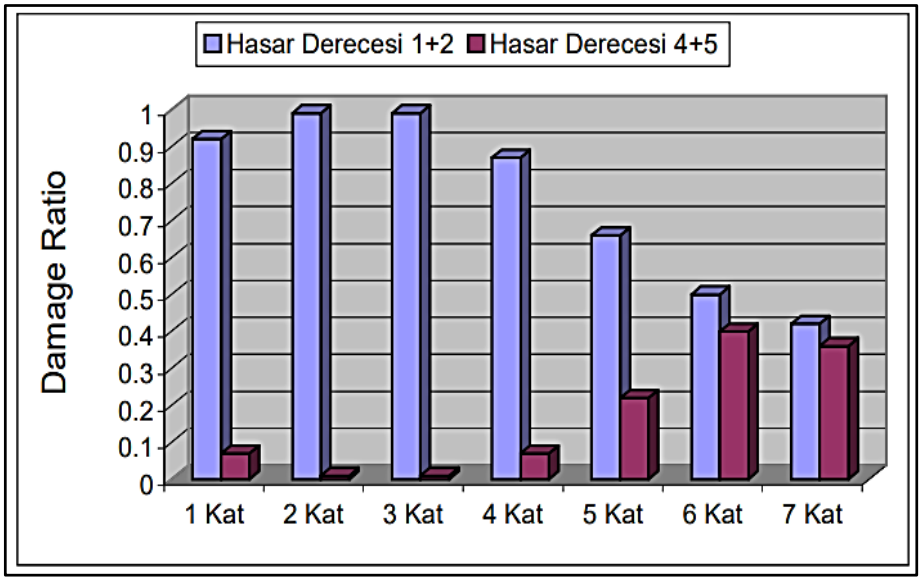

Figure 3.9 Damage Distribution with the Number of stories in Gölcük (Suguoğlu, 2000)

The significance of soil-structure interaction (SSI) in seismic performance, especially for mid-rise reinforced concrete (RC) structures, was highlighted by the 1999 Kocaeli and Düzce earthquakes in Turkey. (Yilmaz, 2022) carried out a thorough investigation of the impact of SSI on mid-rise RC structures with different foundation systems for his master's thesis. According to the study, SSI has a major impact on how buildings respond to earthquakes, particularly those that are built on soft soils. When compared to buildings with rigid foundations, those using flexible foundation systems showed greater inter-story drifts and lateral displacements. The research underlined that underestimating structural needs due to SSI neglect in seismic design could undermine safety. Therefore, improving the resilience of mid-rise RC

structures in earthquake-prone areas requires SSI concerns to be included into seismic design instructions.

3.2.2 2023 Kahramanmaraş Earthquake

Early on February 6, 2023, an earthquake of a magnitude of 7.8 hit the Kahramanmaraş region in southeast Turkey. A magnitude 7.6 earthquake struck the area nine hours later. A large area of Syria and Turkey experienced severe shaking (Modified Mercalli Intensity 6-9) due to the earthquakes' relatively shallow depth of around 10 km. As of March 20, 2023, the total number of fatalities has surpassed 57,000 (50,000 in Turkey and 7,000 in Syria). This incident has become the most deadly in modern Turkish history, surpassing the magnitude 7.8 Erzincan earthquake of 1939, which claimed over 33,000 people's lives. (Spencer et al, 2024), seismic hazard and surface rupture maps is represented in figure 3.10.

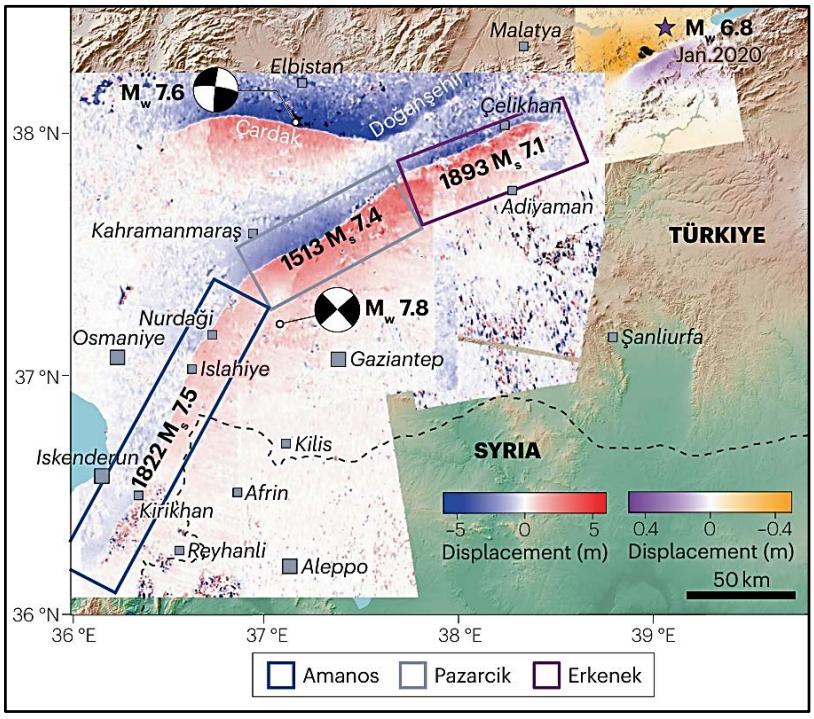

Figure 3.10 Seismic hazard and surface rupture maps of the 6 February 2023 earthquakes (Işık, 2023)

The February 6, 2023, Kahramanmaraş earthquakes in Turkey caused extensive geotechnical damage in all affected regions, revealing critical flaws in soil-structure interaction and ground behavior. Notable landslides included the construction of a landslide dam in Islahiye and a large one on an easy limestone slope in Tepehan. In coastal areas like İskenderun, liquefaction of reclaimed land resulted in substantial ground deformation and subsidence, which led to building tilt and collapse. The significant structural damage in Gölbaşı, Adıyaman, was attributed to problems with soil–structure interaction, highlighting the need of considering local soil conditions when designing for earthquakes. Significant damage was also sustained by 17 earth dams in Turkey and one in Syria, among others, underscoring the earthquakes' profound geotechnical impact on critical infrastructure. (Doğan and Yılmaz, 2024) The soils in the earthquake-affected areas have a weak bearing capacity and a high likelihood of liquefaction, according to tests carried out in the seismic zone. The foundation systems of buildings constructed on agricultural land are often not chosen to fit in with the soil. Examining the figure 3.11 of damages in foundation and soil, shows that the construction often collapsed due to the absence of a basement and the effect of liquefaction on the ground.

Figure 3.11 Damages arose from the Soil and Foundation system (Yön et al., 2024)

(Natur & Güllü, 2024) When SSSI is neglected, foundation shaking, storey drifts, and displacement patterns, especially in the lower levels may be significantly underestimated. Studies conducted after the earthquake show that adjacent structures exacerbate foundation shaking and lateral slope deformations, which affect seismic performance. The interaction effects increased with building density and slope conditions, as seen by the 41.18% increase in foundation shaking and the more than 50% increase in maximum storey drifts on lower levels caused by a nearby building's proximity to the slope.

The results show that in order to more accurately predict structural demand and ensure adherence to performance-based design standards, seismic design codes must explicitly address SSSI issues, especially for sloping terrains and densely populated areas. For more explanation of the figures 3.12 (Factors affected by the 2023 Kahramanmaraş-Pazarcık earthquake), 3.13 (The rocking time history of the building foundation closest to the slope affected by the Kahramanmaraş-Pazarcık earthquake). and 3.14(The building closest to the slope that was affected by same earthquake) respectively and all emphasize the influence of seismic ground motion on slope stability and structural performance, concentrating on foundation rocking and lateral displacement.

They underline the significance of soil-structure-slope interaction in seismically active areas of Kahramanmaraş-Pazarcık earthquake, illustrating that proximity to slopes significantly affects the seismic performance of structures.

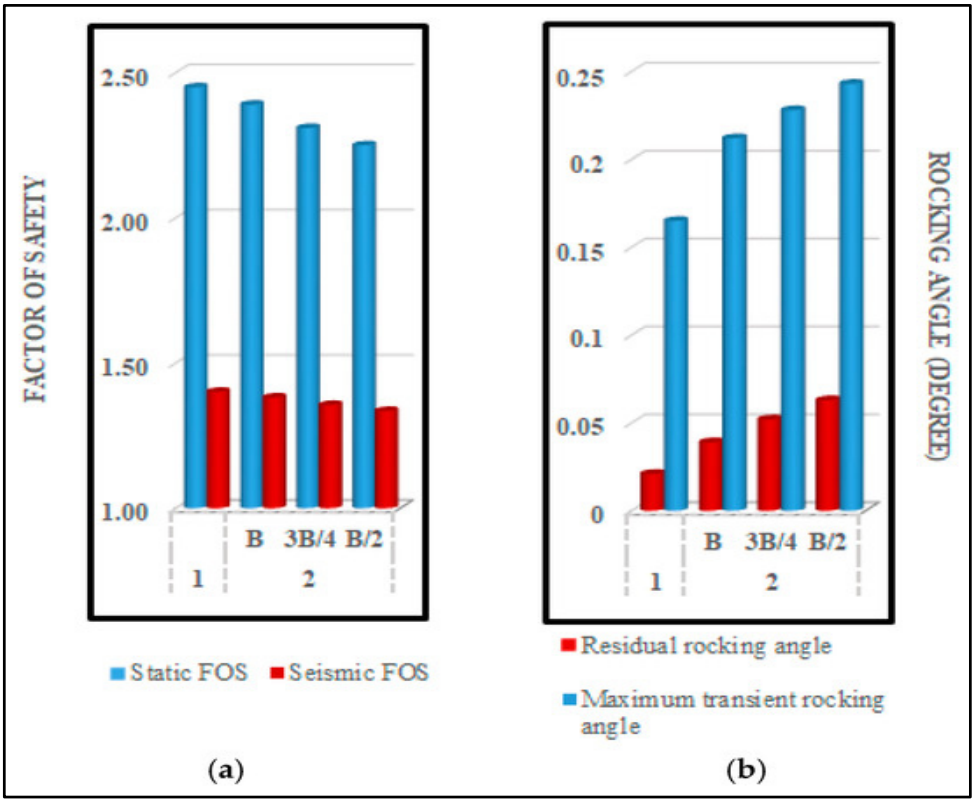

Figure 3.12 Factors Affected By The 2023 Kahramanmaraş-Pazarcık Earthquake: (a) The Shallow Slope's Static-Seismic FOS; (b) The Maximum Transient-Residual Foundation Rocking Angle (Bayraktar et al, 2023)

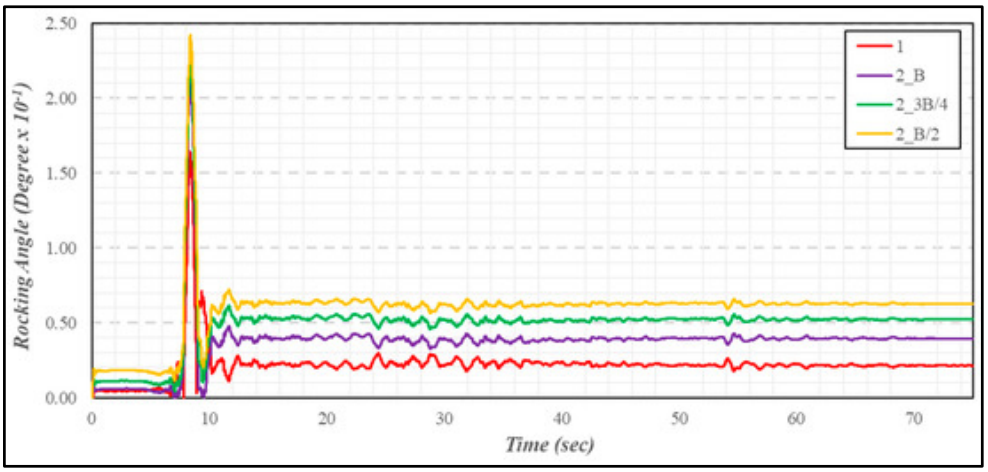

Figure 3.13 The rocking time history of the Building foundation Closest To The Slope Affected By The Kahramanmaraş-Pazarcık Earthquake In 2023 (Bayraktar et al, 2023)

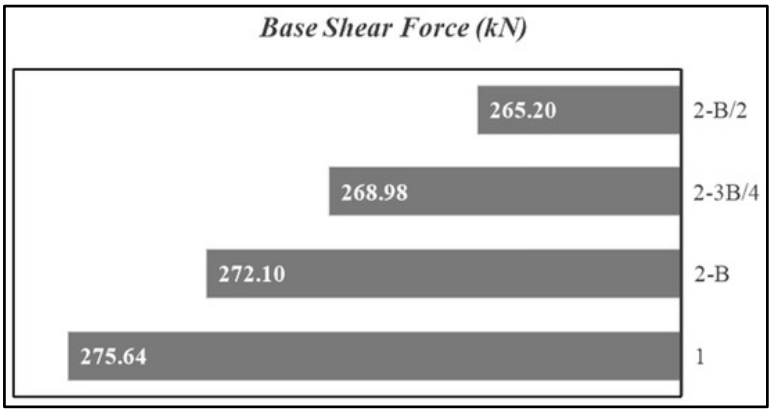

Figure 3.14 The Building Closest To The Slope That Was Affected By The 2023 Kahramanmaraş-Pazarcık Earthquake's Maximum Lateral Displacement (Bayraktar et al, 2023)

3.4 INFLUENCES OF EARTHQUAKES ON SSI PRACTICES IN BOTH COUNTRIES

The need of including soil-structure interaction (SSI) into seismic design approaches has been demonstrated by a study of seismic events in Morocco and Turkey. The 2004 Al Hoceima earthquakes in Morocco and the 1999 Kocaeli and Düzce earthquakes in Turkey provide valuable information, especially about the ways in which soft soils, inadequate foundation systems, and building proximity affect structural performance during seismic events. Morocco's uneven collapse of traditional, non-engineered buildings like masonry and adobe structures in rural areas was mostly caused by local soil characteristics and neglecting. Insufficient seismic detailing combined with the amplification of seismic waves on soft, sloping soils resulted in significant structural damage.

These results clearly demonstrate that Morocco's current seismic design techniques have historically neglected site-specific soil behavior, dangerously underestimating seismic risk. Similarly, post-earthquake research and academic investigations such as Yilmaz's (2022) in Turkey have shown that when SSI is disregarded, mid-rise reinforced concrete buildings with flexible foundations on soft soils experience higher lateral displacements, inter-story drifts, and overall instability.

The findings suggest that rigid foundation assumptions can lead design standards to underestimate the structural requirements under real earthquake conditions, hence compromising safety margins. Furthermore, recent simulations of the Kahramanmaraş-Pazarcık earthquake on February 6, 2023, demonstrated how SSSI significantly raises seismic demands, especially in sloping and heavily populated regions. Buildings next to one other on sloping soft soils at lower altitudes revealed more than 50% increase in maximum story drift and up to 41% increased foundation shaking. This highlights the increasing significance of ground inclination and building closeness, which are often disregarded in traditional seismic regulations.

These geographical and empirical facts lead to four significant implications:

- Underestimating seismic forces results from ignoring SSI and SSSI, especially in areas with heavy construction, steep topography, and soft soils.
- Conventional and informal buildings without professional supervision or adequate seismic features are particularly vulnerable to seismic damage when constructed on flexible or poorly classified soils.
- It is necessary to modify seismic design regulations to explicitly include SSI and SSSI, promote site-specific soil reaction studies, and establish stricter foundation design standards, particularly for mid-rise and rural structures.
- The potential to decrease the number of deaths and financial losses from upcoming earthquakes, as well as awareness and capacity-building

programs for engineers, planners, and the general public, improve resilient urban development.

If Moroccan and Turkish seismic codes are to be strong, they must include advanced SSI modeling, geotechnical site studies, and performance-based design requirements. Without these improvements, structural safety in earthquake-prone areas particularly in rural and sloping regions will remain insufficient. To ensure that the lessons learned from past disasters are fully incorporated into engineering and regulatory practice, future earthquake design should place a high premium on localized soil reactivity, structure interaction effects, and foundation behavior.

CHAPTER 4

4. GEOTECHNICAL EARTHQUAKE ENGINEERING STANDARDS

4.1 INTRODUCTION

For buildings in earthquake-prone areas to be safe and strong, seismic design regulations are essential. In order to reduce possible damage and fatalities, they provide engineers and architects uniform criteria for designing structures that can resist seismic pressures. The Moroccan Seismic Design Code and the Turkish Building Earthquake Code are two well-known seismic design regulations that are compared in this chapter.

The primary objective of this comparison research is to look at the differences and similarities between TBDY 2018 and RPS 2011, especially when it comes to geotechnical earthquake engineering in soil-structure-interaction. The research looks at how each code deals with important issues such soil investigation, soil classifications, importance factors, and foundation. This study's focus is on shedding light on how the regulations in each code affect how well structures deal in earthquakes.

4.2 COMPARATIVE ANALYSIS OF TURKISH AND MOROCCAN SEISMIC PROVISIONS RELATED TO SSI

4.2.1 Site Classification: Ground Types and Vs Criteria

Comparative Evaluation of Local Ground Classification in TBDY-2018 and RPS 2011 categorize soils into identical categories based on characteristics such as shear wave velocity (Vs_{30}), SPT N-values, and undrained shear strength (Cu). The Turkish code provides a more comprehensive and stratified categorization (ZA to ZF) principally based on Vs_{30}, while the Moroccan code

(S1 to S5) depends on a combination evaluation of N_{60}, Cu, and Vs, assuming a more conservative approach for soft and specialized soils.

Variations in Undrained Shear Strength (Cu):

The comparison reveals significant variations in Cu levels within soil classes, which are ZC - S3, ZD - S4, and ZE - S5.

ZC - S3: Cu_{30} > 250 kPa in Turkey vs. > 100 kPa in Morocco

ZD - S4: 100 kPa < Cu_{30} < 250 kPa in Turkey vs. 25–50 kPa in Morocco

ZE - S5: Cu_{30} < 100 kPa (or site-specific) in Turkey vs. < 25 kPa in Morocco (in special conditions)

These differences arise from regional geological variances. Turkish soils, especially in regions such as Istanbul, often demonstrate increased stiffness and density (example, sandstone-claystone with Vs30 approaching 1270 m/s), but Moroccan urban soils (such Rabat or Casablanca) tend to be more compressible and less dense, particularly in Zone II.

The table 4.1 presents the classification of soils according to shear wave velocity (Vs), standard penetration resistance (N-SPT), and undrained shear strength (Su) as per TBDY 2018, while the table 4.2 presents the classification of soil types according to Vs criteria. .

Table 4.1 Site Classification: Ground Types and Vs Criteria (TBDY, 2018)

Local Ground Classes	Type of Soil	$(Vs)_{30}$ [m/s]	$(N_{60})_{30}$ [pulse/30cm]	$(Cu)_{30}$ [kPa]
ZA	Hard and solid rocks	> 1500	-	-
ZB	Rocks that are little worn and medium-solid	760 – 1500	-	-
ZC	Very thick layers of sand, gravel, and stiff clay or rocks that have been used and fragile with a lot of fissures	360 – 760	> 50	> 250

Table 4.1 (Continued) Site Classification: Ground Types and Vs Criteria (TBDY, 2018)

Local Ground Classes	Type of Soil	$(Vs)_{30}$ [m/s]	$(N_{60})_{30}$ [pulse/30cm]	$(Cu)_{30}$ [kPa]
ZD	Medium to firm layers of sand, gravel, or extremely hard clay	180 – 360	15 – 50	70 – 250
ZE	Profiles with layers of loose sand, gravel, or soft to solid clay or a total layer of soft clay (cu < 25 kPa) with a total thickness of more than 3 meters, meeting the parameters of PI > 20 and w > 40%	< 180	< 15	< 70

- ZF - Reasons that need inquiry and review on the site itself:
- 1. Soils that might fall apart after an earthquake (liquefiable soils, very sensitive clays, collapsible weak cemented soils, etc.)
- 2. Clays that are more than 3 meters thick and contain a lot of organic matter in them.
- 3. Clays having a total thickness of more than 8 meters and a high plasticity (PI > 50).
- 4. Soft or medium solid clays that are quite thick (more than 35 m).

Table 4.2 Site Classification: Ground Types and Vs Criteria (RPS, 2011)

Site Class	Soil Type	Standard Penetration Resistance (N_{60})	Undrained Shear Strength (Su) [kPa]	Shear Wave Velocity (Vs) [m/s]
S1: Rock Soil	Rock that is less than 3 m below the foundation is intact.	—	—	Vs ≥ 760
S2: Stiff Soil	Weathered rock; highly stiff, sticky soils; very thick, silty soils; marls or very hard clays	Ns ≥ 50	Su ≥ 100	760 > Vs ≥ 360
S3: Medium Soil	Medium-size sand and gravel; medium-size stiff clay	50 ≥ Ns ≥ 15	100 > Su ≥ 50	360 > Vs ≥ 180
S4: Soft Soil	Loose silty soils	Ns < 15	Su < 50	Vs < 180
S4: Soft Soil (continued)	For soil to be deeper than 3 m, it must have a water content of more than 40% and a plasticity index of more than 20.	—	Su < 25	Vs < 150

The table 4.3 represents the overall comparison of local site classification of both codes standards.

Table 4.3 A comparison of local site classification in TBDY-2018 and RPS2011

Soil Class (TBDY - RPS)	TBDY-2018 (Cu_{30}) [kPa]	RPS-2011 (Cu_{30}) [kPa]	Soil Type (TBDY-2018)	Soil Type (RPS-2011)
ZC - S3	> 250	> 100	Very thick layers of sand, gravel, and hard clay or rocks that have been weathered and are fragile and cracked.	Sand and gravel that is medium dense; clay that is medium stiff
ZD - S4	100 - 250	25 - 50	Sand that is loose, clay that is soft, or silt that is weak	Soils that can be easily compressed or turned into liquid need in-depth geotechnical research.
ZE - S5	< 100 (Site-specific study)	< 25 (Special cases)	Soils that are particularly soft, contain a lot of organic stuff, or can be converted into a liquid or compacted	Soils that can be easily compressed or turned into liquid need in-depth geotechnical research.

The Turkish Building Earthquake Code (TBDY 2018) and the Moroccan Seismic Code (RPS 2011) reveal variances in the symbols and criteria used for

soil type classification. TBDY 2018 classifies local site types from ZA to ZF, mainly according to shear wave velocity (V_{S30}), while RPS 2011 use classifications from S1 to S5, based on a mix of SPT-N_{60} values, undrained shear strength (Su), and shear wave velocity (Vs). A significant difference between TBDY 2018 and RPS 2011 is observed in the undrained shear strength (Su) values calculated for comparable soil conditions. Discrepancies appear in the related classes, including ZC vs. S3, ZD vs. S4, and ZE vs. S5, where the threshold values for Su change. TBDY 2018 emphasizes V_{S30}-based zoning, but RPS 2011 has additional Su limitations, especially for soft and unique soils. The table below compares the undrained shear strength values for corresponding soil classifications in TBDY 2018 and RPS 2011

4.2.2 Local Ground Effect Coefficients

The Turkish Building Earthquake Code (TBDY 2018) and the Moroccan Seismic Code (RPS 2011) derives their seismic design criteria from ground vibrations resulting from earthquakes. The design provisions use a probabilistic seismic hazard methodology, including a 50-year design lifetime with a 10% likelihood of exceedance, equivalent to a 475-year return time, which is a recognized worldwide norm. TBDY 2018 and RPS 2011 use seismic hazard maps that specify spectral acceleration coefficients, essential for determining seismic demand on buildings. These coefficients include two primary vibration periods:

Ss: Coefficient of short-period spectral acceleration (0.2 seconds) S1: Spectral acceleration coefficient at (one second). The coefficients are computed using a 5% damping ratio (in relation to critical damping) and are represented as a fraction of gravitational acceleration (g). Variations in Local Ground Effects TBDY 2018 assigns Fs and F1 independently, taking into account both V_{S30} and seismic zone; coefficients rise for softer soils and elevated ground movements. In TBDY 2018, spectral acceleration values are computed by taking into consideration:

$$SD_S - SM_S = S_S \times F_S - F_a \qquad (4.1)$$

$$SD_1 - SM_1 = S_1 \times F_1 - F_V \quad (4.2)$$

Where:

Ss and S1 represent the designated spectral accelerations. Fs and F1 are the local ground amplification coefficients for their corresponding periods. Conversely, RPS 2011 use a singular coefficient for both short and long durations.

Rather, it employs a singular site coefficient determined by soil classification (S1 to S5)

The coefficients are defined as follows:

S1 (rock or shallow stiff soils): 1.0;

S2 (stiff soils ≥ 30 m or soft soils < 30 m): 1.2;

S3 (soft soils ≥ 15 m or very soft soils < 10 m): 1.4;

S4 (very soft soils ≥ 10 m): 1.8;

S5 (special conditions, example: liquefiable or organic soils): site-specific.

This tabular method misses to distinguish between short-term and long-term coefficients (such as Fs and F1) and presumes a universal amplification factor across the whole design spectrum, the tables 4.5 and 4.6 respectively show the the local ground effect coefficients for short and l second period, both of F1 and Fs.

RPS 2011 defines a singular amplification value for each site, independent of the spectral period. For instance:

S1 = 1.0

S2 = 1.2

S3 = 1.4

S4 = 1.8

S5 = specific-site

The Moroccan code is hence easier to understand although less responsive to spectral change. The table 4.4. compares local ground effect coefficients for the short-period area as outlined in the Turkish Building Earthquake Code (TBDY 2018) and the Moroccan earthquake Code (RPS

2011), emphasizing the distinct approaches each standard adopts for various soil classifications in earthquake design.

Table 4.4 Site Coefficient Based on Soil Nature (RPS, 2011)

Site	Soil Description	Coefficient
S1	Rock at all depths Stiff soils, thickness < 30 m	1
S2	Stiff soils, thickness ≥ 30 m Medium soils, thickness < 30 m	1.2
S3	Medium soils, thickness ≥ 15 m Soft soils, thickness < 10 m	1.4
S4	Soft soils, thickness ≥ 10 m	1.8
S5	Special conditions	*

Table 4.5 Local Ground Effect Coefficients (Fs) For The Short Period Region (TBDY, 2018)

Type of Soil	Ss ≤ 0.25	Ss = 0.50	Ss = 0.75	Ss = 1.00	Ss = 1.25	Ss ≥ 1.50
ZA	0.8	0.8	0.8	0.8	0.8	0.8
ZB	0.9	0.9	0.9	0.9	0.9	0.9
ZC	1.3	1.2	1.1	1.0	1.0	1.0
ZD	2.4	1.9	1.6	1.3	1.1	1.0
ZE	2.4	2.0	1.8	1.5	1.2	0.8
ZF	Site specific analysis					

Table 4.6 Local Ground Effect Coefficients (F1) for 1.0s period (TBDY, 2018)

Yerel Zemin Sınıfı	S1 ≤ 0.10	S1 = 0.20	S1 = 0.30	S1 = 0.40	S1 = 0.50	S1 ≥ 0.60
ZA	0.8	0.8	0.8	0.8	0.8	0.8
ZB	0.8	0.8	0.8	0.8	0.8	0.8
ZC	1.4	1.3	1.2	1.1	1.0	0.9
ZD	2.4	2.2	2.0	1.8	1.7	1.7
ZE	3.5	3.0	2.6	2.3	2.1	2.0
ZF	Site specific analysis					

To resume the comparison of both codes in accordance to local ground effect, the table 4.7 is created.

Table 4.7 Comparison of Local Ground Effect Coefficients in (TBDY 2018, RPS, 2011**)**

Soil Class	Turkey (TBDY2018) – Fs	Morocco (RPS2011)– SiteCoefficient	Soil Description
ZA / S1	Fs = 0.8	1.0	Rock or very stiff soils
ZB / S2	Fs = 0.9	1.2	Stiff soils (≥30m) or medium soils (<30m)
ZC / S3	Fs ≈ 1.0–1.2	1.4	Medium to soft soils
ZD / S4	Fs ≈ 1.3–1.9	1.8	Soft soils (≥10m thickness)
ZE / S5	Fs ≈ 2.0–2.4	*	Very soft soils or special site conditions

Table 4.7 (Continued) Comparison of Local Ground Effect Coefficients in TBDY 2018 and RPS2011

Soil Class	Turkey (TBDY2018) – Fs	Morocco (RPS2011)-Site Coefficient	Soil Description
ZF / —	Site-specific analysis required	—	Custom behavior analysis required

This table combines the local ground effect coefficients used in the Turkish Seismic Code (TBDY 2018) with the Moroccan Seismic Code (RPS 2011). Turkey employs variable coefficients (Fs) based on short-period spectral acceleration (Ss) and soil classification (ZA–ZF), while Morocco specifies a fixed coefficient for each soil category (S1–S5).

4.2.3 Seismic hazards distribution in Turkey and Morocco

4.2.3.1 Turkey

Previous earthquakes have exposed several issues, such as insufficient reinforcing, low concrete integrity, inadequate lateral stiffness, weak ductility, and insufficient column strength. These factors have exacerbated the susceptibility of structures during earthquake events. The seismic hazard map of Turkey, shown in figure 4.1, was first published in 1972 and subsequently revised in 1996. The graphic categorizes the nation into five separate zones according to the degree of seismic risk. The first zone denotes regions with high seismic activity risk, whilst the fifth zone signifies locations with less seismic exposure (Ilki, Celep, 2012).

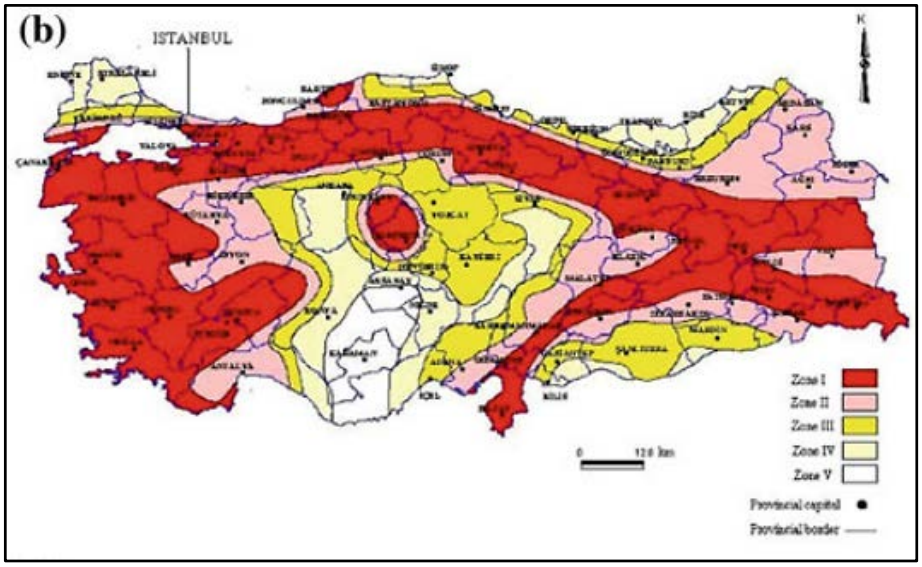

Figure 4.1 Seismic hazard distribution in Turkey until 2012 (Ilki,Celep, 2012).

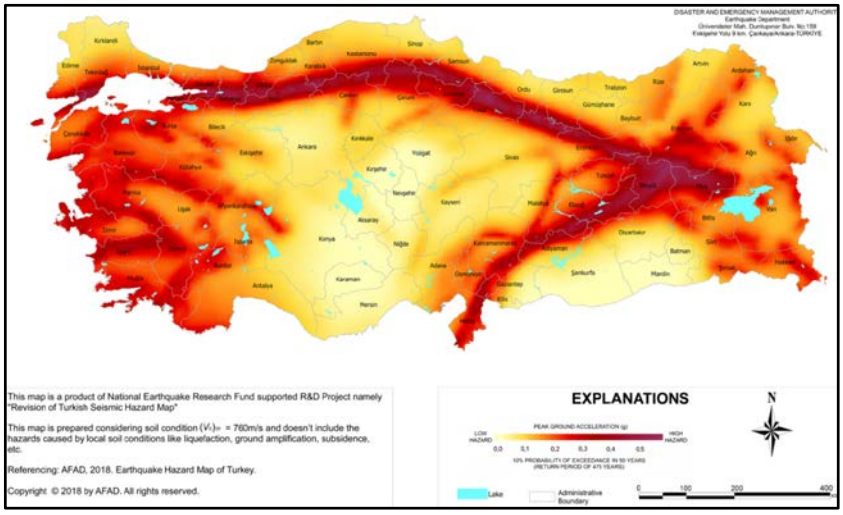

Figure 4.2 Seismic hazard distribution in Turkey (AFAD,2018)

The revised map was created with the more comprehensive data. The new map displays peak ground acceleration values, in contrast to the old graphic, which illustrated earthquake zones as we can compare from both figures. In the updated map, danger levels rise from yellow to red. (AFAD), as it is observed in figure 4.2.

4.2.3.2 Morocco

(Ziraoui et al, 2024) The RPS 2000 version 2011 employs a zonal technique to simplify the computation of seismic loads and to unify structural design criteria over extensive areas of the nation. This involves separating the nation into many zones of uniform seismicity, each showing a comparable degree of seismic danger with a certain probability of occurrence. The seismic zone map in figure 4.3 created by the RPS 2000 has five zones corresponding to the highest horizontal ground acceleration with a 10% probability of occurring during a 50-year period. This probability is considered realistic, given it applies to moderate earthquakes that are expected to occur several times over a structure's lifetime. In each zone, the factors that delineate the seismic danger, such as horizontal ground acceleration, are regarded as constant with:

Zone 1: Amax/g=0.04

Zone 2: Amax/g=0.07

Zone 3: Amax/g=0.1

Zone 4: Amax/g=0.14

Zone 5: Amax/g=0.18

The map of seismic zones in Morocco is presented in Figure 4.2.

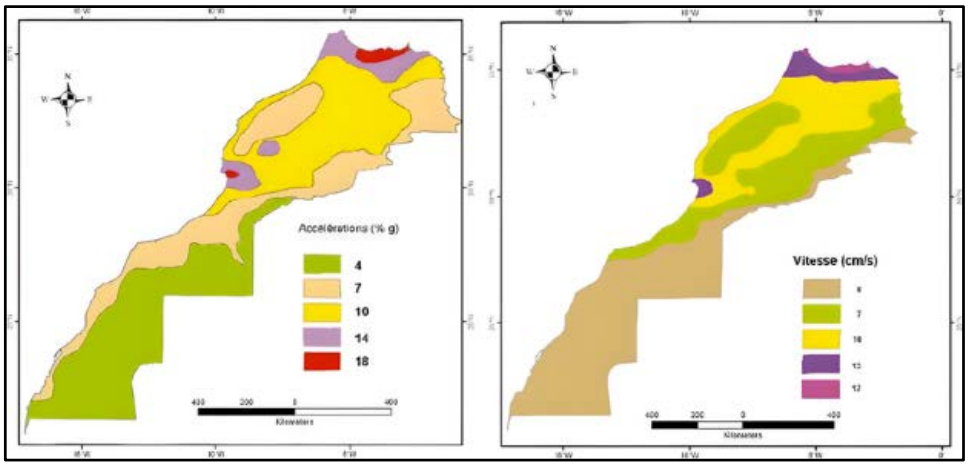

Figure 4.3 Map of the five seismic zones of Morocco (RPS, 2011)

4.2.4 Seismic Spectral Acceleration Formulas and Response Spectrum Input

The spectrum of the elastic response using modular functions that are dependent on natural period (T), soil factor (S), and peak ground acceleration (ag), Se (T) is defined in both of these standards. Furthermore, the Turkish Building Earthquake Code (TBDY 2018) establishes the vertical elastic design spectrum, which is represented by the symbol SeD(T). This spectrum is in addition to the horizontal design spectrum. This spectrum is used for the purpose of assessing the vertical acceleration demand on structures, which is particularly significant for tall buildings and essential infrastructure applications, the design spectral acceleration is presented in figure 4.4.

According to TBDY 2018:

$S_{eD}(T) = (0.32 + 0.48 \times T / T_{AD}) \times S_{DS}$ for $0 \leq T \leq T_{AD}$ (4.3)

$S_{eD}(T) = 0.8 \times S_{DS}$ for $T_{AD} \leq T \leq T_{BD}$ (4.4)

$S_{eD}(T) = 0.8 \times S_{DS} \times T_{BD} / T$ for $T_{BD} \leq T \leq T_{LD}$ (4.5)

Where:

S_{DS} is the design spectral acceleration over short intervals (same as horizontal)

T_{AD}, T_{BD}, and T_{LD} refer to vertical spectrum transition times computed as:

$T_{AD} = T_A / 3$ (4.6)

$T_{BD} = T_B / 3$ (4.7)

$T_{LD} = T_L / 2$ (4.8)

These expressions are important when evaluating vertical accelerations that can affect structural elements differently from horizontal loads.

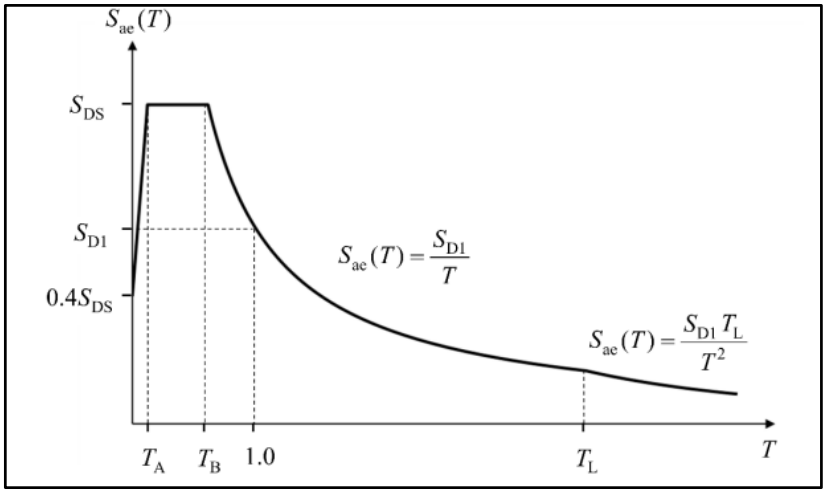

Figure 4.4 Design spectral acceleration according (TBDY, 2018)

Represented by the ratio of spectral zones Za and Zv, the Moroccan seismic code (RPS 2011) specifies the spectral response using a dynamic amplification factor (D). Standard damping is 5%; the amplification factor changes with T, the vibration period. A correcting factor m = $(5/x)^{0.4}$ is used for different damping levels.

Table 4.8 Spectral amplification factor (D) formulas (RPS, 2011)

Za / Zv Ratio	T ≤ 0.25 s	0.25 <T<0.50	T ≥ 0.50s
1 <	1.9	1.9	$1.20 \times T\text{^}(-2/3)$
1 =	2.5	$-2.4 \times T + 3.1$	-
1 >	3.5	$-6.4 \times T + 5.1$	-

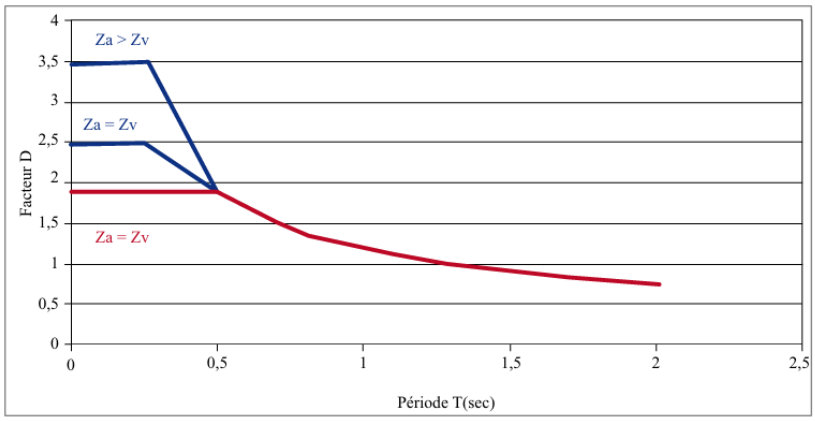

Figure 4.5 Spectral Amplification Factor D according to Moroccan Code (RPS, 2011)

Compared to previous codes, the spectral response of the Moroccan seismic code (RPS, 2011) is not explicitly expressed in terms of an explicit Se (T) formula. Rather, the building of the design spectrum is predicated on the dynamic amplification factor D, which varies with the ratio of the spectral acceleration at short intervals (Za) to that at long periods (Zv). As created in table 4.8, across three time intervals: $T \leq 0.25$ s, $0.25 < T < 0.5$ s, and $T \geq 0.5$ s, the amplification factor D is depending on the value of Za/Zv, each interval has its own formulation either larger than, equal to, or less than 1, the curves are showed in figure 4.5.

Additionally, the Moroccan code adjusts for damping values different from the standard 5% by int Furthermore, the Moroccan code includes a scaling factor $m = (5/x)\text{^}0.4$, where x is the real damping ratio, therefore modifying for values varying from the usual 5%. This suggests that, before the application in numerical models such as PLAXIS, the last spectrum used for structural analysis is a modified form of the base curve that requires hand changes. By contrast, the design spectrum is clearly defined by the Turkish seismic code (TBDY 2018) utilizing well-structured formulas for horizontal and vertical spectral accelerations, respectively, indicated as Se(T) and SeD(T).

Based on transition periods TA, TB, and TL, the design spectrum is established across piecewise segments varying depending on the local ground class (ZA to ZE). Directly included in the code, these formulae are instantly available for time history or response spectrum analysis in PLAXIS.

In contrast to the Moroccan code, TBDY 2018 defaults to a 5% damping ratio, including the effects of soil conditions directly into the spectrum via site categorization and significance factors. Consequently, the design process is increasingly automated and incorporated into structural analysis procedures, removing the need for external spectrum corrections or amplification factors.

The Moroccan code-based spectrum (RPS 2011) continues to use piecewise elastic response formula. According to Za/Zv ratios. The soil factor S (1.0-1.8) multiplies ag (ground acceleration), with transitions defined at T = 0.25 s and 0.5 s. The differences are created in table 4.9.

Table 4.9 Comparison of Spectrum Types for both of Code Standards

Characteristic	TBDY 2018 (Turkey)	RPS / Springer (Morocco)
Spectrum Type	Multi-slope elastic spectrum	Elastic+performance-based
Composition	Piecewise, based on Ss, S1, TA, TB, TD	Piecewise in RPS 2011; efficiency spectrum in article
Transitional Phases	TA, TB, TD, TL (site-defined)	0.25 s and 0.5 s (RPS), unspecified in PBSD graph
Spectral Inputs	$SDS = SS \times FS, SD1 = S1 \times F1$	$Sa = V/M$ from pushover
Significance of SSI	Direct input to PLAXIS via Se(T)	Ideal for nonlinear SSI modeling with capacity demand
Design Style	Code-specified elastic spectrum	Performance-based for crucial structures

4.2.5 Earthquake Design Class and Building Importance Factor

The Turkish Building Earthquake Code 2018 (TBDY 2018) and the Moroccan Seismic Design Code (RPS 2011) admit the need of modifying seismic design forces according to a structure's significance, although they vary in their classification of structures and their distribution of Importance Factors (I).

In TBDY 2018, the significance of buildings is classified under the idea of Bina Kullanım Sınıfı (BKS), or building use class, which is divided into three categories: BKS=1, BKS=2, and BKS=3. For BKS=1, including essential structures like hospitals, emergency operation centers, and structures essential for post-earthquake operations (such, military, civil defense), an importance factor of 1.5 is used. This illustrates the Turkish code's emphasis on earthquake safety for essential infrastructure. The Moroccan RPS 2011 categorizes buildings according to their occupancy and structural objective. The Moroccan code assigns a significance factor of 1.4 to 1.5 for Category III and IV buildings, which include vital facilities such as hospitals, fire stations, and key communication centers. This alignment in critical categories indicates a mutual acknowledgment of the operational continuity requirements of these facilities during seismic events. For structures of moderate significance, including schools, government structures, and substantial public-use facilities (example: stadiums, malls, etc), TBDY 2018 designates BKS=2, with an importance factor of 1.2. The RPS 2011 employs a comparable degree of conservatism, generally defining a significance factor of 1.2 for these structures, although the Moroccan code is somewhat simpler in its categorization approach.

For typical structures, such as buildings, small offices, commercial units, and some industrial buildings, both codes specify a fundamental important factor of 1.0. This comprises constructions whose collapse, while undesirable, would not result in mass fatalities or significant disruption. The table 4.10 outlines the categorization of key factors for both TBDY 2018 and RPS 2011.

TBDY 2018 and RPS 2011 categorize buildings according to their significance and occupancy classification, influencing seismic load computations.

Table 4.10 Earthquake Design Class and Building Importance Factor in both TBDY (2018) and RPS (2011)

Standard	Importance Class	Importance Factor (I)	Examples
TBDY 2018	Class I	BKS = 1 1.5	Hospitals, emergency buildings
TBDY 2018	Class II	1.4	Schools, public buildings
TBDY 2018	Class III	BKS = 2 1.2	Commercial/residential buildings
TBDY 2018	Class IV	BKS = 3 1.0	Temporary or agricultural structures
RPS 2011	Category A	1.5	Critical infrastructure, hospitals
RPS 2011	Category B	1.3	High-occupancy buildings
RPS 2011	Category C	1.0	Ordinary use buildings
RPS 2011	Category D	0.8	Low-occupancy or temporary use

4.2.6 Structural Period, Natural Frequency and Resonance Considerations

The fundamental vibration period T, which defines the mass and stiffness of the structure, may be determined by appropriate dynamic analysis or by using Rayleigh's approach. However, empirical formulae can be used under certain specific situations.

4.2.6.1 Turkish Seismic Code (TBDY 2018)

The basic period T may be calculated using the below simplified formulas:

For reinforced concrete or braced steel frameworks:

$T = 0.075 \times H\text{^}0.75$ (4.9)

Where H represents the overall height of the building

The dynamic technique method must fulfill these requirements:

a) Spectral response is dependent upon the exact specific site.

b) Direct time-history analysis must use site-specific accelerograms.

c) The effective seismic load (Vt) should not be less than 90% derived from the corresponding static method.

Significant application for SSI analysis and resonance evaluation

The above expressions correlate mass and stiffness with structural period. It is essential in resonance assessment, where matching between soil period and structure period may improve the response.

Empirical Period Formula

In accordance to TBDY 2018, the estimated fundamental vibration period TpA is presented by:

$TpA = Ct \times Hn\text{^}¾$ (4.10)

Where:

TpA: estimated duration (s)

Ct: Coefficient depending upon type of structure (0.10 for RC frames, 0.08 for steel frames, 0.07 for other types)

Hm: Overall height of the structure (m)

1.2 Rayleigh Limit

The Rayleigh approach may be used to investigate the modal period T_p, but it should not surpass 1.4 times the empirical period:

$T_p \leq 1.4 \times T_pA$ (4.11)

Conditions of dynamic method

Dynamic analysis may be used just when height or regularity criteria are not met. Essential prerequisites requirements include:

The spectral response should be site-specific.

Time-history analysis must use site-compatible accelerograms.

The resulting base shear (V_t) must be not less than 90% of the static equivalent base shear.

4.2.6.2 Moroccan Seismic Code (RPS 2011)

Empirical Period Formulas

According the Moroccan standards, RPS 2011, the fundamental period T can be represented by various formulas:

$T = 0.075 \times H\text{^}0.75$ for RC/steel braced frames (4.12)

$T = 0.085 \times H\text{^}0.75$ for rigid steel frames (4.13)

$T = 0.09 \times H / \sqrt{L}$ for structures with walls (4.14)

$T = 1.8 \times \sqrt{(mH/EI)}$ for cantilever buildings (4.15)

$T = 2N(N+1) \times \sqrt{(M/k)}$ for buildings with infill panels (4.16)

Dynamic Method

RPS 2011 permits dynamic analysis with site-specific spectral response or time-history input. The dynamic base shear should not be inferior than 90% of the static base shear.

Concerning SSI

Both standards codes integrate SSI effects by connecting the structure's mass and stiffness to the period T. Resonance may occur when soil and structure periods coincide resulting in amplified responses. The comparison is represented in table 4.11.

Table 4.11 Comparison of TBDY(2018) and RPS(2011)

Characteristic	TBDY 2018 (Turkey)	RPS 2011 (Morocco)
Empirical Period Formula	$TpA = Ct \times Hn\text{^}¾$	$T = C \times H\text{^}0.75$ or $T = 0.09 \times H/\sqrt{L}$
C_t / C Coefficients	0.10 (RC), 0.08 (Steel), 0.07 (Others)	0.075 to 0.085 based on type of structure
Rayleigh Limit	Tp ≤ 1.4 × TpA	Implicitly indicated, however regulated by base shear
Dynamic Method	Mandatory if height or irregularity criteria are present	Used if necessary by site circumstances
Accelerogram Requirement	Site-specific accelerograms are necessary	Site-specific accelerograms are required
Base Shear Control	Vt ≥ 90% of static equivalent	Vt ≥ 90% of static equivalent
SSI Consideration	Directly influences Se(T) and period Tp values	Consequences through soil classification and dynamic amplification

The determination of the natural period (T) influences the input of the response spectrum. Both standards include calculations or empirical guidelines based on height and structural classification, for a clear description of the differences, the table 4.12 shows the formulas used in each code.

Table 4.12 Structural Period, Natural Frequency, and Resonance Considerations in both Codes

Standard	Formula/Method	Notes
TBDY 2018	$T = Ct * H\hat{}x$ (empirical)	Ct and x vary according to the structural system
TBDY 2018	Modal analysis (dynamic)	Preferred for irregular or tall buildings
RPS 2011	$T = 0.1 \cdot N$	N = number of stories (approximate)
RPS 2011	$T = 2\pi\sqrt{(m/k)}$	For regular systems, based on rigidity and mass

4.3.7 Foundation Design Provisions: Shallow and Deep Foundations

Shallow Foundation Design in Morocco (RPS 2011)

According to the Moroccan Seismic Design Code (RPS 2011), shallow foundations must be designed considering both permanent (dead loads, permanent imposed loads) and dynamic actions resulting from seismic loads. The standard non-seismic design methods are generally applied. The design must verify soil bearing capacity, settlement, and the rotation of the foundation. Specific safety coefficients are provided:

1.5 with respect to ultimate bearing capacity

1.2 with respect to sliding

1.2 with respect to settlement

Furthermore, foundations must comply with limitations on vertical displacements as stated in the technical specifications of the project. In seismic zones, additional attention is required to verify the soil's equilibrium state before, during, and after vibration effects. The effect of liquefaction, lateral spreading, and seismic amplification must be evaluated. Although no specific formula is given in RPS 2011 for shallow foundation capacity, general

empirical and analytical approaches are accepted as long as they ensure compliance with serviceability and safety requirements.

4.3.7.1 Shallow Foundation Design in Turkey (TBDY 2018)

The Turkish Building Earthquake Code (TBDY-2018) allows the use of shallow foundations when the soil's bearing capacity at shallow depth is sufficient, particularly when bedrock is encountered at shallow levels. It is applicable when the foundation width (B) is larger than the foundation depth (D), usually with D ≤ 3 m. Groundwater conditions must also be evaluated.

The ultimate bearing capacity of shallow foundations is calculated using Hansen's equation, which includes shape, depth, inclination, ground, and load factors:

$$q_k = cN_c s_c d_c i_c g_c b_c + qN_q s_q d_q i_q g_q b_q + 0.5\,\gamma \grave{B} N_\gamma s_\gamma d_\gamma i_\gamma g_\gamma b_\gamma \quad (4.17)$$

Where:

- q_k = ultimate bearing capacity
- c = cohesion of soil
- q = surcharge (overburden) pressure
- γ = unit weight of soil
- B = width of foundation
- N_c, N_q, N_γ = bearing capacity factors based on φ (internal friction angle)- s, d, i, g, b = shape, depth, inclination, ground, and base factors for each term

The TBDY-2018 provides a consistent methodology for calculating and validating foundation performance, especially under seismic loads. It requires a factor of safety of at least 3.0 under static loading and adjusts values for seismic effect.

4.3.8 Liquefaction Resistance Criteria

4.3.8.1 Liquefaction and Settlement Criteria in Morocco (RPS 2011)

According to the Moroccan Seismic Design Code (RPS 2011), liquefaction is defined as the phenomenon where seismic loads densify granular soils, which rapidly increases pore water pressure and reduces effective stress, leading to a sudden loss of shear strength. The RPS emphasizes that foundation soils in seismic zones should be verified to ensure they are not prone to liquefaction. If they are, appropriate engineering measures must be applied to mitigate the risk. Liquefaction susceptibility is assessed using parameters such as grain size distribution, grain shape, in-situ unit weight, and effective vertical stress (σ′vo), especially within the top 20 meters of the soil profile. The RPS does not define a specific formula but identifies soils as susceptible if they meet characteristics like a saturation degree Sr ≈ 100%, Cu ≤ 15, D50 between 0.05 mm and 1.5 mm, and a liquid limit LL ≤ 35%. Fine silty sands and clays with low plasticity (IL < 0.75) are also flagged. Granular soils matching these parameters are deemed to fall within the liquefaction risk zone. Although RPS 2011 does not prescribe numeric liquefaction resistance calculations, its approach relies on visual and field assessments supported by geotechnical parameters.

4.2.8.2 Liquefaction and Settlement Criteria in Turkey (TBDY 2018)

The Turkish Building Earthquake Code (TBEC / TBDY-2018) implements a rigorous, quantitative framework to assess liquefaction by comparing liquefaction resistance to induced shear stress during an earthquake. The liquefaction resistance (τ_R) is calculated using:

$$\tau_R = CRR_{M7.5} C_M \sigma'_{Vo} \quad (4.18)$$

Where:

CRR_M7.5: Cyclic Resistance Ratio for a moment magnitude of 7.5, calculated as:

$$RR_{M7.5} = \frac{1}{34-N_{1,60f}} + \frac{N_{1,60f}}{135} + \frac{50}{(10N_{1,60f}+45)^2} - \frac{1}{200} \qquad (4.19)$$

N_1,60f: SPT value corrected for fines content

(Idriss & Seed's, 1997) C_M: Earthquake magnitude correction factor

$$C_M = \frac{10^{2.24}}{M_W^{2.56}} \qquad (4.20)$$

σ′vo: Effective vertical stress at the depth considered.

To determine the earthquake-induced shear stress (τ_earthquake), TBDY uses:

$$\tau_{\text{earthquake}} = 0.65\sigma_{Vo}(0.45SD_S)r \quad (4.21)$$

Where:

σ_vo: Total vertical stress

SDS: Short-period spectral acceleration coefficient

r_d: Stress reduction coefficient based on depth.

These formulas allow the engineer to calculate the factor of safety against liquefaction by comparing τ_R and τ_earthquake. TBDY-2018 requires this safety factor to be FS ≥ 1.10. The methodology offers high precision by incorporating site-specific dynamic soil properties, spectral response data, and seismic hazard parameters.

In summary, there are notable distinctions between the two codes. TBDY-2018 places a greater emphasis on calculating liquefaction resistance using detailed formulas based on cyclic resistance ratios (CRR_M7.5), design earthquake magnitude correction (C_M), effective vertical stress (σ′vo), and earthquake-induced shear stress. These are integrated into analytical equations that enable engineers to compute liquefaction risk quantitatively. In contrast, the Moroccan RPS 2011 approach is more qualitative and relies on assessing field parameters such as grain size, soil plasticity, saturation, and effective stress without direct computation of τ_R or τ_earthquake. Moreover, TBDY requires a safety factor of FS ≥ 1.10, while RPS 2011 does not specify a numerical threshold. These variations reflect the differences in seismic risk levels, geotechnical practices, and soil characteristics of each country. The Turkish Earthquake Code (TBDY 2018) defines a comprehensive and

prescriptive methodology for using SPT in liquefaction analysis, including correction factors and threshold charts. In contrast, the Moroccan code RPS 2011 includes the use of SPT and CPT to evaluate liquefaction potential.

CHAPTER 5

5. CASE STUDY & METHODOLOGY

5.1 OVERVİEW OF CASE STUDY

5.1.1 Story Building with Raft Foundation

The case study in this thesis research is based on the **Benleo Park Acıbadem project** of **30.622,26** m^2, a premium residence has been selected, located in **Acıbadem/Üsküdar/Istanbul/Turkey, strated the construction in 2018**. The project has its realistic geotechnical data availability, located in a seismically active region, and structural typology that aligns with the scope of this thesis. Developed by Esta Construction, Benleo Park Acıbadem consists of 8 Mid-rise buildings with modern architectural and structural designs. The top views of the project and its located area are shown in figures 5.1 and 5.2.

Figure 5.1 Top View of the Benleo Project

The chosen case study of a 15-story reinforced concrete structure with a raft foundation corresponds to the research objectives of this thesis, which aims to evaluate soil-structure interaction (SSI) under certain seismic code conditions. This kind of building provides a reasonable and crucial scenarios for SSI studies, due to the effect of height, and foundation type. A raft foundation interacts generally with the underlying soil, so it is very sensitive to geotechnical changes and seismic stresses.

Figure 5.2 Top View of the Benleo Project

There are eight basement levels, one ground floor, eight regular floors, and one attic floor in the Benesta Acibadem Project. The structure's floor heights are 2.9 meters in the eighth basement, 4.0 meters in the seventh, and 3.4 meters between the sixth and seventh basements. The height of the eighth and ninth floors is 3.6 m. The building will be used as a residence. It will be built using a traditional reinforced concrete technology and be a reinforced concrete building. In this study, a specific 15-story reinforced concrete building (A4) with a raft foundation was chosen as the representative structure for Soil-Structure Interaction (SSI) analysis, as shown in the figure 5.3, and in figure

5.4 shows the visiting day of the construction site in order to observe the building and collect informations concerning analysis.

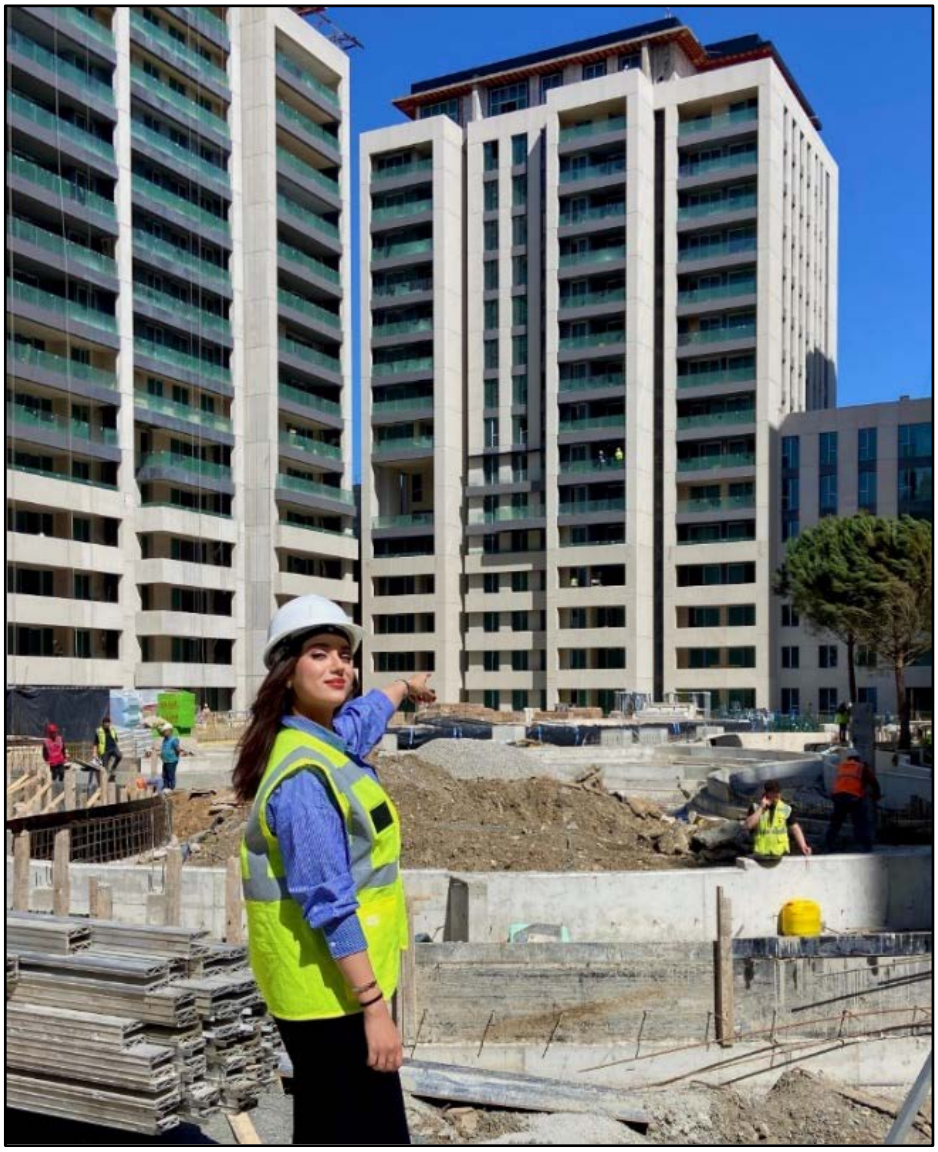

Figure 5.3 Front View Of Block A4 Chosen For Case Study From Site Of Construction

Figure 5.4 Observation Of The Building A4 While Site Visit

5.1.2 Numerical Models : 2D and 3D

5.1.2.1 3D Model (ETABS)

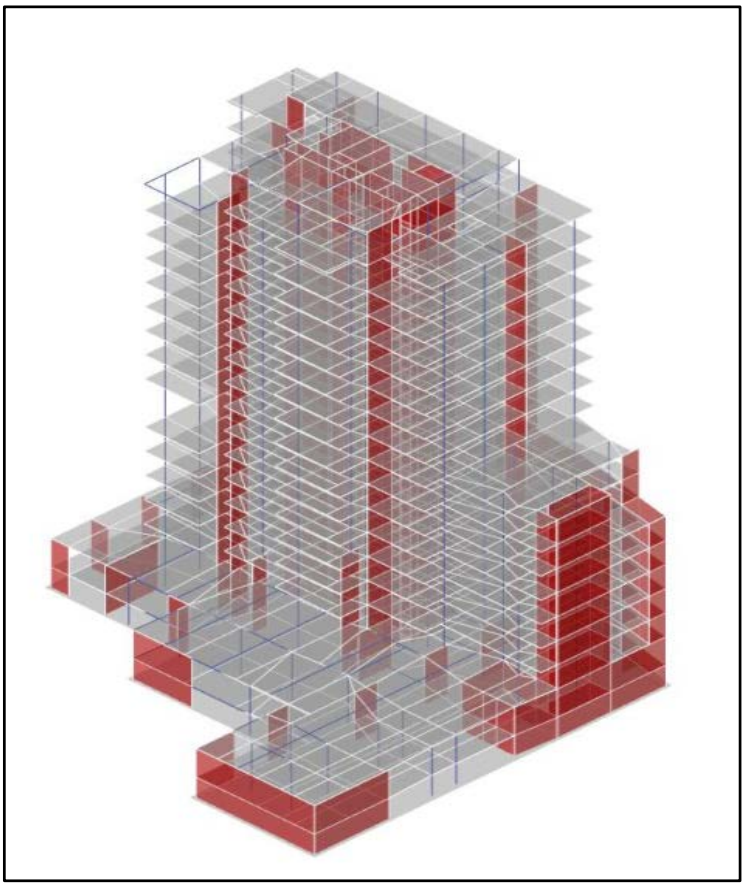

Figure 5.5 Structure A4 Block (3D view by ETABS)

The figure 5.5 shows the ETABS 3D structural model of Structure A4 Block, illustrating the internal structural system used for analysis and design. The model includes beams, columns, shear walls, and slab systems, allowing comprehensive performance-based seismic and static assessments. This perspective emphasizes the structural framework underlying SSI modeling, developed during the comprehensive structural design process by AGM Mühendislik (May, 2022).

5.1.2.2 2D Model (AUTOCAD)

Figure 5.6 Section Plan Of Block A4 (1/100)

The architectural design project prepared by TAGO Architecture was taken as the basis for the structural design. This figure 5.6 shows cross-section of the A4-Block's 2D architectural representation produced in AutoCAD of 1/100 scale. The model shows in details the outward geometry, height, floor measures, and footprint of the building. Using this plan, the building design, foundation layout, and structural measurements were all determined upon; these elements were then included into the PLAXIS 2D model to recreate reasonable load transfer with the appropriate building dimensions, that are :

Dimensions:

Height of building: 51.50 m

Height of single-floor: 3.4 m

Width of foundation (x-direction): 25.50 m

Thickness of Foundation(y-direction): 7 m

5.2 GEOTECHNICAL DATA (TURKEY)

The Turkish Standards and other relevant requirements listed below were employed in the structural foundation design.

TS 498 Calculation values of loads to be considered when Structural Elements are measured.Turkish Building Earthquake Regulation TBDY-2018.

As suggested by the appropriate soil report, the structure's foundation was found to be a raft foundation. The geotechnical report includes detailed calculations related to the foundation.

Boreholes excavations were done at eight different points in the investigation region, ranging in depth from 21.0 to 44.0 meters. Three distinct boreholes machines were used for the drilling of the units. As shown in the figure 5.7, drilling machines and sample boxes are connected:

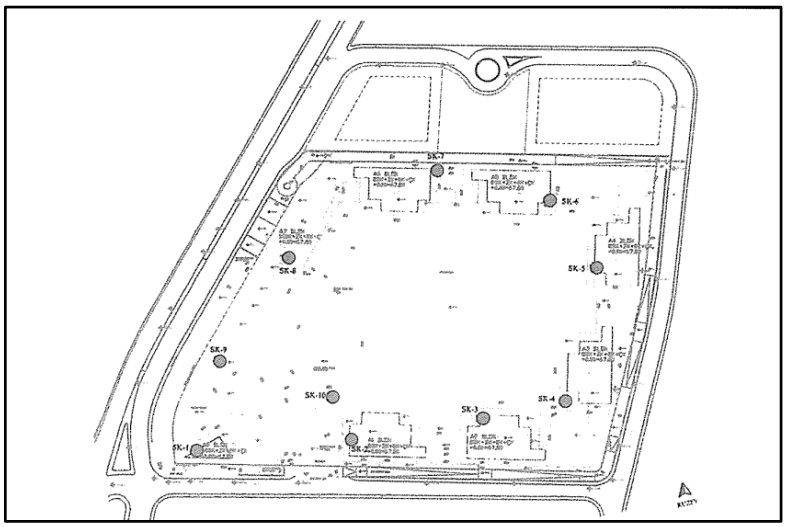

Figure 5.7 Drilling Location Map

Figure 5.8 Sample Box Display Of Borehole SK 5 Investigation

The figure 5.8 shows extracted soil core samples from a geotechnical drill performed at the project construction site. The samples are arranged in labeled core boxes for visual examination and categorization. The sign at the top specifies borehole identification (SK 5), depth intervals, and fundamental field observations. This picture illustrates a segment of the geotechnical research process, used to determine soil stratigraphy, consistency, and composition crucial data for numerical modeling and soil-structure interaction analysis.

Table 5.1 Borehole Results Of Sk5

Borehole No.	Depth (m)	Coordinates (X, Y)	Elevation (Z)	Layer Depth (m)	Lithology / Formation
SK5	40.0	420940.0184, 4541819.552	68.15	0–20	Fill / Artificial Fill
				20–40	Sandstone-Mudstone / Denizli Köyü

Formation

The table 5.1 presents the geotechnical and geological values and parameters are obtained from borehole SK5, which was drilled as part of the site investigation for the building that was selected from the project in the case study.

The borehole reaches a depth of 40.0 meters and is located at the geographic coordinates of X: 420940.0184, Y: 4541819.552, with a soil surface elevation of 68.15 meters. Three separate geological layers, each showing different depositional and structural features, compose the subsurface conditions found at the SK5 site. A small fill layer that is about two meters thick can be observed at the top of the profile. This layer is made up of various man-made materials that were probably added during earlier grading or building processes, so it will not be taken into consideration, while modeling the soil characteristics in finite element PLAXIS2D, because it is usually composed of a mixture of trash and it has an uneven texture and inconsistent grain structure. A considerable alluvial deposit lies under the fill, ranging in depth from 2 meters to around 20 meters. This layer's natural fluvial origin is indicated by its yellowish-brown shade color and coarse and fine gravelly stream material.

Between 20 meters and the ultimate borehole depth of 40 meters, the soil evolves into a more cemented and geologically detailed structure. The bottom layer is grayish to ash-colored and has evidence of weathering, including visible fractures and fissures. It comprises clastic veins and is mostly clayey in nature, with sporadic interlayers of limestone, sandstone, and mudstone. The existence of various rock types indicates sedimentary origins and affects the variety in stiffness and permeability throughout the layers of rock. This layer is crucial for engineering study due to its influence on bearing capacity and its interaction with foundation components. A soil profile of the borehole used in the case study is presented in the figure 5.9.

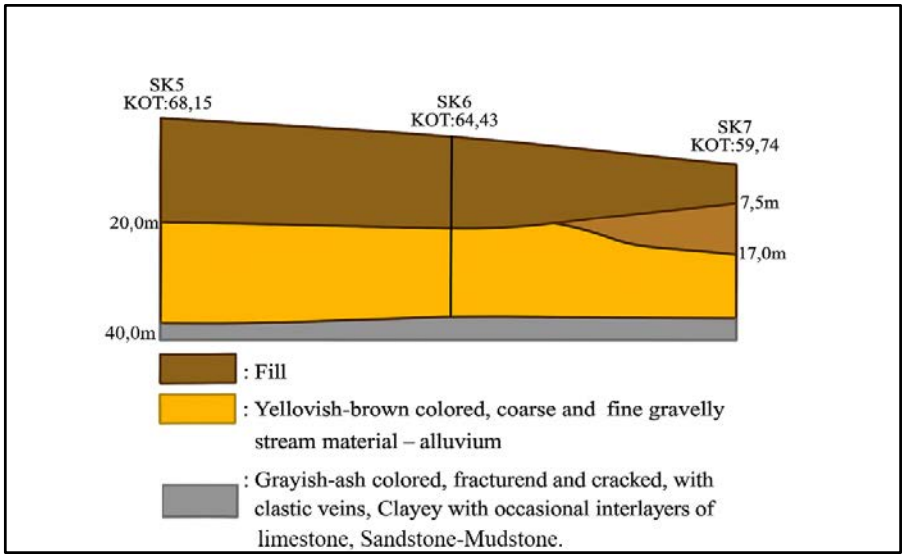

Figure 5.9 Soil profile of boreholes SK5, SK6, SK7

In determining the design parameters for the soils, the outcomes were used together with the physical characteristics that were assessed by laboratory tests on representative samples obtained from the drillings.

The appropriate strength and deformation characteristics of the soils under short-term (undrained) and long-term (drained) conditions for geotechnical analysis include cohesion (cu c'.), shear strength (τ), deformation modulus (E, E') values, and natural and water-saturated unit weights (γn, γsat) values, which were determined in accordance with AASHTO LRFD Bridge Design Specifications (2012), Bowles (1996), Stroud (1989), and laboratory experimental findings. The parameters are shown in the table 5.2.

Table 5.2 Soil Parameters Used In PLAXIS Input (Turkey)

Parameter	Value
Unit weight, γn/γsat(kN/m^3)	**20/21**
Modulus of Elasticity, E'ref (MPa)	**150**
Cohesion, c'(KPa)	**25**
Shear strength angle	**36**

5.3 GEOTECHNICAL DATA (MOROCCO)

This study's selection of Moroccan soil characteristics is based on geotechnical data that accurately reflects the usual local soil conditions in Moroccan specific chosen area (Kenitra/Rabat) in 2023. These parameters were selected to represent actual site features, enabling a significant comparison with Turkish soil data under equivalent structural and loading circumstances. The objective is to isolate the impact of soil characteristics on soil-structure interaction (SSI) behavior in the simulation. Similar to Turkish geotechnical findings, the Moroccan soil model employs field-derived data including unit weight, modulus of elasticity, cohesion, and internal friction angle to effectively assess the foundation reaction in regard to the RPS 2011 seismic code. The drill investigation area shown below (Figure 5.10) demonstrates the real subsurface stratigraphy used for modeling, and the borehole simple box results are presented in figure 5.11, while the corresponding table encapsulates the essential geotechnical parameters found and that will be used in PLAXIS for simulation.

Figure 5.10 Boreholes Location Map

Figure 5.11 Sample Box Display Of Borehole SCP1 Investigation

Table 5.3 Soil Parameters Used In PLAXIS Input (Morocco)

Parameter	Value
Unit weight, γn/γsat(kN/m^3)	**19/20**
Modulus of Elasticity, E'ref (MPa)	**160**
Cohesion, c'(KPa)	**6**
Shear strength angle	**30.7**

5.4 COMPARISON OF MOROCCAN VS TURKISH SOIL PARAMETERS WITH STANDARDS CODES

5.4.1 Unit Weight (γn/γsat)

This unit weights of the study are related to the soil types specified in the codes, even though neither TBDY 2018 nor RPS 2011 provides specific values for each type of soil. A predicted range for ZB-class soils, which usually represent medium-dense sands or stiff fine-grained soils, was used in the Turkish example, with a unit weight of 20 kN/m³. These numbers match with what was investigated in the Turkish soil case study.

The soil in Moroccan case study is composed of sandstone blocks and sand with varying degrees of cementation; the unit weight for these materials is 19 kN/m³. To represent the actual field conditions in Northern Morocco, this value is appropriate for granular soils with varied degrees of compaction and rock fragment inclusions. The numerical models are consistent with the soil categorization context given in TBDY 2018 and RPS 2011, and they also accurately reflect the site's geology.

5.4.2 Modulus of Elasticity (E'ref)

The relative stiffness of the soil profiles under static and dynamic loading was taken into account in the selection of the modulus of elasticity (E′ref) as 150 MPa for the Turkish case and 160 MPa for the Moroccan case. The chosen modulus is in agreement with the mechanical properties of medium-dense sands or stiff clays for the Turkish case study, which is TBDY 2018's ZB soil classification. Although TBDY 2018 doesn't provide E′ values directly, it does categorize soils according to shear wave velocity (Vs) and SPT values; ZB is defined as Vs30 between 375 m/s and 750 m/s and $N6_0$ values typically vary between 30 and 50. In Turkish geotechnical practice, empirical correlations like $E' \approx 3.5 \cdot N60$ provide E′ values between 130 MPa and 180 MPa, confirming that 150 MPa is a reasonable and conservative input. However, the soil from

Morocco was found to be a partially cemented granular, consisting of sand with various levels of cementation and sandstone inclusions. The 2011 RPS indicates that while specific modulus values are not given, soil is classified into groups, such S2 or intermediate granular soil, based on qualitative descriptors and normal mechanical behavior. Depending on the local stratigraphy and compaction, the E′ values for granular soils with mild cementation in Moroccan geotechnical practice usually vary between 140 MPa and 180 MPa. With RPS 2011 imposing less seismic demand than TBDY 2018, and with stiffer local behavior, the selected value is160 Mpa.

5.4.3 Cohesion (c′)

The behavior of ZB-class soils, which in Turkey are usually considered as stiff silty clays or partly cemented sands, was represented by a cohesion value of 25 kPa in the model. While the Turkish seismic code doesn't provide specific cohesiveness values, it does provide practitioners with ranges of geotechnical parameters that they can operate within it. For cohesive soils with medium to high strength, the typical Turkish value is between 20kPa and 30 kPa. Furthermore, due to the code's stringent requirements for foundation stability, including the verification of base shear capacity, sliding, and bearing resistance under seismic loading, it is essential to select a greater cohesiveness in order to maintain sufficient safety margins.

Sand with soft particles or weathered inclusions would be examples of a weakly cemented granular deposit with a cohesion value of 6 kPa in the Moroccan model. In Morocco, seismic standards require broad mechanical qualities, not precise numerical restrictions. Low cohesion values are allowed in the Moroccan code due to its reliance on global safety factors and larger soil classifications, which do not require the same degree of comprehensive shear-failure assessment as the Turkish code. Under seismic stress, the Moroccan simulations showed greater lateral and vertical motions, which may be more compatible with the design strategy.

5.4.4 Shear Strength Angle (φ′)

In accordance with the Turkish seismic design approach for ZB-class soil, the Turkish model's friction angle is 36°, it represents the behavior of medium-dense to dense granular soil. Although numerical friction angle values are not provided by TBDY 2018, soils are classified according to shear wave velocity and field behavior. Geotechnical parameters may be defined using either laboratory or empirical data. The chosen value fulfills the requirements of TBDY 2018 for foundation behavior and total soil-structure interaction, which include minimized sliding risk, more restrictive seismic performance and verification processes. The moderately compacted sandy soil with different cementation and sandstone fragments was reflected in the Moroccan case studied model with a reduced friction angle of 30.7° in comparison with 36°. Seismic design practice in Morocco places an emphasis on more general qualitative soil descriptions rather than specific mechanical parameter limitations; this soil profile is in line with this strategy. Values around 30°-32° are common in granular soils with less compaction. According to RPS 2011, which does not prioritize comprehensive slide or lateral stability tests as much as TBDY 2018.

5.5 NUMERICAL MODEL AND ANALYSIS INPUT

The figure 5.12 illustrates the numerical model constructed in PLAXIS 2D, developed to simulate the soil-structure interaction (SSI) behavior of a building supported by a raft foundation. The model consists of three primary components: applied structural loads, the raft foundation, and the underlying soil mass, modelled using the hardening soil model, in accordance to case study conditions, to reflect nonlinear stress–strain behavior.

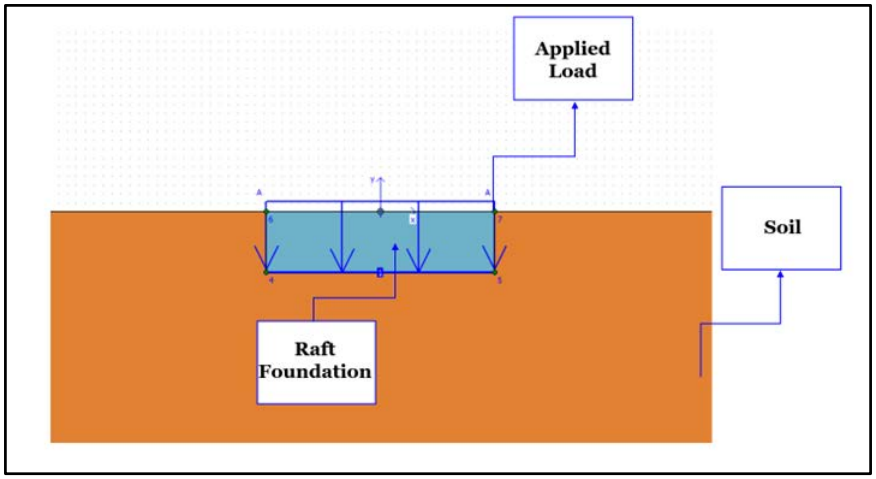

Figure 5.12 2D Model of Building + Foundation + Soil (PLAXIS 2D)

5.5.1 Applied Load Generation In PLAXIS

In this study, a specific 15-story reinforced concrete building (A4) with a raft foundation of 7m depth and unit weight of $\gamma = 24$ kN/m³ were chosen as the representative structure for soil-structure interaction analysis, under three different loads combinations that were taken from geotechnical report situated as:

Service load combination : G+Q **= 39.20** ton/ m² = **384.55** kN/ m²

Factored load combination : 1.4G+1.6Q **= 56** ton/ m² **= 549.36** kN/ m²

Seismic load Combination : G+Q+E **= 43.50** ton/ m² = **426.74** kN/ m²

Where:

G: Dead Load

Q: Live Load

E: Seismic Load

Self-Weight-Foundation reaction : $\gamma \times H$ = 24 × 7 = 168 kN/ m²

The foundation's self-weight should only be turned on if it wasn't previously incorporated into the structural load combination. Not taking into account the self-weight load in the material characteristics is crucial, nevertheless, when loads are pre-calculated and include the weight of the foundation and prevent adding the weight 2 times.

The Final used load values are:

1. Concerning 1st load combination (G+Q) is **216.5 kN/ m²**
2. Concerning 2nd load combination (1,4G + 1,6Q) is **381.36 kN/ m²**
3. Concerning 3rd load combination (G+Q+E) is **258.73 kN/ m²**

The figure 5.13 shows the typology of the Plaxis 2D model that represents the loads, foundation and soil profile.

5.5.2 Foundation Generation in PLAXIS

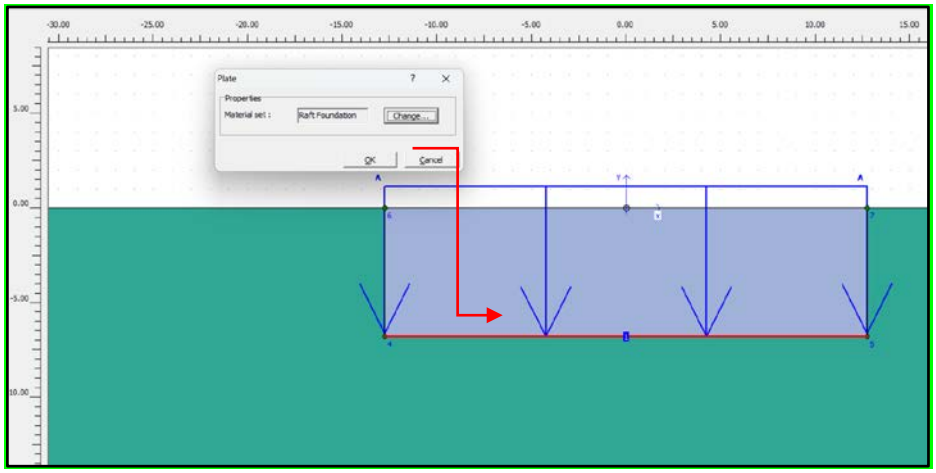

Figure 5.13 Modelled Raft Foundation Represented As Plate In PLAXIS 2D

In the example project chosen in case study, the type of foundation that was used is: raft foundation, in the PLAXIS model is represented as plate, as is it is shown in the figure 5.13, with parameters:

Axial Stiffness: EA= 4,2 .107 KN/m

With E (Young's Modulus of concrete) = 3.107kN/m ²

A (Cross-sectional area) = 1,4 m²

Flexural Rigidity: EI = 6,86 .106 kNm²/m

With the same value of E (Elasticity / Young's Modulus)

I (Moment of Inertia) = $\frac{B \times H^3}{12} = \frac{1 \times 1{,}4^3}{12} = 0.228666667\ m^4$

d = 1,4m

w = 5KN/m

5.4.3 Boundaries Setup

After entering all material properties, geometry, and load combinations into PLAXIS, the next step is to define the model boundaries to ensure accurate simulation of soil behavior. Typically, the lateral boundaries are set far enough from the foundation to minimize boundary effects, and the bottom boundary is fixed to simulate the natural soil constraint, the figure 5.14 shows how those boundaries look like in the software.

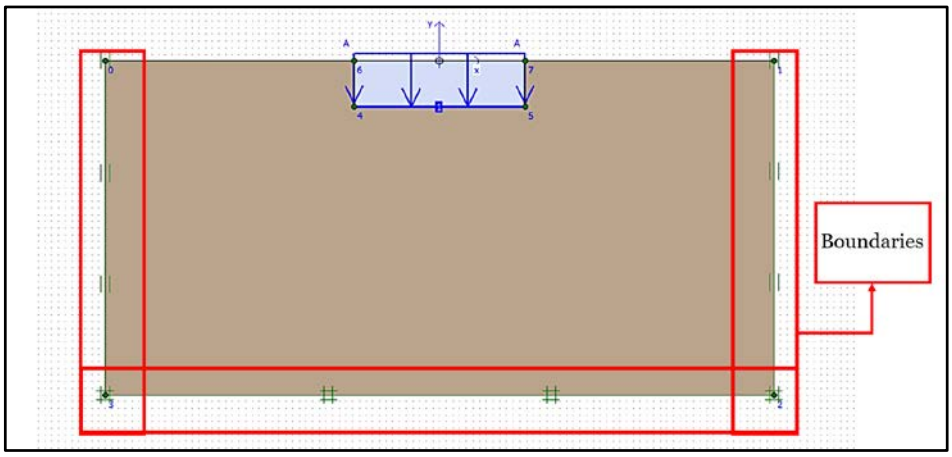

Figure 5.14 Define Boundaries In The Model (PLAXIS)

5.6. EVALUATION OF PLAXIS RESULTS

5.6.1 Deformation Of Mesh Results

Once boundaries have been correctly distributed, the mesh is formed, thus, this stage is essential for numerical precision, as the mesh determines the discretization and computation of the soil-structure interaction. Sometimes, surrounding the foundation zone, a finer mesh is used to increase result accuracy.

The computation steps are defined after the creation of mesh. Based on the data, many important outputs, such total displacement, horizontal displacement, shear strain distribution, total stress fields, and over-

consolidation ratio(OCR) were obtained. For Turkish and Moroccan case studies, these results provide an idea on how the soil and foundation react to the applied loads and assist to assess settlement, deformation patterns, and soil strength behavior under seismic and fixed loading circumstances. The mesh of both cases (Turkish soil and Moroccan soil deformation meshes under same load conditions are shown in figures 5.15 and figure 5.16, respectively)

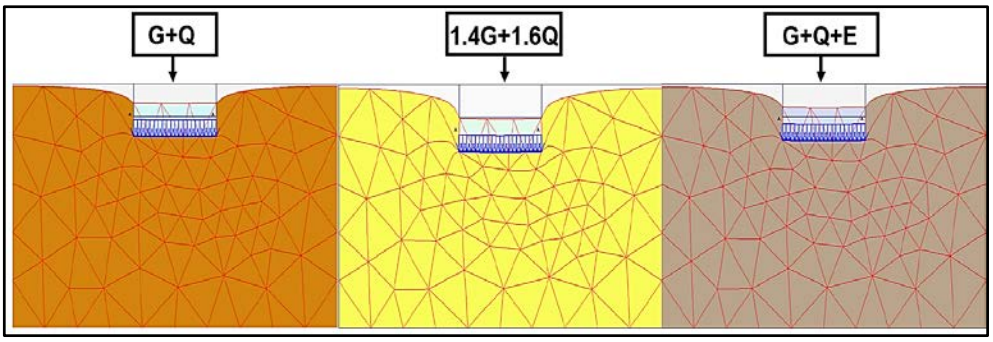

Figure 5.15 Load Distribution And Mesh Generation For Three Different Load Combinations (Turkish Soil Parameters)

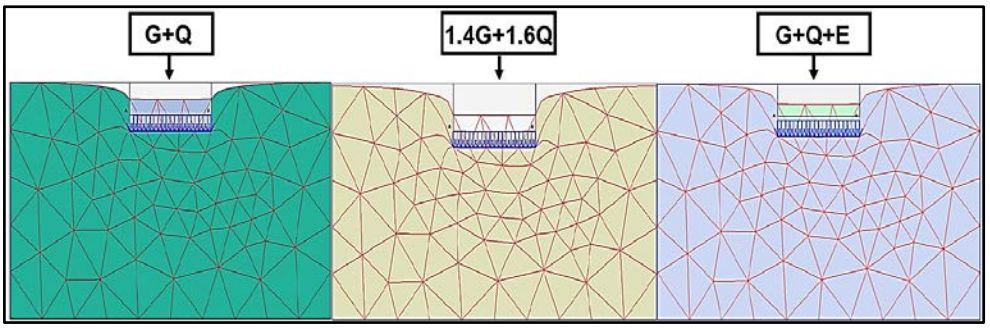

Figure 5.16 Load Distribution And Mesh Generation For Three Different Load Combinations (Moroccan Soil Parameters)

5.6.2 Vertical Displacement Results (Settlement)

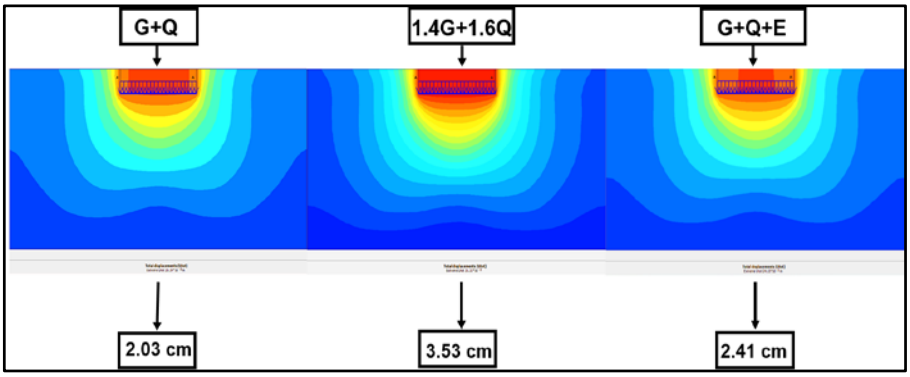

Figure 5.17 Vertical displacement results (Turkey)

The displacement results indicate the maximum settlement under the raft foundation. When soil-structure interaction is recognized, the settlement values for each load combination are:

G + Q**: 2.03 cm**

1.4G + 1.6Q**: 3.53 cm**

G + Q + E**: 2.41 cm**

As it is shown in figure 5.17, the value of settlement increases in factored load combination's similuation. The settlement of earthquake-induced load is less than extreme static combination load value because it uses improved static loads which function constantly and uniformly on the foundation.

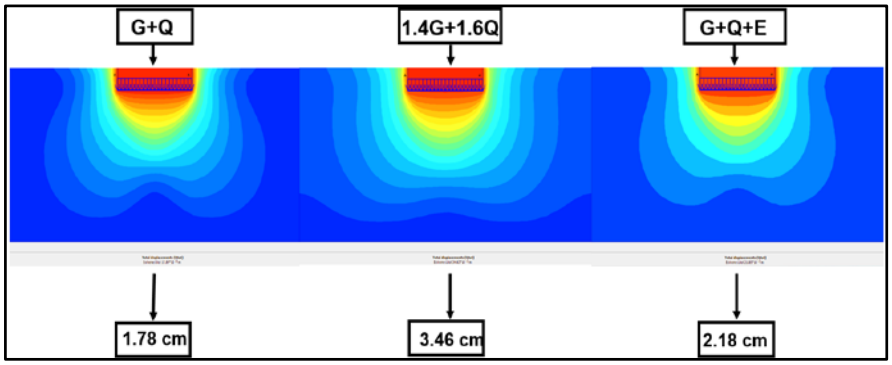

Figure 5.18 Vertical Displacement Results (Morocco)

Concerning the effect of Moroccan soil parameters effects results:

G + Q: **1.78 cm**

1.4G + 1.6Q: **3.46 cm**

G + Q + E: **2.18 cm**

As it is shown in Figure5.18, with the largest settlement considering the factored static combination. The magnitudes are lower than Turkey's values in all load combinations cases.

5.6.3 Horizontal Displacement Results

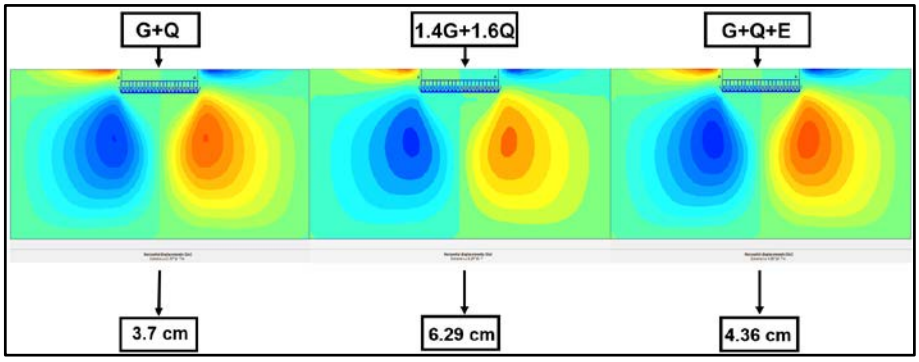

Figure 5.19 Horizontal Displacement Results (Turkey)

Under different types of loads, as observed in figure 5.19, these contour plots show how the earth and building system move laterally, or horizontally. Since it influences structure drift, internal stresses, and soil sliding behavior, horizontal displacement is particularly relevant for evaluating seismic performance, the results of displacement under combinations are as follow:

G + Q**: 3.70 cm**

1.4G + 1.6Q**: 6.29 cm**

G + Q + E**: 4.36 cm**

The higher horizontal displacement is produced by the calculated static load, most likely as a result of enhanced shear stress and plastic deformation in

the soil. Seismic loading (G+Q+E) also results in significant lateral displacement as a result of inertia effects and dynamic wave propagation.

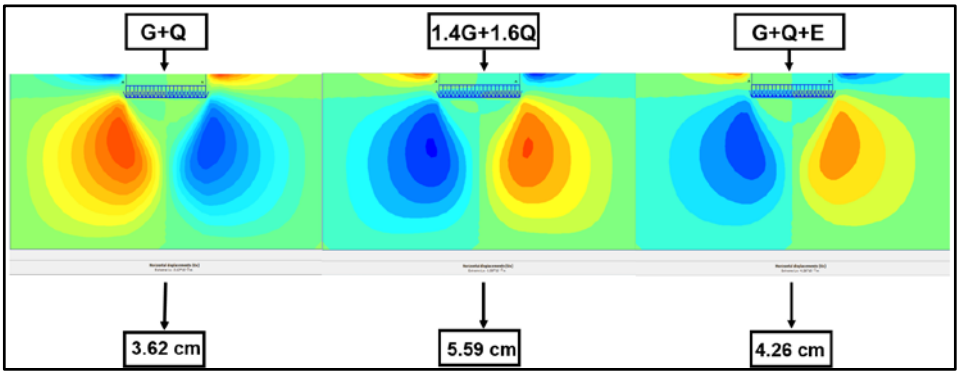

Figure 5.20 Horizontal Displacement Results (Morocco)

Concerning the effect of Moroccan soil parameters effects results in horizontal displacement, as illustrated in figure 5.20:

G + Q**: 3.62 cm**

1.4G + 1.6Q**: 5.59 cm**

G + Q + E**: 4.26 cm**

The combination of 1.4G and 1.6Q shows the highest horizontal displacement, as was shown in the Turkish example, whereas the seismic load causes only minor movement. Less variation in load types compared to the Turkish model suggests that the soil in the location of Moroccan case study is more uniformly stiff laterally.

5.6.4 Shear Strain Results

Shear strain (ε) is known by its indication of the intensity of internal deformation of the soil located under load. The figure 5.21 demonstrates the results under load combinations of Turkish soil parameters case.

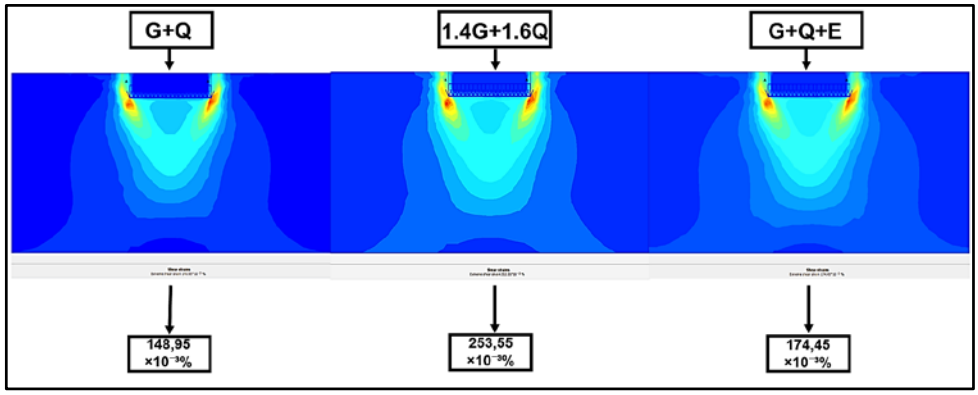

Figure 5.21 Shear Strains Results (%) (Turkey)

The results of displacement under combinations are as follow:

G + Q**: 148,95 × 10⁻³ %**

1.4G + 1.6Q**: 253,55 × 10⁻³ %**

G + Q + E**: 174,45 × 10⁻³%**

In the figure 5.21, it is observed that under the factored static load (1.4G + 1.6Q), the shear strain is higher, indicating that the shear stress has been increased. Because of dynamic redistribution and potential stress relief zones, the seismic load (G + Q + E) causes slightly greater shear strain than the basic load (G + Q), but less than the factored static load combination.

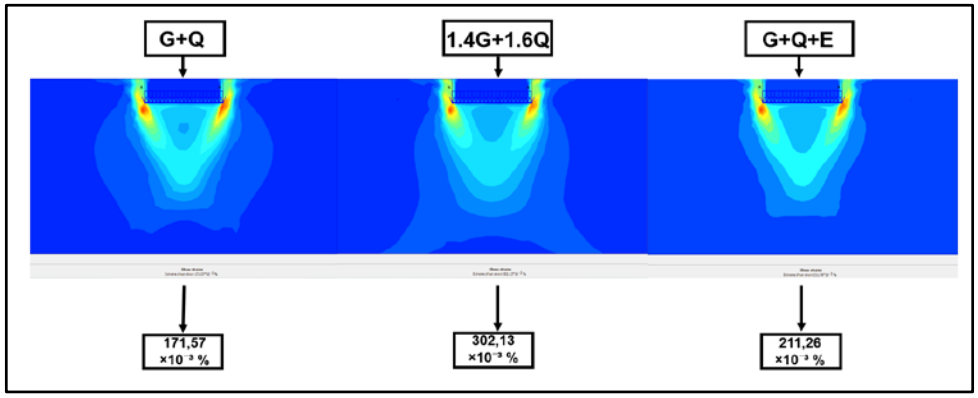

Figure 5.22 Shear Strains Results (%) (Morocco)

Concerning the effect of Moroccan soil parameters effects results:

G + Q**: 171,57 × 10⁻³ %**

1.4G + 1.6Q**: 302,13 × 10⁻³ %**

G + Q + E**: 211,26 × 10⁻³ %**

As it is observed in figure 5.22 that the highest shear strain arises in the 1.4G + 1.6Q combination. Moroccan soil (case study) has almost highest shear strain values compared to Turkish soil (case study) across all loading scenarios.

5.6.5 Total Stresses Results

Concerning the results of total stresses, that is reffered to the combined of all loads acting on thr soil mass of turkish soil parameters, are showed as follow in figure 5.23:

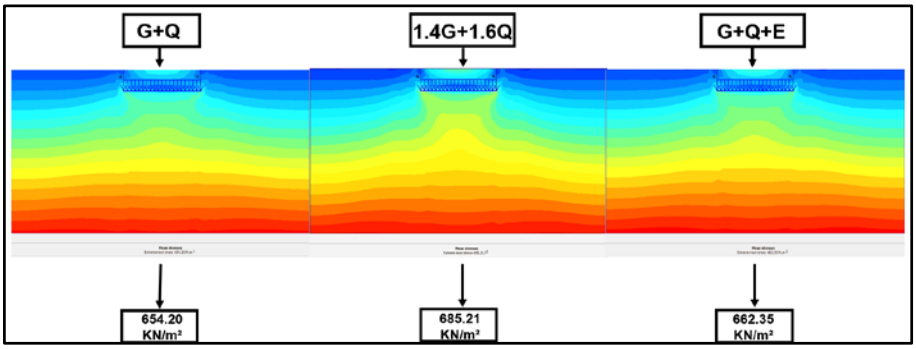

Figure 5.23 Total Stresses Results (KN/m²) (Turkey)

G + Q: **654.20 kN/m²**

1.4G + 1.6Q: **685.21 kN/m²**

G + Q + E: **662.35 kN/m²**

The combination of 1.4G and 1.6Q produces the maximum stress, which is expected given the increased static loading. The seismic load (G + Q + E) results in marginally reduced total stress compared to the calculated static situation, due to their short-term redistribution of forces and the transient characteristics of dynamic loads. Total stress denotes the cumulative impact of all forces exerted on the soil mass, that includes:

Dead load (G)

Live load (Q)

Seismic load (E) (when relevant).

This is essential in SSI since it affects bearing capacity, settling, and potential soil failure mechanisms under load.

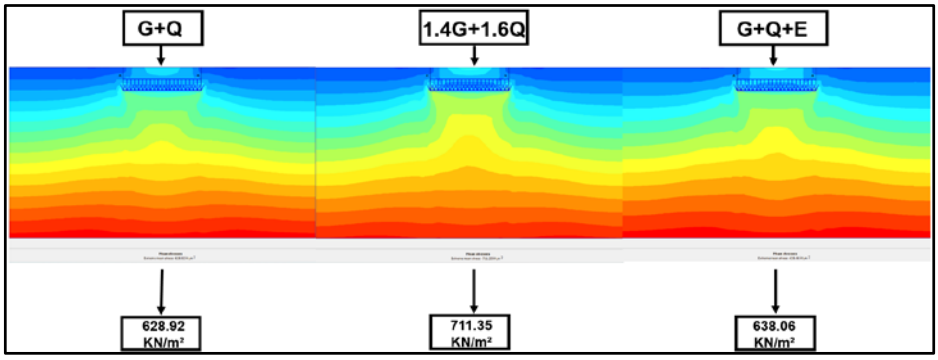

Figure 5.24 Total Stresses Results (KN/m²) (Morocco)

According to the total stress of Moroccan soil parameters effects results shown in figure 5.24:

G + Q: **628.92 kN/m²**

1.4G + 1.6Q: **711.35 kN/m²**

G + Q + E: **638.06 kN/m²**

Findings show that for the Moroccan case study that it has similar results, nevertheless, it is notable that the 1.4G + 1.6Q stress surpasses the value of Turkish case study under the same combination. This indicates that the Moroccan model has an increased stress accumulation, possibly due to reduced redistribution or increased concentration of stress under the foundation zone.

5.6.6 Over-Consolidation Ratio Results

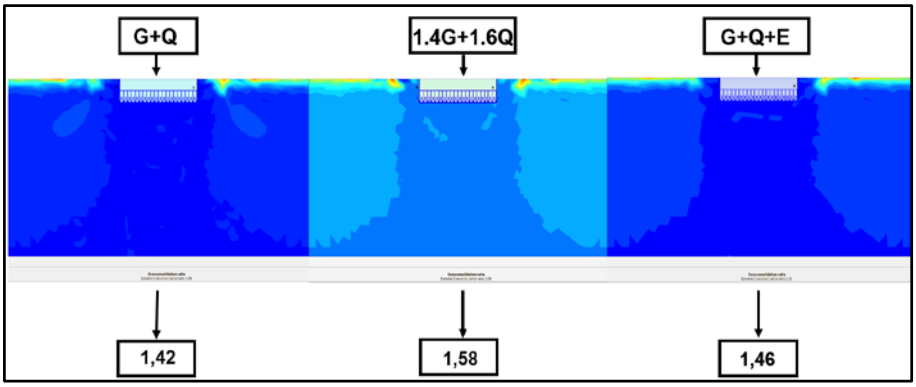

Figure 5.25 Over Consolidation Ratio Results (Turkey)

The figure 5.25 illustrates the over-consolidation ratio (OCR) for the model using Turkish soil properties across three load combinations. The soil is consistently over-consolidated, indicating a prior stress history that exceeds the imposed loads.

G + Q: **1.42**. (Marginally over-consolidated, the soil effectively withstands standard service loads.)

1.4G + 1.6Q = **1.58** (As it is greater than 1 ,the results remains within the soil's stress history.)

G + Q + E: **1.46** (Seismic stress causes a slight increase, however the soil stays stable.)

This behavior demonstrates moderate rigidity and acceptable resistance to settlement under both static and dynamic situations, consistent with Turkish soil parameters.

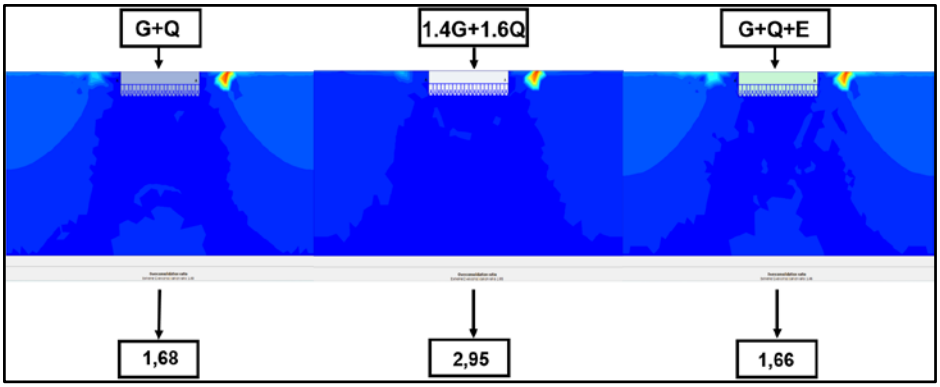

Figure 5.26 Over Consolidation Ratio Results (Morocco, 2018)

The findings of Moroccan soil characteristics under load combinations shown in figure 5.26, in line with OCR, demonstrate enhanced over-consolidation behavior, particularly at higher load combinations, signifying increased stiffness and reduced compressibility, as shown by the results:

G + Q: **1.68** (Effective over-consolidation under service load)

1.4G + 1.6Q: **2.95** (Significant resistance to structural stresses; remarkable stiffness.)

G + Q + E: **1.66** (While seismic forces were applied, soil is definitely over-consolidated.)

These results indicate higher soil strength and a low possibility of settlement under both gravitational and seismic loads, in accordance with Moroccan soil conditions. The values of all PLAXIS output parameters for both case studies , Turkish and Moroccan soil parameters are summarized in tables 5.5 and 5.6.

Table 5.4 Summarized Values Of Turkish Case Stydy's Outpus

Type of Load Combination	Total Vertical Displacement (Settlement) (cm)	Total Horizontal Displacement (cm)	Total Stress (σ) (KN/m²)	Total Strain (ε) (%)	Over Consolidation Ratio
Q+G	2.03	3.7	654.20	$148{,}95\times10^{-3}$	1.42
1.4G + 1.6Q	3.53	6.29	685.21	$253{,}55\times10^{-3}$	1.58
G+Q+E	2.41	4.36	662.35	$174{,}45\times10^{-3}$	1.46

Table 5.5 Summarized Values Of Moroccan Case Stydy's Outpus

Type of Load Combination	Total Vertical Displacement (Settlement) (cm)	Total Horizontal Displacement (cm)	Total Stress (σ) (KN/m²)	Total Strain (ε) (%)	Over Consolidation Ratio
Q+G	1.78	3.62	628.92	$171{,}57\times10^{-3}$	1.68
1.4G + 1.6Q	3.46	5.59	711.35	$302{,}13\times10^{-3}$	2.95
G+Q+E	2.18	4.26	638.06	$211{,}26\times10^{-3}$	1.66

5.6.7 Bending Moment Results

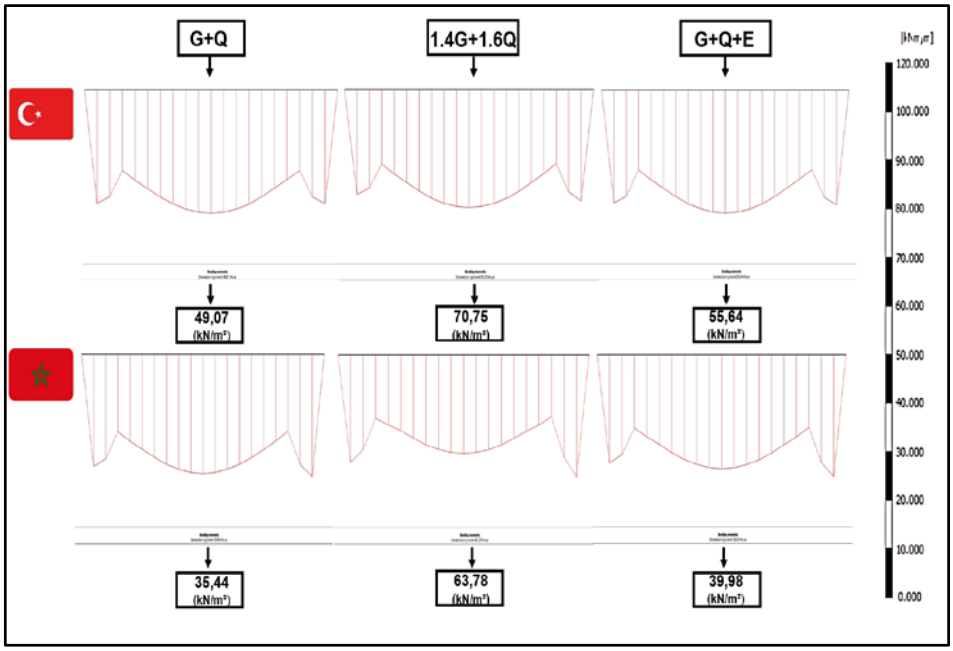

Figure 5.27 Bending Moment Results, Both For Turkish And Moroccan Soil Parameters Under Similar Conditions

Table 5.6 Table Of Bending Moment Values Of Both Conditions

Load Combination	Bending Moment (Turkey) (kN/m²)	Bending Moment (Morocco) (kN/m²)
G + Q	49.07	35.44
1.4G + 1.6Q	70.75	63.78
G + Q + E	55.64	39.98

When different types of loads are placed on the soil-structure system, the bending moment values show how it reacts, the values are presented in 2 different ways, first in diagrams, that represents the ouputs of models in Plaxis 2D, in figure 5.27, and conclusion of numerical results for both countries were created in table 5.4. The Turkish model consistently has higher bending

moments than the Moroccan model. This means that the structure parts are under more stress.

G+Q: The Turkish base has more breaking stress when it's under service loads, possibly because the soil isn't enough stiff.

1.4G + 1.6Q: When the maximum load is applied, both values increase, but Turkey still has higher bending in comparison with Moroccan's case study's result, which means that more load gets transferred to the soil.

G + Q + E: When earthquake loads are added, bending moments increases in both cases, but the values are higher in Turkey. The Turkish model always has higher bending moments, which means that the structural parts are under more stress because the soil has deformed more. The Moroccan cases study's model, on the other hand, has stronger ground (as seen from the OCR values), which means that the base breaks less. This shows how the features of the soil affect how stress is distributed in a structure when the load changes.

CONCLUSION AND SUGGESTIONS

Turkey and Morocco are considered as seismically active countries; hence, knowing how each nation's seismic code controls soil-structure interaction (SSI) is actually important. This is the main objective of the research: to compare the Turkish building earthquake code (TBDY 2018) and the Moroccan Seismic Design Code (RPS 2011) in accordance with SSI by evaluating the simulation's findings that consist of the analysis of three load combinations applied in a raft foundation's building (case study) under two different soil parameters (Morocco and Turkey).

Concerning the content of thesis chapters, it begins with an introduction that explains the need for seismic design in Turkey and Morocco in creating building safety. Setting the framework for a comparison between TBDY 2018 and RPS 2011 describes the research aims and helps to have the adequate answers to the research's questions. In the second chapter, a detailed literature review was conducted, including geotechnical earthquake engineering and SSI, which contains seismic wave propagation, soil behavior, and SSI processes, giving a theoretical foundation for the research. The literature was carried out in order to compare Turkish and Moroccan seismic criteria by examining previous research and established standards. The chapter that follows examines the most important latest earthquakes in both countries. Concerning Turkey: 1999 Kocaeli and 2023 Kahramanmaraş, and Morocco: 2004 Al Hoceima and 2023 Al Haouz. This section assesses the contribution of SSI to structural damages and emphasizes the influences of earthquakes on SSI practices in both countries.

One of the primary objectives of the study is the comparison of TBDY 2018 and 2011which is the main content of the third chapter. It was found that while RPS 2011 remains more general and prescriptive, TBDY 2018 provides a more comprehensive and performance-based approach to SSI after their comparison. Both deals with some important points of SSI element and most

important regulations, but Turkey is considered more detailed in comparison with Moroccan's standards codes. Just after this chapter, a numerical case study was carried out to evaluate, in line with the soil-structure interaction effects, the impact of each country's soil characteristics on the same type of foundation and same loading circumstances. In this chapter, the software chosen is PLAXIS 2D, known for its effectiveness in modeling, in order to evaluate the impact of code-specific variations on displacements, stress, strain, over-consolidation ratio, and moment diagram outputs. The last part of the thesis summarizes all the chapters results and emphasizes the answers to the research questions in detail, giving an explanation of the software findings. The research is closed by the problematic solution and recommendations concerning the main issue.

The literature review emphasizes an organized comprehension of soil-structure interaction (SSI), mentioning its significance in seismic design. It defines essential SSI processes, distinguishing between kinematic and inertial effects, and clarifies the inadequacy of fixed-base models for practical study. Theoretical modeling methodologies, such as wave propagations, are examined together with international seismic standards like Eurocode 8 and ASCE 7, highlighting differences in the evaluation of soil-structure interaction (SSI). The study defines critical geotechnical factors like stiffness, strength, and dynamic inputs. Key output indicators, displacements, stresses, pore pressures, and foundation forces are examined to comprehend the impact of SSI on structural behavior. The literature provides a solid basis for comparing Turkish and Moroccan codes. After research on historical earthquakes in Morocco and Turkey, it shows that there is a need to include soil-structure interaction (SSI) and structure-soil–structure interaction (SSSI) in seismic design. The analysis after disasters occurred in both countries show that neglecting site-specific conditions, particularly on soft or inclined soils, results in overestimated seismic demands, increased structural damage, and reduced safety margins, especially in Morocco, as traditional buildings still exist and are easy to destroy during earthquake events. Improving seismic resilience necessitates

performance-based methodologies, higher foundation standards, and heightened awareness among engineers and planners, particularly in rural and topographically complicated regions. Chapter four examines the comparative analysis of TBDY 2018 and RPS 2011, highlighting two fundamentally distinct methodologies for controlling soil-structure interaction (SSI) under seismic loading: characterized by analytical and numerical methods. Turkey's TBDY 2018 presents a more detailed and structurally unified code, including comprehensive spectrum acceleration formulas, requirements for dynamic analysis, and liquefaction criteria based on precise geotechnical data. In contrast, Morocco's RPS 2011 employs a framework with simpler modeling guidelines, facilitating practical implementation but with some important missing points necessary for complicated SSI circumstances. The comparative examination of TBDY 2018 (Turkey) and RPS 2011 (Morocco) shows notable common points and some differences in the evaluation of aspects affecting soil-structure interaction (SSI). The variations are presented as follows:

Classification of Soil

Soil classification is essential in both codes standards in order to evaluate a structure's seismic response and determining adequate foundation design. The Turkish standard classifies soils into six categories (ZA to ZF), while the Moroccan code has a similar framework, ranging from S1 to S5. Both approaches use similar categorization metrics: shear wave velocity (Vs), standard penetration resistance (SPT-N_{60}), and undrained shear strength (Su) with a difference in type of shear velocity, Turkey is based on Vs30, while Morocco is based on Vs. Turkey takes into consideration Vs30 value to capture the overall dynamic behavior of the top 30 meters of soil, aligning with international standards, while Morocco uses local Vs values based on dominant soil layers, reflecting a simpler, more empirical approach to site classification.However, the criteria defining each standards class varied, highlighting variations in national seismic concerns. For example, the Turkish code categorizes ZC soils in intermediate soil classes as having Vs30 values

between 360m/s-760 m/s and Su exceeding 250 kPa, while Morocco's S2 class similarly specifies these soils with Vs ranging from 360-760 m/s but allows Su values as low as 100 kPa. This signifies a more rigid interpretation of stiffness in the Turkish code. In low-value classifications, the Turkish ZD soil category permits Vs30 ranging from 180 m/s to 360 m/s with Su values between 70 kPa and 250 kPa, but Morocco's S3 class accommodates Su values as low as 50 kPa, highlighting a more conservative methodology in Turkish engineering design. In soft soils (ZE–SE), the Turkish code restricts Su to below 70 kPa and Vs30 to less than 180 m/s, but the Moroccan code adopts a more progressive limit of Su < 50 kPa with the same Vs value. Both regulations recognize the need for specialized geotechnical investigations in problematic soils (ZF in Turkey, S5 in Morocco). The Moroccan code classifies S5 soils with a plasticity index (PI) of more than 75 and a thickness exceeding 8 meters, whereas the Turkish code stipulates a PI greater than 50 and a depth greater than 8 meters. Turkey is demonstrating a more conservative approach to soil classification than Morocco.

Building Importance Factor

The Turkish code categorizes four important classes, from Class I (essential facilities such as hospitals) with a value of 1.5, to Class IV (temporary or agricultural constructions) with a factor of 1.0. Conversely, RPS 2011 employs four classifications (A to D), defining Category A for critical infrastructure at 1.5 and Category D for low-occupancy or temporary structures at 0.8. The categories demonstrate similar structural priorities. The difference point is that TBDY 2018 takes into consideration building use classes (BKS) that are able to offer a more detailed framework, notably noticeable in structures of moderate significance, such as residential and commercial buildings, which are assigned a reduced factor (1.2) in TBDY 2018 and 1.3 in RPS2011. Both codes provide seismic design parameters based on a 475-year return time with a 10% probability of exceedance and 5% critical decreasing,

aligning international design standards while preserving national priorities in risk classification.

Local Ground Effect Coefficient

Both Moroccan and Turkish code standards use fundamentally distinct methodologies in determining local ground effect coefficients, which directly influence the amplification of seismic demand in soil-structure interaction evaluations. TBDY 2018 uses a dual coefficient system, Fs and F1, which changes based on soil classification (ZA to ZF) and spectral acceleration levels (Ss and S1), permitting a more dynamic response to seismic loading. For instance, Fs values in Turkey reach a maximum of 3.5 for extremely soft soils (ZE), whereas Morocco limits this to 1.8 for similar S5 soils. The difference can be related to Turkey's more seismically active tectonic area and more soil variability, requiring higher sensitivity in code restrictions. The Turkish model is more technically strong for advanced numerical modeling since it individually addresses short- and long-period impacts, which are crucial for high-rise buildings. In contrast, RPS 2011 employs a singular coefficient based only on site categorization (S1 to S5), which, while easier to use, fails to account for frequency-dependent soil behavior. In conclusion, the Moroccan technique supports simplicity in seismic design, while the Turkish way more effectively clarifies the complex relationship between seismic waves and soil categories, providing a more precise foundation, especially for PLAXIS SSI simulations input and structural safety evaluation.

Spectrum Input

Concerning seismic spectral acceleration models, in both code standards it shows significant differences in technical clarity, practical implementation, and incorporation into soil-structure interaction (SSI) simulations. The Turkish code (TBDY 2018) offers a more detailed and analytically effective approach. The clear mathematical formulas for both horizontal and vertical spectral accelerations, Se(T) and SeD(T), provide a simple and exact approach for

numerical implementations. The integration of spectral transition periods such as TA, TB, and TL, customized for local soil classifications (ZA–ZE), improves the precision of ground motion representation and more effectively reflects the dynamic characteristics of soils over different period rangesModeling buildings on soft or layered soils is important, since these soils may increase seismic shaking or generate resonance, significantly affecting the accuracy and safety of structural design. Conversely, while the Moroccan code (RPS 2011) incorporates the dynamic amplification factor (D) and modifies for damping changes using the $m = (5/x)^{0.4}$ factor, its application in numerical modeling is indirect. The lack of a definitive Se(T) formula and dependence only on Za/Zv ratios may add subjective variability in manual spectrum modifications. Furthermore, the absence of a vertical spectrum component in the Moroccan code may inadequately reflect the vertical acceleration impacts that may significantly influence thin or vertically irregular buildings, which are explicitly addressed by TBDY 2018.

Natural Frequency and Resonance

The evaluation of a structure's basic period (T) is essential in seismic analysis, especially for soil-structure interaction (SSI), where an alignment of the structure's natural period with the main soil period may result in resonance and significant deformation. Both TBDY 2018 and RPS 2011 recognize this risk and provide simple and analytical techniques for estimating T, but with varying degrees of rigidity and assumptions appropriate to their respective national circumstances. The Turkish standard (TBDY 2018) employs an empirical formula, $T = Ct \cdot H\text{^}0.75$, with Ct=0.10 for RC frames, which provides a conservative assessment of flexibility appropriate to Turkey's diverse geological conditions, including both rigid rocks and alluvial basins. The limiting of dynamic periods to 1.4 times the empirical value (Rayleigh requirements) guarantees that modal periods are physically reasonable and prevents the underestimation of base shear forces. This measure is especially important in soft soil areas (ZD, ZE), where amplification effects are

significant. It is observed that the limit is acceptable and essential, since above it might artificially reduce the seismic demand and alter the SSI-induced period extension. Conversely, the Moroccan standard (RPS 2011) presents additional formulas, $T = 0.09 \times H / \sqrt{L}$ for wall systems and $T = 1.8 \times \sqrt{(mH/EI)}$ for cantilevers, providing enhanced flexibility to various structural configurations. These expressions effectively characterize the behavior of slender or rigid structural systems. Nonetheless, the absence of a specific upper limit, such as the 1.4 times limit in TBDY, may lead to an underestimation of seismic demand unless confirmed by modal dataIn both codes, the need for site-compatible accelerograms is crucial for attaining realistic response analysis, particularly when soil-structure interaction effects can change the structure's dominant vibration mode. It is concluded after code evaluation that SSI extends the basic time by decreasing effective stiffness, especially in soft soils, which corresponds with the design reasoning of TBDY's categorization (ZA to ZE) and RPS's soil-dependent amplification factors. The elongation of this period must be carefully controlled to avoid excessive extension, as it may shift the structure into a domain of increased spectral demand, especially around peak amplification areas. In summary, the Turkish code offers a more systematic and conservative framework characterized by well-defined empirical limits and dynamic modeling restrictions. The Moroccan code offers more architectural design allowance but requires the engineer's critical evaluation to prevent overly safe assumptions.

Foundation

The differences in shallow foundation design methodologies between the two codes directly reflect the seismic risk profile of both countries. Turkey's TBDY 2018 employs a strict, parameter-driven process that aligns with international standards. Employing Hansen's bearing capacity formula, augmented by seismic-specific modifications (such as shape, depth, and inclination factors), permits designers to modify foundation capacity to actual and complicated circumstances, particularly in areas characterized by

significant seismic activity and diverse soil types. The need for a safety factor of at least 3.0 under static loads indicates a substantial safety margin, essential for metropolitan areas with multistory or inconsistent structures. Conversely, Morocco's RPS 2011 provides a performance-based framework that does not prescribe exact formulas. The guideline emphasizes adherence to fundamental geotechnical concepts such as bearing capacity, settlement, and sliding, supported by empirical methodologies and international safety factors. The use of 1.5 for strength and 1.2 for sliding and settlement shows a simpler and prescriptive methodology, likely designed for simple implementation in projects with insufficient subsurface data and less important infrastructure. This may be useful in low- to moderate seismic zones or for standard residential constructions, which is not the case for a seismically active nation. It means that some studies are required for foundation sections in Moroccan code standards.

Liquefaction

The Turkish and Moroccan code standards methodologies regarding liquefaction demonstrate both advanced technology and the area's seismic situation. TBDY 2018 employs a quantitative, performance-oriented approach, aligned with international best practices in seismic geotechnical engineering. This is due to Turkey's elevated seismic risk and history of catastrophic earthquakes (e.g., 1999 Kocaeli, 2023 Kahramanmaraş), which required rigorous, scientifically based procedures. The use of SPT-based CRR formulas, stress correction factors, and a specified factor of safety ($FS \geq 1.10$) makes TBDY exceptionally appropriate for numerical modeling in finite element software like such as PLAXIS and consistent validation of designs. In contrast, Morocco's RPS 2011 provides practical criteria for identifying vulnerable soils based on textural, plasticity, and saturation thresholds. This indicates a more prescriptive and visual methodology, emphasizing actual field diagnostics rather than numerical calculation. It occurred by data unavailability, decreased historical seismicity, or a conservative regulatory tradition. This qualitative

method, sufficient for standard design, may cause uncertainty in numerical simulations or complicated urban developments without additional site-specific assessments. In conclusion, the difference in liquefaction methodologies between the two codes consists of regional reflection engineering development, risk assessment, and data accessibility.

To summarize, both codes standards aims are about providing structural safety under seismic loads, but Turkey's TBDY 2018 provides a more resilient and detailed foundation for advanced SSI modeling and performance-based design. However, Morocco's RPS 2011 standards provide significant practical guidance for preliminary hazard assessment, particularly in resource-constrained settings. Although these differences, both standards recognize the significance of soil classification, foundation type, and seismic demand scaling, highlighting a mutual commitment to structural safety. The variation in stiffness define limits of boundaries, important factors, and base shear techniques that emphasize the need for context-specific refinement in code provisions. This suggest a need for seismic code revision, especially for Morocco, for higher performance-based safety, particularly in areas where local soil characteristics and seismic activity require specific SSI modeling approaches, because Morocco, like in Turkey, has recently known a high seismic intensity.

Table 6.1 Key Parameter Differences for SSI Modeling TBDY 2018 vs RPS 2011

Parameter	**TBDY 2018 (Turkey)**	**RPS 2011 (Morocco)**
Soil Classes	ZA-ZF(based on Vs30)	S1-S5(based on Vs, SPT-N and Su)
Soil Factor (S)	1.0–2.4	1.0–1.8
Importance Factor (I)	1.0–1.5(based on building use class)	0.8–1.5(based on building function)
	Multi-slope	Piecewise by Za/Zv

Se (T) formula	piecewise(TB,TC,TD,TL)	
Liquefaction	SPT, Su-based	SPT-based charts
Foundation Type	Raft, pile, mat with detailed SSI provisions.	Shallow or deep with general rules.

The table 6.1 presents a comparative summary of key geotechnical and seismic parameters that influence soil–structure interaction (SSI) modeling under the Turkish Building Earthquake Code (TBDY 2018) and the Moroccan Seismic Code (RPS 2011). These parameters directly affect the input conditions, seismic demand, and response interpretation in numerical tools such as PLAXIS 2D.

In the analysis section, the aim is to describe the analysis found by using finite element software (PLAXIS 2D). The evaluations were done on a 15-story building (from the realistic Turkish project done by ESTA Construction Company). The data of foundation and structure geometry, in addition to soil geotechnical data, were useful to be able to analyze the SSI in accordance with TBDY2018. As this project was built based on the same code standards. Concerning the loads, from the geotechnical report, three types of combination equation loads were applied. Then, three types of analysis were done: Q+G, 1.4G+1.6Q, and G+Q+E to better observe the effects between soil and structure in different aspects and be able to analyze if some changes should be made to improve or to achieve more reliable results. About the Moroccan side's case, to be able to compare the results, it was considered that the same building, foundation, and load conditions were applied in Moroccan soil conditions. What would the results be? In the next part, the charts demonstrate the variations of both countries in accordance wi th seismic code standards.

Vertical Displacement (Settlement)

Table 6.2 Total Vertical Displacement Comparison

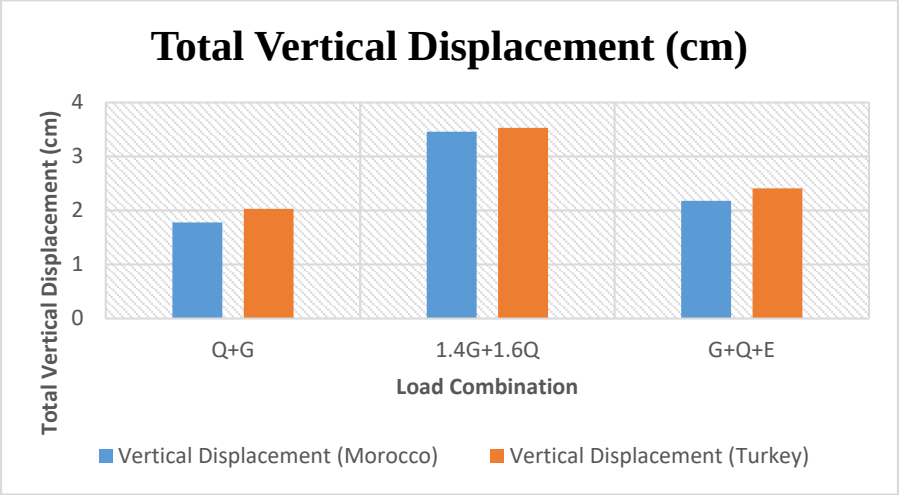

The first analysis were about vertical displacement (settlement) under all load combinations, for both cases, as it is shown in figure 6.1. It is observed that Turkish soil had slightly higher settlement values in all load combinations. Where it reached in second loads combination scenario 3.53 cm compared to 3.46 cm in Morocco. Turkish soil had slightly higher settlement values in all load combinations. This corresponds with the fact that Turkish soil's 150 MPa modulus of elasticity (E) was a little less than Morocco's 160 MPa, which increased compressibility. This is related to the values of the elasticity modulus, even though there is a 10 MPa difference and the Turkish soil is stiffer than the Moroccan soil (by comparing cohesion and friction angles), but in soil mechanics and soil-structure interaction, small changes in the elasticity modulus can lead to noticeable results.

Total Horizontal Displacement

Table 6.3 Total horizontal displacement comparison chart results

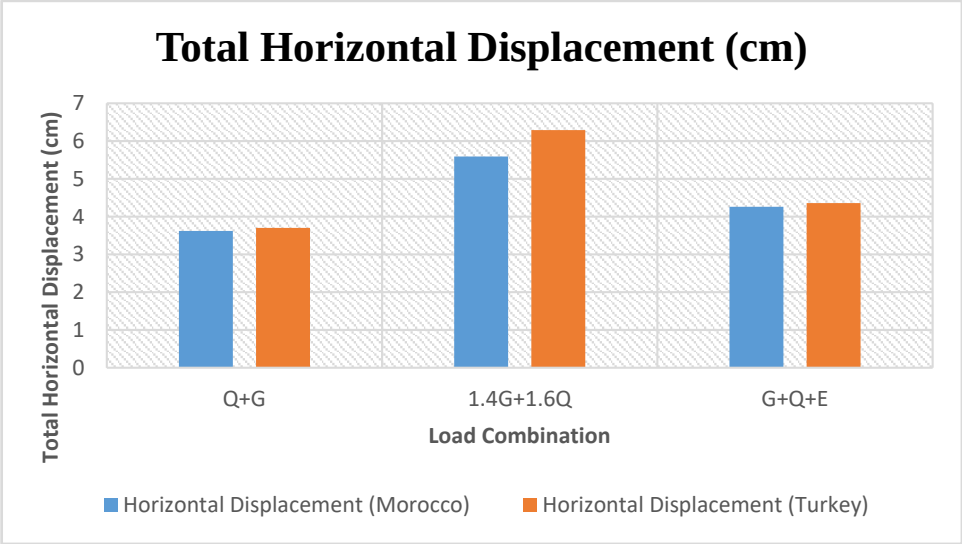

Considering horizontal displacement analysis is important in accordance with soil-structure interaction to ensure accurate seismic performance assessment and safe structural design. In Figure 6.2, it is observed that under the 1.4G + 1.6Q combination, the largest horizontal displacement in Morocco was 5.59 cm, but in Turkey it reached 6.29 cm, demonstrating an ongoing pattern of higher displacements in the same case study. Concerning the variations in results with the same cause of the vertical displacement case, in this part, the variations are related also to the spectral acceleration values. Although spectral accelerations were not directly input into the program, the high seismic demand in Turkish design practice is influenced by the use of detailed site classifications and conservative base shear provisions in TBDY 2018. In contrast, the Moroccan RPS 2011 uses a smoother D-factor-based spectrum, leading to relatively more low-load effects values.

Total Stress and Strain

Table 6.4 Shear Strains Comparison Graph Chart Results

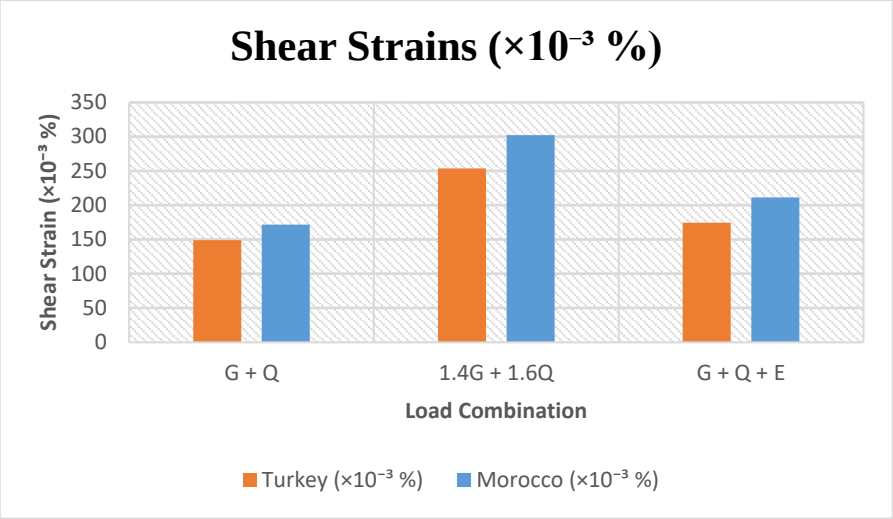

Table 6.5 Total Stress Comparison Chart Results

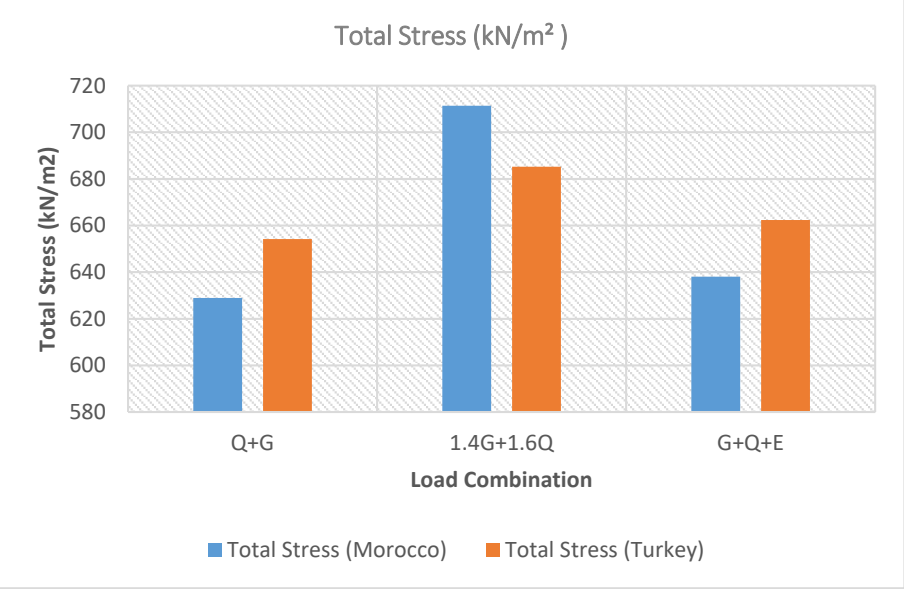

As it is known, the shear stress is the force applied to the soil due to structural or seismic loads per unit area, while the shear strain is the deformation of this area caused by that stress. The results with Moroccan soil parameters are more resistant to deformation when the stress levels are higher, as shown in figure 6.3 (711.35 kN/m² compared to 685.21 kN/m² of Turkish soil parameters under 1.4G + 1.6Q). Even though settlement is lower in Moroccan case, the internal energy absorption (strain) is greater, as shown by larger strain values in figure 6.4 (up to 302.13×10^{-3}%).Although the Turkey soil case study experiences greater displacements, its reduced strain values reflect a totally different results behavior. The reason is the early yielding and sliding, rather than straining, is possible because of less internal distortion caused by reduced OCR (over-consolidation ratio) and E (elasticity modulus) values.

Over Consolidation Ratio (OCR)

Table 6.6 Over-Consolidation Ratio Comparison Chart Results

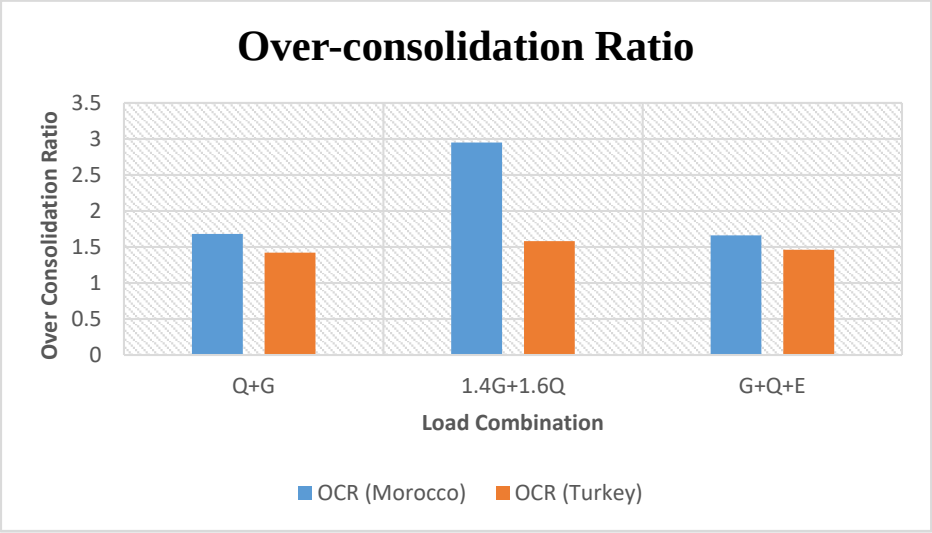

It appears that the soils in the Moroccan case study were more rigid and pre-consolidated. After evaluating figure 6.5, the OCR values in that country's model are much higher (up to 2.95) compared to the Turkish soil case study

(max 1.58). Better resilience to shear deformation and low settlement values are supported by this. According to the code's interpretation, the Moroccan design emphasizes the use of soils that are either naturally compacted or treated, which makes them safer, in accordance with its empirical liquefaction evaluation technique. In Turkey, OCR values are generally lower due to more rigid (or denser) soils, aligning with the conditions in TBDY 2018 for numerical liquefaction evaluations and the use of CRR (cyclic resistance ratio) and shear stress ratio computations.

Bending Moment

Table 6.7 Bending Moment Comparison Chart Results

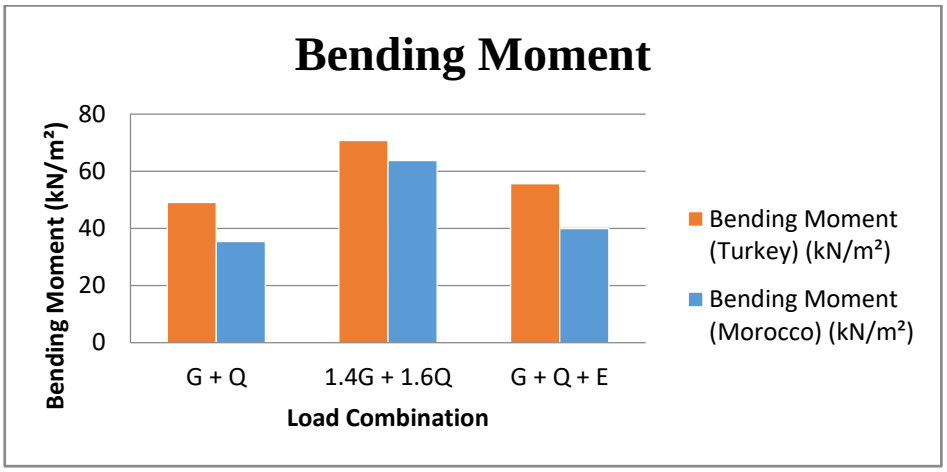

The analysis of bending moments under equivalent loading conditions showed in figure 6.6 describes consistently elevated values in the Turkish model. This conclusion is directly associated with the reduced soil stiffness (E = 150 MPa) and lower OCR values observed in the Turkish soil's case study, contributing to increased foundation deformation and elevated internal stresses. On the other hand, the Moroccan soil case study, characterized by its greater stiffness (E = 160 MPa) compared to the Turkish case study's stiffness value and over-consolidation, distributes stresses uniformly, resulting in less bending of structural parts. The findings confirm the impact of soil stiffness and

consolidation behavior on moment in foundation systems, highlighting that soil-structure interaction effects are more significant when the supporting soil is softer or more deformable.

After a detailed codes standards comparison of TBDY2018 and RPS2011 concerning the main parameters that may affect the soil structure interaction, and after analyzing the outputs of case studies, the evaluations that concerns how the soil are affected by the structure under various types of loads consists of : settlement, horizontal displacement, strain, shear stress, over-consolidation ratio and bending moment results. It was found that there is a direct and indirect relationship between the findings values and the soil parameters in accordance to codes standards. From the obtained findings analysis, it is recommended that future research and engineering practices should prioritize the integration of soil-structure interaction with numerical modeling before constructing. This is essential because the findings demonstrated that small variations in parameters such as modulus of elasticity (E) and over-consolidation ratio (OCR) can significantly change displacement, stress distribution, and deformation patterns, especially under combined static and seismic loading. Verified geotechnical data improves the accuracy of models, resulting in safer and more efficient structure designs. In addition to revising Moroccan code standards, as it was found in the comparison codes section that there are a lot of missing key parameters and investigations concerning soil-structure interaction, and for Morocco, considered an active tectonic area, it is mandatory to take precautions before the damages.

REFERENCES

ASCE. (2022). Minimum design loads and associated criteria for buildings and other structures (ASCE/SEI 7-22). American Society of Civil Engineers.

Ateş, Ş., Toprak, S., & Özçep, F. (2024). *Geotechnical and Structural Damages Caused by the 2023 Kahramanmaraş Earthquake ın Gölbaşı, Adıyamanç.*

Auersch, L. (2025). Dynamic compliance functions of surface foundations on layered soil: Rigid and flexible plates. *Journal of Geotechnical and Geoenvironmental Engineering.*

Bard, P. Y. (1999). Local effects on strong ground motion: Physical background and engineering consequences. *In Proceedings of the Advanced Study Course on Seismic Risk.*

Bard, P. Y., & Durand, S. (1986). Ground motion amplification and vertical motions on a large scale. *Earthquake Engineering & Structural Dynamics.*

Bielak, J., Loukakis, K., Hisada, Y., & Yoshimura, C. (2003). Domain Reduction Method for Three-Dimensional Earthquake Modeling in Localized Regions. Part I: Theory. *Bulletin of the Seismological Society of America, 93(2),* 817–824.

Brinkgreve, R. B. J., Kumarswamy, S., Swolfs, W. M., & Waterman, D. (2019). *PLAXIS 2D 2019 Material Models Manual.* Bentley Systems Netherlands B.V.

Budhu, M. (2010). *Soil Mechanics and Foundations.* Wiley.

Chandiwala, A., Savaliya, M., & Vasanwala, S. (2018). Soil-Structure Interaction on Pile Raft Foundation in Multi-Storey RC Building with Vertical Irregularity. *Proceedings of Indian Geotechnical Conference 2018.*

Chellai, E.H., Bouchta, A., Ammor, A., & Gauraz, A. (2024). Post-earthquake geotechnical and structural damage assessment following the 2023 Al Haouz earthquake in Morocco. *Case Studies in Earthquake Engineering, 6,* 100148.

Chennaoui Aoudjehane, H., & Messaoudi, M. (2024). The 2023 Morocco earthquake: A brief overview. *Earth and Marine Science and Technology, 2(4),* 1–7.

Cherkaoui, T.-E., & El Hassani, A. (2012). Seismicity and Seismic Hazard in Morocco: 1901–2010. *Bulletin de l'Institut Scientifique, Rabat, Section Sciences de la Terre, 34*, 45–55.

Chopra, A. K. (2012). *Dynamics of structures: Theory and applications to earthquake engineering* (4th ed.). Prentice Hall.

Clough, R. W., & Penzien, J. (1975). *Dynamics of structures.* McGraw-Hill.

Clough, R. W., & Penzien, J. (1993). *Dynamics of structures* (2nd ed.). McGraw-Hill.

Deverchère, J., et al. (2009). Crustal strain patterns in the central-western Mediterranean from GPS data. *Geophysical Journal International, 178(1)*, 430–446.

Di Capua, G., Facciorusso, J., Grelle, G., & Marino, S. (2024). Lessons learned from the 2023 Al Haouz earthquake in Morocco: Earthquake environmental effects and engineering geology perspectives. *Engineering Geology, 337*, 107402.

Dominguez, J. (1993). *Boundary elements in dynamics.* Computational Mechanics Publications.

El Janous, S., Abid, M. A., Afras, A., & El Ghoulbzouri, A. (2024). Evaluation of the Seismic Susceptibility in the North of Morocco Considering the Soil-Structure Interaction.

Elmrabet, T., Nour, A., & Rachid, E. (2014). The Al Hoceima (Morocco) earthquakes of 1994 and 2004: Control of damage patterns by active fault geometry and structural inheritance. *Journal of Geodynamics.*

Erdik, M. (2017). Seismic design of buildings in Turkey: Past, present, and future. *Earthquake Engineering and Engineering Vibration, 16(1)*, 1–12

Fardis, M. N. (2009). *Seismic design, assessment and retrofitting of concrete buildings: Based on EN-Eurocode 8.* Springer.

Gazetas, G. (1991). Formulas and charts for impedances of surface and embedded foundations. *Journal of Geotechnical Engineering, 117(9)*, 1363–1381

Gulhane, P., & Bajad, M. N. (2018). Analysis of soil-structure interaction using elastic continuum model. *International Journal of Geotechnical Engineering.*

Güllü & Natur. (2024). Simulation study on SSSI of mid-rise buildings near slopes during the 2023 Kahramanmaraş earthquake. *Natural Hazards.*

Horvath, J. S. (2002). An overview of the use of EPS geofoam (expanded polystyrene) in geotechnical applications. *Geotextiles and Geomembranes.*

Huang, Y., Li, X., & Chen, Y. (2018). Seismic wave amplification through layered soil profiles. *Soil Dynamics and Earthquake Engineering, 114*, 453–466.

Idriss, I. M., & Sun, J. I. (1992). SHAKE91: A computer program for conducting equivalent linear seismic response analyses of horizontally layered soil deposits. *University of California, Davis.*

Işık, E. (2023). Structural Failures of Adobe Buildings during the February 2023 Kahramanmaraş (Türkiye) Earthquakes. *Applied Sciences, 13(15)*, 8937

Kerr, A. D. (1964). Elastic and viscoelastic foundation models. *Journal of Applied Mechanics, 31*, 491–498.

Kerr, A. D., & Rhines, F. N. (1967). A viscoelastic foundation model for the dynamic analysis of beams. *International Journal of Solids and Structures, 3(4)*, 445–464.

Kowalska, B. (2012). Determination of soil parameters using CPTu and DMT tests. *Annals of Warsaw University of Life Sciences – SGGW. Land Reclamation, 44(2)*, 219–228.

Koçkar, M. K., Ercan, Ö., & Arslan, M. H. (2024). Observed Damage Behavior of Earth Dams During the 2023 Kahramanmaraş Earthquakes. *Geotechnical and Geological Engineering, 42*, 1673–1692.

Kramer, S. L. (1996). *Geotechnical earthquake engineering.* Prentice Hall. Lysmer, J., & Richart, F. E. Jr. (1966).

Dynamic response of footings to vertical loading. *Journal of Soil Mechanics and Foundations Div, ASCE, 92(SM1)*, 65–91.

Madabhushi, S. P. G., & Haigh, S. K. (2014). Centrifuge modelling of seismic soil–structure interaction in soft clay. *Soil Dynamics and Earthquake Engineering, 66*, 125–138.

Malusà, M. G., Ellero, A., & Ottria, G. (2024). Tectonics of the Mw 6.8 Al Haouz earthquake (Morocco) reveals minor role of asthenospheric upwelling. *Tectonophysics.*

Mekki, M. (2014). Seismicity and Seismic Hazard in Morocco. *University of Science and Technology of Oran.*

Motallebiyan, A., Bayat, M., & Nadi, B. (2020). Analyzing the Effects of Soil-Structure Interactions on the Static Response of Onshore Wind Turbine Foundations Using Finite Element Method. *Civil Engineering Infrastructures Journal, 53(1)*, 189–205.

Mylonakis, G., & Gazetas, G. (2000). Seismic soil-structure interaction: Beneficial or detrimental? *Journal of Earthquake Engineering, 4(3)*, 277–301.

Mylonakis, G., & Nikolaou, S. (2010). Soil-structure interaction effects on the seismic response of structures. *In Earthquake Geotechnical Engineering for Protection and Development of Environment and Constructions* (pp. 105–118). CRC Press.

Mylonakis, G., Nikolaou, S., & Gazetas, G. (2006). Footings under seismic loading: Analysis and design issues with emphasis on bridge foundations. *Soil Dynamics and Earthquake Engineering, 26(9)*, 824–853.

Nouri-Borujerdi, A., & Rahgozar, M. A. (2018). Evaluation of SSI effects on seismic performance of moment-resisting RC frames considering soil nonlinearity. *Earthquake Engineering and Engineering Vibration, 17(1)*, 137–151.

Orak, Y., Filiz Orak, Safiye Göçer, & Mehmet Doğanay. (2023). Earthquake in Türkiye: Impact on Health Services and Infection Threats. *Journal of*

Pitilakis, K., Anastasiadis, A., & Raptakis, D. (2004). Design spectra and soil classification for seismic code provisions. *In Proceedings of the 13th World Conference on Earthquake Engineering.*

Pitilakis, K., Riga, E., & Anastasiadis, A. (2015). Design and evaluation of ground motion scenarios for seismic microzonation. *Soil Dynamics and Earthquake Engineering, 69*, 142–163.

Poulos, H. G., & Davis, E. H. (1974). *Elastic solutions for soil and rock mechanics.* Wiley.

Reissner, E. (1958). On bending of elastic plates. *Quarterly of Applied Mathematics, 16*, 153–165.

Selvadurai, A. P. S. (1979). *Elastic analysis of soil-foundation interaction.* Elsevier.

Spencer, K.D., et al. (2024). Modulation of anxiety-like behavior in galactooligosaccharide-fed mice. *Brain, Behavior, and Immunity, 121*, 229–243.

Stewart, J. P., & Fenves, G. L. (1998). System identification for evaluating soil-structure interaction effects in buildings. *Journal of Engineering Mechanics, 124(4),* 385–397.

Stewart, J. P., Fenves, G. L., & Seed, R. B. (2014). Seismic soil-structure interaction in buildings. *Journal of Geotechnical and Geoenvironmental Engineering, 140(4),* 04013021.

Sucuoglu, H., & Yazgan, U. (2001). The 1999 Kocaeli and Düzce (Turkey) Earthquakes. *Proceedings of the International Conference on the 2001 Bhuj Earthquake and Advances in Earthquake Science, Kanpur, India.*

Tokimatsu, K., & Seed, H. B. (1987). Evaluation of settlements in sands due to earthquake shaking. *Journal of Geotechnical Engineering, 113(8),* 861–878.

Van der Woerd, J., et al. (2014). The Al Hoceima (Morocco) 2004 earthquake: Postseismic deformations from SAR interferometry, field observations, and tectonic implications. *Journal of Geodynamics, 77,* 89–109.

Veletsos, A. S., & Meek, J. W. (1974). Dynamic behavior of building-foundation systems. *Earthquake Engineering & Structural Dynamics, 3(2),* 121–138

Veletsos, A. S., & Newmark, N. M. (1960). Effect of foundation compliance on earthquake response. *Journal of the Engineering Mechanics Division, 86(EM2),* 67–94.

Wen-hwa-Wu. (2025). Comparison of base shear response spectrum to different earthquakes. *ResearchGate Scientific Figure.*

Winkler, E. (1867). *Die Lehre von der Elastizität und Festigkeit (The theory of elasticity and strength).* H. Dominicus.

Wolf, J. P. (1985). *Dynamic soil-structure interaction.* Prentice Hall.

Yang, Z., & Elgamal, A. (2004). Influence of damping formulation on the seismic response of a saturated porous medium. *International Journal for Numerical and Analytical Methods in Geomechanics, 28(9),* 861–879

Yilmaz, E. (2022). Soil-structure interaction effects on seismic performance of mid-rise RC buildings with different foundation systems [Master's thesis, Middle East Technical University]. *METU Thesis Database.*

Yılmaz, M. T., & Doğan, T. (2024). Evaluation of the seismic response of reinforced concrete buildings in the light of lessons learned from the February 6, 2023, Kahramanmaraş (Türkiye) earthquake sequences. *Natural Hazards.*

Yılmaz, Mehmet, & Serkan Aydın, editors. (2025). *Research and Findings in Engineering Sciences*. Bookchapter.org.

Zhang, J., Zhang, Y., & Tang, H. (2014). Seismic soil–structure interaction analysis using finite element method in time domain. *Soil Dynamics and Earthquake Engineering, 55*, 92–102.

APPENDICES

APPENDIX A. Comparison of Codes Standards

Table 6.1 Key Parameter Differences for SSI Modeling TBDY 2018 vs RPS 2011

Parameter	TBDY 2018 (Turkey)	RPS 2011 (Morocco)
Soil Classes	ZA-ZF(based on Vs30)	S1-S5(based on Vs, SPT-N and Su)
Soil Factor (S)	1.0–2.4	1.0–1.8
Importance Factor (I)	1.0–1.5(based on building use class)	0.8–1.5(based on building function)
Se (T) formula	Multi-slope piecewise(TB,TC,TD,TL)	Piecewise by Za/Zv
Liquefaction	SPT, Su-based	SPT-based charts
Foundation Type	Raft, pile, mat with detailed SSI provisions.	Shallow or deep with general rules.

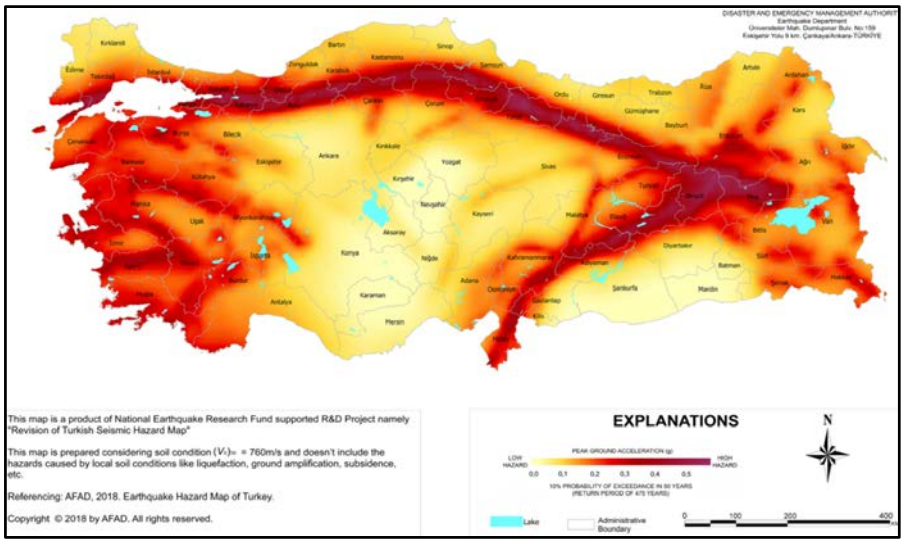

Seismic hazard distribution in Turkey (AFAD,2018)

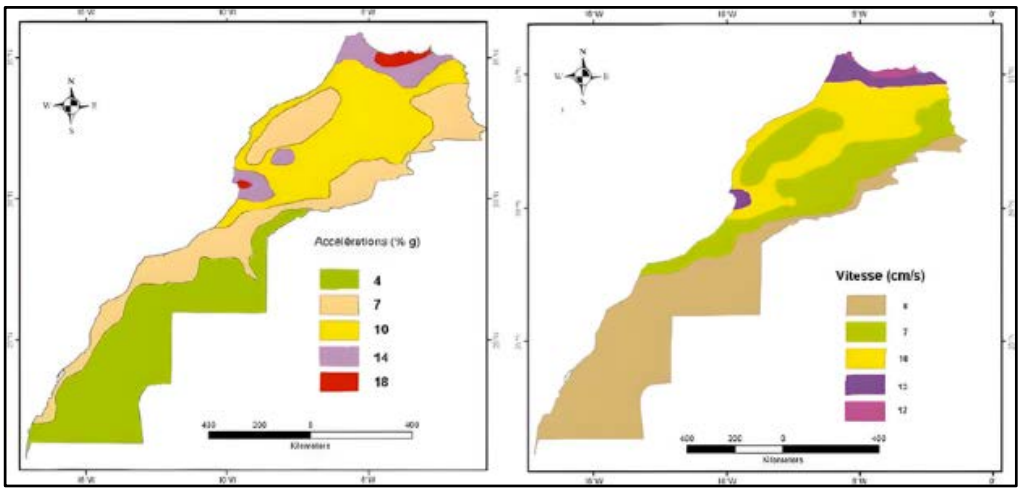

Map of the five seismic zones of Morocco (RPS 2011)

APPENDIX B. Input PLAXIS Parameters

Table 5.2 Soil parameters used in PLAXIS input (Turkey)

Parameter	Value
Unit weight, γn/γsat(kn/m^3)	**20/21**
Modulus of Elasticity, E'ref (MPa)	**150**
Cohesion, c'(KPa)	**25**
Shear strength angle	**36**

Table 5.3 Soil parameters used in PLAXIS input (Morocco)

Parameter	Value
Unit weight, γn/γsat(kn/m^3)	**19/20**
Modulus of Elasticity, E'ref (MPa)	**160**
Cohesion, c'(KPa)	**6**
Shear strength angle	**30.7**

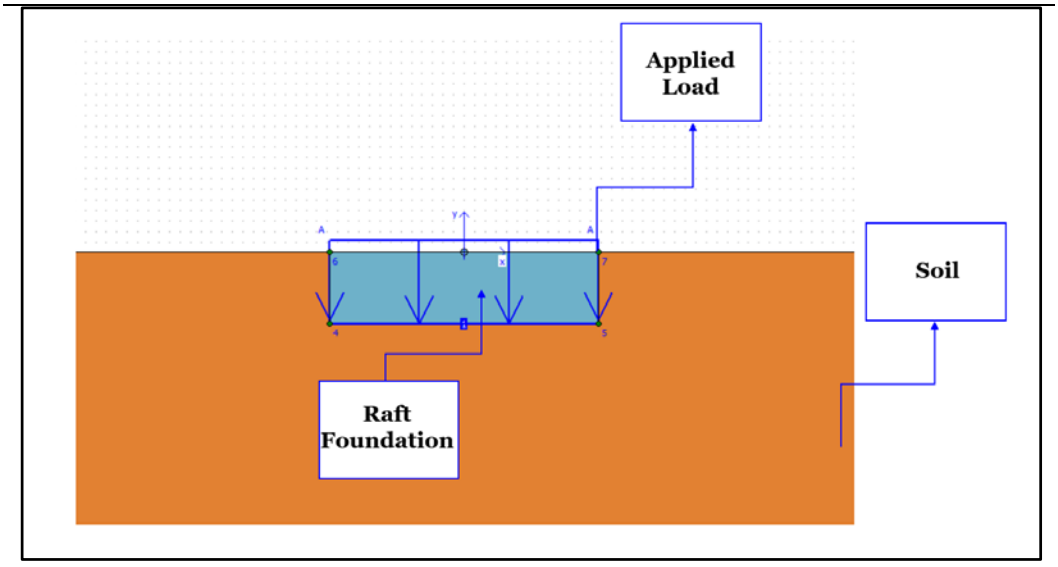

2D Model of Building + Foundation + Soil (PLAXIS 2D)

APPENDIX C. Output PLAXIS Results

Table 5.4 Summarized values of Turkish case stydy's outputs

Type of Load Combination	Total Vertical Displacement (Settlement) (cm)	Total Horizontal Displacement (cm)	Total Stress (σ) (KN/m²)	Total Strain (ε) (%)	Over Consolidation Ratio
Q+G	2,03	3,7	654.20	$148{,}95\times10^{-3}$	1,42
1,4G + 1,6Q	3,53	6,29	685.21	$253{,}55\times10^{-3}$	1,58
G+Q+E	2,41	4,36	662.35	$174{,}45\times10^{-3}$	1,46

Table 5.5 Summarized values of Moroccan case stydy's outpus

Type of Load Combination	Total Vertical Displacement(Settlement) (cm)	Total Horizontal Displacement (cm)	Total Stress (σ) (KN/m²)	Total Strain(ε) (%)	Over Consolidation Ratio
Q+G	1.78	3.62	628.92	$171{,}57\times10^{-3}$	1.68
1,4G + 1,6Q	3.46	5.59	711.35	$302{,}13\times10^{-3}$	2.95
G+Q+E	2.18	4.26	638.06	$211{,}26\times10^{-3}$	1.66

Table 5.6 Table of bending moment values of both conditions

Load Combination	Bending Moment (Turkey) (kN/m²)	Bending Moment (Morocco) (kN/m²)
G + Q	49.07	35.44
1.4G + 1.6Q	70.75	63.78
G + Q + E	55.64	39.98

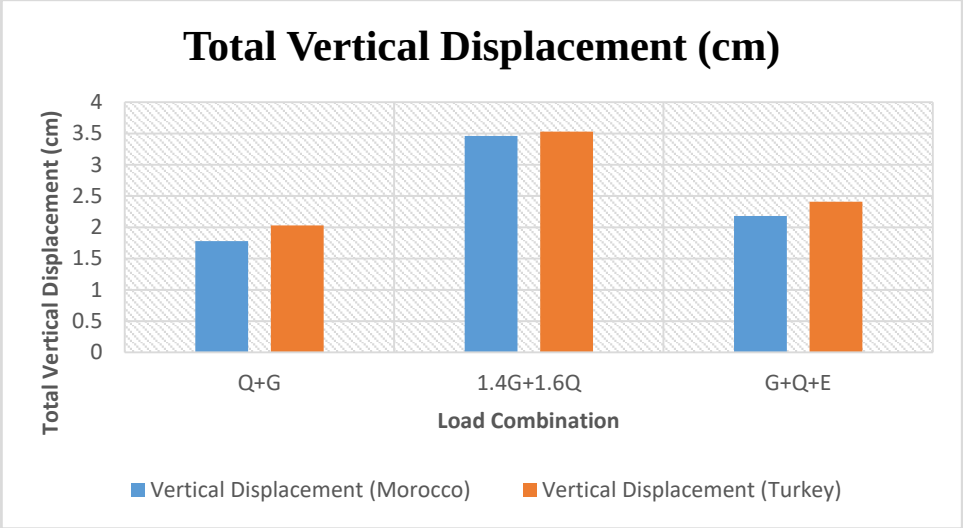

Total vertical displacement comparison

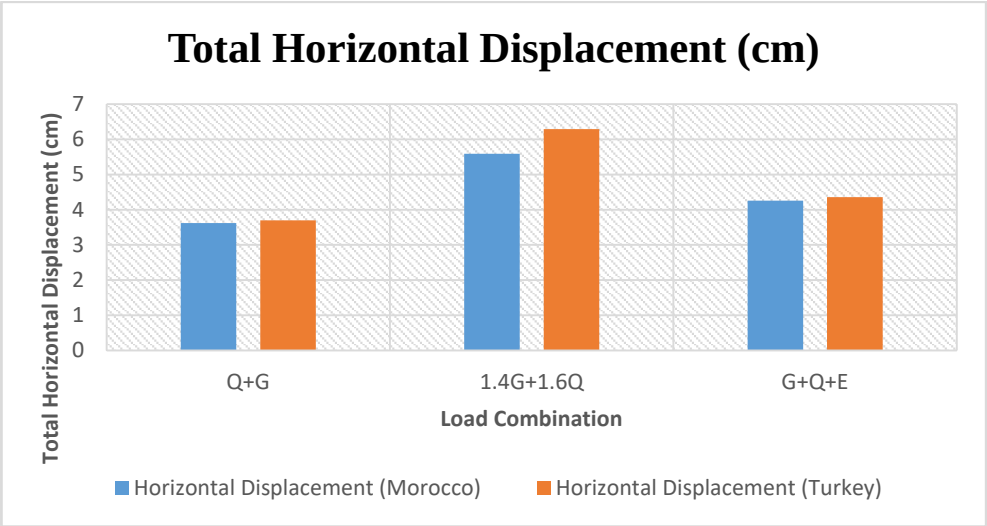

Total horizontal displacement comparison chart results

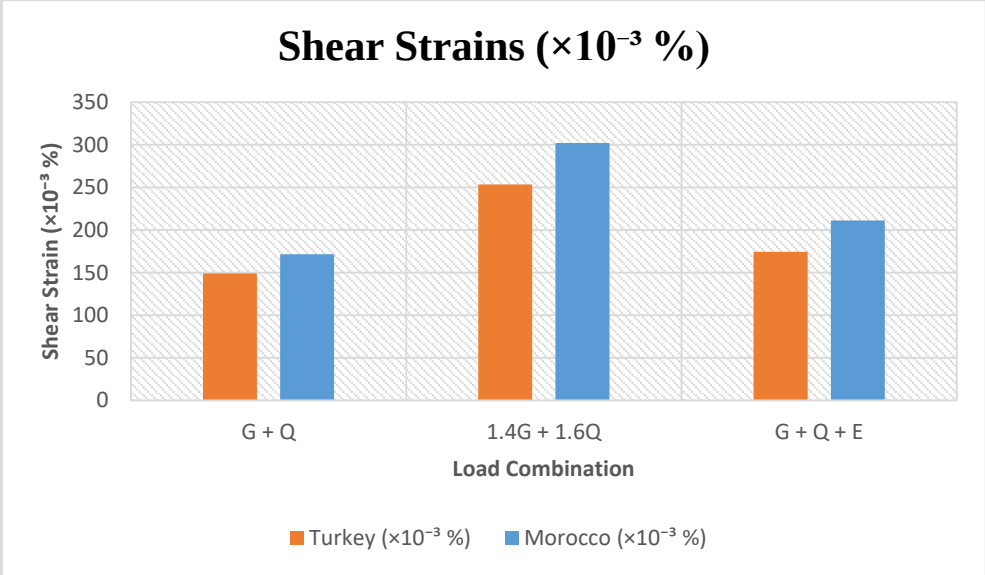

Shear strain comparison chart

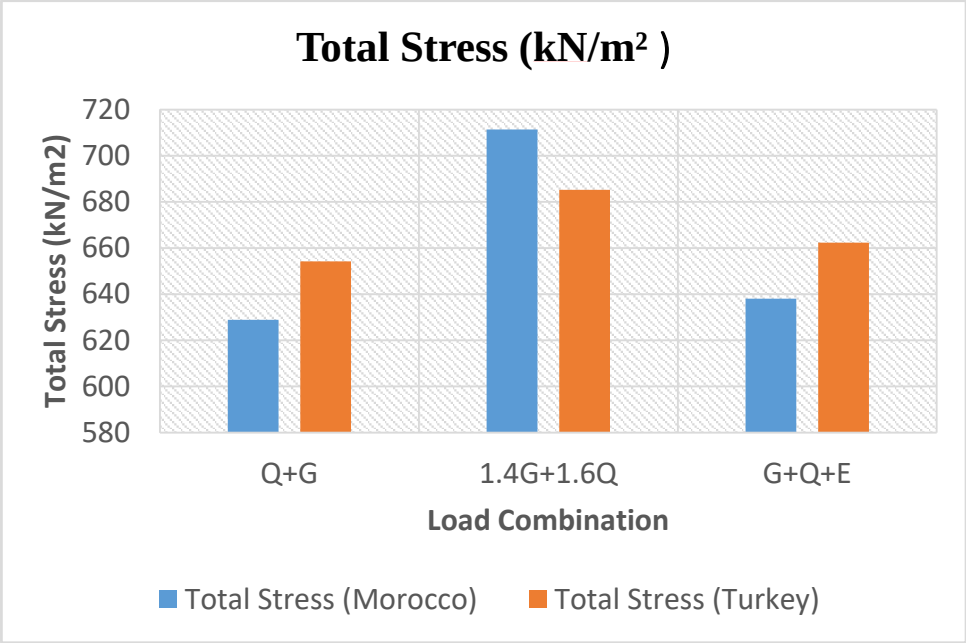

Total stress comparison chart results

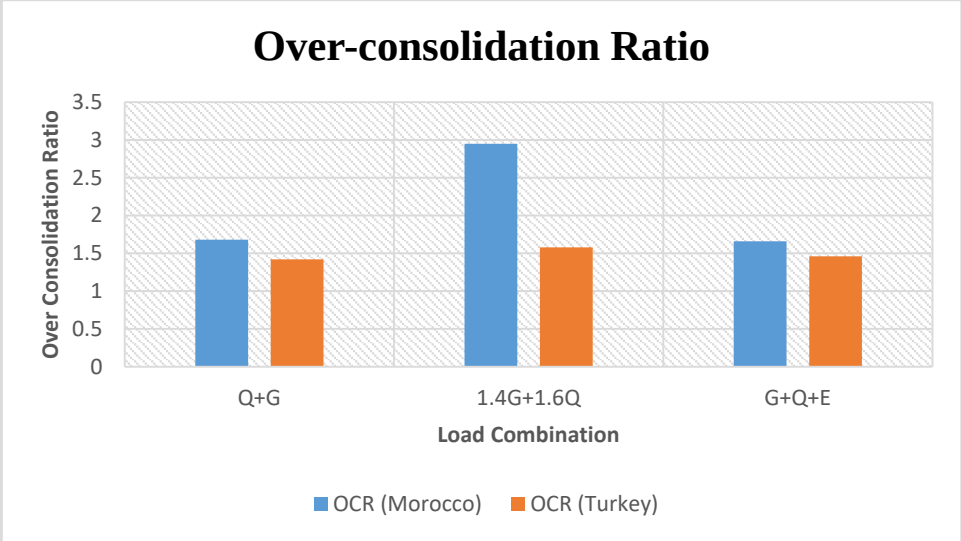

Over-consolidation ratio comparison chart results

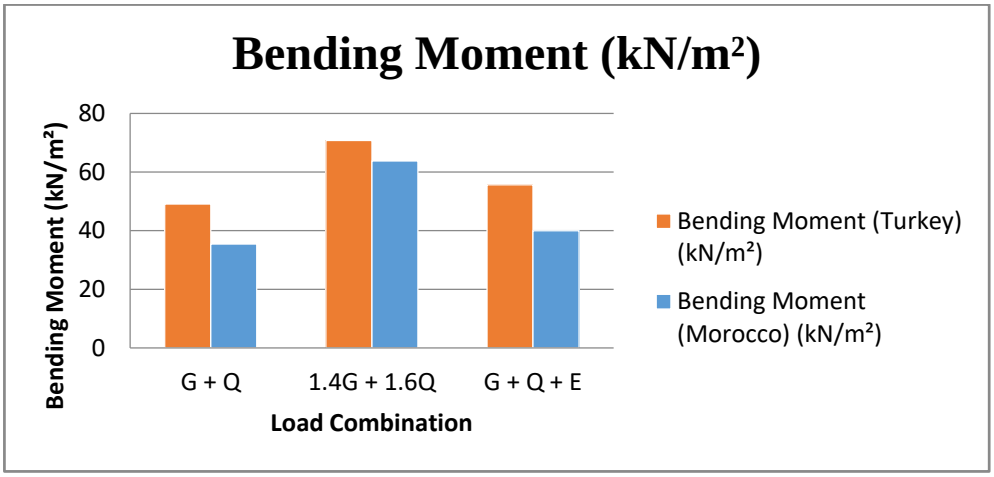

Bending moment comparison chart results

CURRICULUM VITAE